

# Deep Conditional Distribution Learning via Conditional Föllmer Flow

Jinyuan Chang<sup>1,2</sup>, Zhao Ding<sup>3</sup>, Yuling Jiao<sup>3,4</sup>, Ruoxuan Li<sup>3</sup>, and Jerry Zhijian Yang<sup>3,4</sup>

<sup>1</sup>*Joint Laboratory of Data Science and Business Intelligence, Southwestern University of Finance and Economics, Chengdu, Sichuan 611130, China*

<sup>2</sup>*Academy of Mathematics and Systems Science, Chinese Academy of Sciences, Beijing 100190, China*

<sup>3</sup>*School of Mathematics and Statistics, Wuhan University, Wuhan, Hubei 430072, China*

<sup>4</sup>*Hubei Key Laboratory of Computational Science, Wuhan, Hubei 430072, China*

## Abstract

We introduce an ordinary differential equation (ODE) based deep generative method for learning conditional distributions, named *Conditional Föllmer Flow*. Starting from a standard Gaussian distribution, the proposed flow could approximate the target conditional distribution very well when the time is close to 1. For effective implementation, we discretize the flow with Euler’s method where we estimate the velocity field nonparametrically using a deep neural network. Furthermore, we also establish the convergence result for the Wasserstein-2 distance between the distribution of the learned samples and the target conditional distribution, providing the first comprehensive end-to-end error analysis for conditional distribution learning via ODE flow. Our numerical experiments showcase its effectiveness across a range of scenarios, from standard nonparametric conditional density estimation problems to more intricate challenges involving image data, illustrating its superiority over various existing conditional density estimation methods.

*Keywords:* conditional distribution learning, deep neural networks, end-to-end error bound, ODE flow.

## 1 Introduction

With the rapid advancements in data storage technology and the accessibility of more powerful computing resources, our human society is taking significant strides into the era of Artificial Intelligence (AI). Recent influential Artificial General Intelligence (AGI) products, like ChatGPT, Stable Diffusion, and Sora have demonstrated remarkable capabilities in

generating high-quality text, image, or video content based on user-provided prompts, which are making a revolutionary shift in the way we live and work. Notably, Statistics plays a crucial role in the development of these AGI products. A fundamental statistical problem involved is how to generate samples efficiently following a learned high-dimensional conditional distribution (Liu et al., 2024; Esser et al., 2024).

Intuitively, to solve this fundamental statistical problem, we can first estimate the conditional distribution and then generate samples from the obtained estimation. A wealth of classical literature has already delved into nonparametric conditional distribution estimation, including smoothing methods (Rosenblatt, 1969; Hyndman et al., 1996; Chen and Linton, 2001; Hall and Yao, 2005), regression reformulation (Fan et al., 1996; Fan and Yim, 2004), basis function expansion (Sugiyama et al., 2010; Izbicki and Lee, 2016, 2017). Nevertheless, all these methods suffer from the “curse of dimensionality”, where their performance declines drastically as the dimensionality of the related variables increases. Therefore, such two-step strategy lacks the ability to handle the problem in high-dimensional scenarios. To address this issue, recent years have seen some novel methods. Benefiting from the advancements in deep generative models, these methods mainly focus on estimating the samplers directly. For instance, Zhou et al. (2023) introduce a deep generative approach called GCDS utilizing Generative Adversarial Networks (GANs) (Goodfellow et al., 2014). With a theoretical guarantee, GCDS succeeds in estimating a high-dimensional conditional sampler. However, GANs are known to suffer from training instability (Karras et al., 2019) and mode collapse, necessitating considerable engineering efforts and human tuning. Hence, the performance of GAN-based deep generative models is usually less than satisfactory.

The recent breakthrough in deep generative models, known as the diffusion model (Ho et al., 2020), gains notable attention for its superior sample quality and significantly more

stable training process in comparison with GANs. The basic idea in [Ho et al. \(2020\)](#) is training a denoising model to progressively transform noise data to samples following the target distribution, which is equivalent to learning the drift term of a stochastic differential equation (SDE) ([Song et al., 2021](#)). Following this, research on SDE-based generative models has flourished. A mainstream direction involves utilizing an Ornstein-Uhlenbeck process to transform the target distribution into a Gaussian distribution ([Ho et al., 2020](#); [Song et al., 2021](#); [Meng et al., 2021](#)). Then, solving the time-reversed SDE will yield a sampler. The error analysis of SDE-based generative models can be found in, for example, [Wang et al. \(2021\)](#), [De Bortoli \(2022\)](#), [Chen et al. \(2023c\)](#), [Oko et al. \(2023\)](#), [Lee et al. \(2023\)](#), [Chen et al. \(2023a\)](#), and [Benton et al. \(2023\)](#).

Based on the fact that learning the drift term of an SDE corresponds to learning the velocity field of a certain ordinary differential equation (ODE), [Song et al. \(2021\)](#) also consider an ODE-based generative model defined over infinite time interval  $(0, \infty)$ . However, solving infinite time ODEs usually leads to numerical instability ([Butcher, 2016](#)), which could be improved within the framework of stochastic interpolation. There, finite time ODEs can be constructed to transform standard Gaussian distribution into target distributions. Built on this, several ODE-based generative models have been proposed, see, for example, [Liu et al. \(2023a\)](#), [Albergo and Vanden-Eijnden \(2023\)](#), [Xu et al. \(2022\)](#), [Liu et al. \(2023b\)](#), and [Gao et al. \(2023\)](#). Despite their achievement, aforementioned SDE/ODE-based methods are not designed to generate samples from conditional distributions. Lately, there have been proposals of several SDE/ODE-based generative models for conditional sampling ([Shi et al., 2022](#); [Albergo et al., 2023b](#); [Huang et al., 2023](#); [Zheng et al., 2023](#); [Wildberger et al., 2023](#)), while consistency of the learned conditional distribution has not been studied in these works.

In this paper, we introduce a novel ODE-based conditional sampling method named *Conditional Föllmer Flow*, which has the following main advantages:

- Firstly, we propose an ODE system over a unit time interval, and both the velocity field and the ODE flow itself exhibit Lipschitz continuity, mathematically ensuring robustness in training and sampling processes. This assures that our method excels in managing high-dimensional problems and can handle both continuous and discrete variables. Furthermore, our proposed ODE-based method maps random Gaussian noises to some samples with distribution arbitrarily close to the target conditional distribution, which allows us to utilize the noise-sample pairs generated by the ODE-based method to train a new end-to-end neural network using least square fitting. Ideally, the end-to-end neural network takes Gaussian noises as input and produces the corresponding samples as output. It is important to note that the sampling time of the ODE-based method on a time grid with size  $N$  is of order  $\mathcal{O}(N)$ . However, once the end-to-end network is trained, the time required to generate a new sample is significantly reduced to  $\mathcal{O}(1)$  since only a single network evaluation is needed. See more detailed discussion on this in the last paragraph of Section 3. It is worth emphasizing that the end-to-end generator cannot be derived from the SDE-based method due to its inherent stochastic nature for each particle.
- Secondly, under some mild conditions, we demonstrate that the distribution of the generated samples will converge in probability to the target conditional distribution with a certain rate, which is rarely observed in previous works. Several similar results have emerged in the analysis of general SDE-based methods, while in the context of ODE-based counterparts, comparable analytical findings primarily surface when assuming uncheckable regularity of the target velocity field (Chen et al., 2023d, 2024).

As for the conditional scenario, [Huang et al. \(2023\)](#) has extended the SDE/ODE-based methods ([Albergo et al., 2023a](#)) and conducted stability analysis of their proposed SDE. However, their analysis depends on the examination of two separate neural networks and fails to account for errors introduced by sampling algorithms. More importantly, such analysis framework only works for the SDE-based method but is not applicable to the ODE-based method. To the best of our knowledge, our work presents the first in-depth convergence analysis of ODE-based conditional generative methods.

- Thirdly, we conduct a series of numerical experiments and provide a comprehensive assessment of the versatility and efficacy of the conditional Föllmer flow. In small-scale and low-dimensional scenarios, our method exhibits comparable or superior performance to traditional conditional density estimation methods, suggesting its robustness and applicability in conventional settings. Furthermore, our approach excels in high-dimensional examples such as image generation and reconstruction where traditional methods encounter difficulties, which highlights its adaptability to modern data challenges.

The rest of this paper is structured as follows. In [Section 2](#), we provide notation and formally introduce the concept of the conditional Föllmer flow. In [Section 3](#), we elucidate how to employ the conditional Föllmer flow to design numerical algorithms for conditional sampling. In [Section 4](#), we analyze the convergence of our numerical scheme, and present a comprehensive error analysis. In [Section 5](#), we conduct numerical experiments to demonstrate its performance. Finally, in [Section 6](#), we discuss our work and outline some future directions. All technical proofs are provided in the supplementary material.

## 2 Preliminaries

### 2.1 Notation

For a vector  $\mathbf{x} = (x_1, \dots, x_d)^T \in \mathbb{R}^d$ , the  $\ell^2$ -norm and  $\ell^\infty$ -norm of  $\mathbf{x}$  are, respectively, denoted by  $\|\mathbf{x}\|_2 := \sqrt{\sum_{i=1}^d x_i^2}$  and  $\|\mathbf{x}\|_\infty := \max_{1 \leq i \leq d} |x_i|$ . For a probability density  $\pi$  and a measurable function  $f : \mathbb{R}^d \rightarrow \mathbb{R}$ , the  $L^2(\pi)$ -norm of  $f$  is defined as  $\|f\|_{L^2(\pi)} := \sqrt{\int f^2(\mathbf{x})\pi(\mathbf{x}) \, d\mathbf{x}}$ . For a vector function  $\mathbf{v} : \mathbb{R}^d \rightarrow \mathbb{R}^d$ , its  $L^2(\pi)$ -norm is defined as  $\|\mathbf{v}\|_{L^2(\pi)} := \|\|\mathbf{v}\|_2\|_{L^2(\pi)}$ . We denote by  $\text{tr}(\cdot)$  the trace operator on a square matrix. The  $d$ -dimensional identity matrix is denoted by  $\mathbf{I}_d$ . We use  $\mathcal{U}(a, b)$  to denote the uniform distribution on interval  $(a, b)$ , and use  $\mathcal{N}(\mathbf{0}, \mathbf{I}_d)$  to denote the  $d$ -dimensional standard Gaussian distribution. For two positive sequences  $\{a_n\}_{n \geq 1}$  and  $\{b_n\}_{n \geq 1}$ , the asymptotic notation  $a_n = \mathcal{O}(b_n)$  denotes  $a_n \leq Cb_n$  for some constant  $C > 0$ . The notation  $\tilde{\mathcal{O}}(\cdot)$  is used to ignore logarithmic terms. Given two distributions  $\mu$  and  $\nu$ , the Wasserstein-2 distance is defined as  $W_2^2(\mu, \nu) := \inf_{\pi \in \Pi(\mu, \nu)} \mathbb{E}_{(\mathbf{x}, \mathbf{y}) \sim \pi} (\|\mathbf{x} - \mathbf{y}\|_2^2)$ , where  $\Pi(\mu, \nu)$  is the set of all couplings of  $\mu$  and  $\nu$ . A coupling is a joint distribution on  $\mathbb{R}^d \times \mathbb{R}^d$  whose marginals are  $\mu$  and  $\nu$  on the first and second factors, respectively.

### 2.2 Conditional Föllmer Flow

Suppose that we have a random vector  $\mathbf{X} \in \mathbb{R}^{d_x}$ , where  $d_x$  may be quite large, and a condition variable  $\mathbf{Y} \in \mathbb{R}^{d_y}$  related to  $\mathbf{X}$ , forming a pair  $(\mathbf{X}, \mathbf{Y})$ . The marginal densities of  $\mathbf{X}$  and  $\mathbf{Y}$  are denoted as  $p_x(\mathbf{x})$  and  $p_y(\mathbf{y})$ , respectively, while the joint density of  $(\mathbf{X}, \mathbf{Y})$  is denoted as  $p_{x,y}(\mathbf{x}, \mathbf{y})$ . Using  $p_{x|y}(\mathbf{x}|\mathbf{y})$  to represent the conditional density of  $\mathbf{X}$  given  $\mathbf{Y} = \mathbf{y}$ , our interest lies in efficiently sampling from  $p_{x|y}(\mathbf{x}|\mathbf{y})$ . Such interest is underscored by recent advancements in AGI products such as Stable Diffusion and Sora, which specialize

in sampling from distributions with  $\mathbf{Y}$  representing user-provided multimodal prompts and  $\mathbf{X}$  standing for high-dimensional textual, image, or video content corresponding to  $\mathbf{Y}$ . Notably, we actually are not concerned about the specific functional form of  $p_{x|y}(\mathbf{x}|\mathbf{y})$  in these samplings. This is quite reasonable, since even if we are able to obtain such functional form in high-dimensional scenarios – given its impracticality – designing sampling algorithms based on it, e.g. high-dimensional MCMC, still remains intensely challenging. Therefore, instead of focusing on  $p_{x|y}(\mathbf{x}|\mathbf{y})$  itself, opting to directly learn a sampler proves to be much more practical.

We first introduce the so-called *Conditional Föllmer Flow*, a novel ODE-based method, which can map random Gaussian noises to some samples with distribution arbitrarily close to the target conditional distribution.

**Definition 1 (Conditional Föllmer Flow)** *If  $\mathbf{Z}(t, \mathbf{y})$  solves the following ODE for any  $\mathbf{y} \in [0, B]^{d_y}$ :*

$$d\mathbf{Z}(t, \mathbf{y}) = \mathbf{v}_F(\mathbf{Z}(t, \mathbf{y}), \mathbf{y}, t) dt, \quad t \in [0, 1), \quad (1)$$

*with  $\mathbf{Z}(0, \mathbf{y}) \sim \mathcal{N}(\mathbf{0}, \mathbf{I}_{d_x})$ , then we call  $\mathbf{Z}(t, \mathbf{y})$  the conditional Föllmer flow and  $\mathbf{v}_F$  the conditional Föllmer velocity field associated to  $p_{x|y}(\mathbf{x}|\mathbf{y})$ , respectively, where the velocity field  $\mathbf{v}_F$  is defined by*

$$\mathbf{v}_F(\mathbf{x}, \mathbf{y}, t) = \frac{\mathbf{x} + \mathbf{s}(\mathbf{x}, \mathbf{y}, t)}{t}, \quad t \in (0, 1), \quad (2)$$

*for  $\mathbf{v}_F(\mathbf{x}, \mathbf{y}, 0) = \mathbb{E}(\mathbf{X}|\mathbf{Y} = \mathbf{y})$ , and*

$$\mathbf{s}(\mathbf{x}, \mathbf{y}, t) = \nabla_{\mathbf{x}} \log f_t(\mathbf{x}|\mathbf{y}), \quad t \in [0, 1), \quad (3)$$

*with  $f_t(\mathbf{x}|\mathbf{y})$  denoting the conditional density of  $t\mathbf{X} + \sqrt{1-t^2}\mathbf{W}$  given  $\mathbf{Y} = \mathbf{y}$ , and  $\mathbf{W} \sim \mathcal{N}(\mathbf{0}, \mathbf{I}_{d_x})$  independent of  $(\mathbf{X}, \mathbf{Y})$ .*

It is easy to see that in Definition 1,  $f_0(\mathbf{x}|\mathbf{y}) = \mathcal{N}(\mathbf{0}, \mathbf{I}_{d_x})$ . Meanwhile, we will always use  $\mathbf{W}$  to denote a standard Gaussian random vector independent of  $(\mathbf{X}, \mathbf{Y})$  in the remaining text.

For the convenience of later discussion, we introduce the concept of flow map from ODE theory. Simply put, for an ODE system:  $d\mathbf{x}_t = \mathbf{v}(\mathbf{x}_t, t)dt$ , its flow map  $\Phi_t(\cdot)$  is defined as  $\Phi_t(\mathbf{x}_0) = \mathbf{x}_t$ , where  $\mathbf{x}_0 \in \mathbb{R}^d$  is the initial value of the ODE, and  $\mathbf{x}_t$  is the ODE solution at time  $t$  with initial value  $\mathbf{x}_0$ . Thus,  $\Phi_t(\cdot)$  determines a mapping from  $\mathbb{R}^d$  to  $\mathbb{R}^d$ . Based on this, we propose the definition of *Conditional Föllmer Flow Map*.

**Definition 2 (Conditional Föllmer Flow Map)** *We refer to the flow map related to the conditional Föllmer flow  $\mathbf{Z}(t, \mathbf{y})$  or the conditional Föllmer velocity field  $\mathbf{v}_F$  as the conditional Föllmer flow map, denoted by  $\mathbf{F}_t(\cdot, \mathbf{y})$ .*

Note that given  $\mathbf{y} \in [0, B]^{d_y}$ ,  $\{\mathbf{Z}(t, \mathbf{y})\}_{t \in [0, 1]}$  form a family of random vectors, and all the randomness originates from the initial point  $\mathbf{Z}(0, \mathbf{y})$  which follows the standard Gaussian distribution  $\mathcal{N}(\mathbf{0}, \mathbf{I}_{d_x})$ , as the subsequent evolution is determined by a deterministic ODE system. Theorem 1 ensures that as  $t \rightarrow 1$ , the density of  $\mathbf{Z}(t, \mathbf{y})$ , or equivalently expressed as  $\mathbf{F}_t(\mathbf{Z}(0, \mathbf{y}), \mathbf{y})$ , can arbitrarily approach the target conditional density  $p_{x|y}(\mathbf{x}|\mathbf{y})$ . For brevity, we will use  $\mathbf{Z}_t^{\mathbf{y}}$  to represent  $\mathbf{Z}(t, \mathbf{y})$  in the remaining text.

**Theorem 1** *Let Assumptions 1 and 2 in Section 4 hold. Then, for any  $\mathbf{y} \in [0, B]^{d_y}$ , the conditional Föllmer flow  $(\mathbf{Z}_t^{\mathbf{y}})_{t \in [0, 1]}$  associated to  $p_{x|y}(\mathbf{x}|\mathbf{y})$  is a unique solution to the ODE in Definition 1. Also, we have  $\mathbf{F}_t(\mathbf{Z}_0, \mathbf{y}) \sim f_t(\mathbf{x}|\mathbf{y})$  for  $t \in [0, 1)$ , where  $f_t(\mathbf{x}|\mathbf{y})$  is specified in Definition 1 and  $\mathbf{Z}_0 \sim \mathcal{N}(\mathbf{0}, \mathbf{I}_{d_x})$ . Moreover, for any  $\mathbf{y} \in [0, B]^{d_y}$ , we have  $W_2^2(f_t(\mathbf{x}|\mathbf{y}), p_{x|y}(\mathbf{x}|\mathbf{y})) \leq 4d_x(1-t) \rightarrow 0$  as  $t \rightarrow 1$ .*

The proof of Theorem 1 is given in Section A of the supplementary material.

### 3 Sampling Procedure

Leveraging insights from [Albergo et al. \(2023a\)](#) and [Gao et al. \(2023\)](#), we introduce the following proposition, which first offers an alternative expression for  $\mathbf{v}_F$  in the conditional expectation form. Based on such form, it then constructs a quadratic objective function for which  $\mathbf{v}_F$  stands out as the unique minimizer.

**Proposition 1** *For the conditional Föllmer velocity field  $\mathbf{v}_F$  on  $[0, T]$  with  $T < 1$ , the following two assertions are satisfied.*

(i)  $\mathbf{v}_F$  has a conditional expectation form

$$\mathbf{v}_F(\mathbf{x}, \mathbf{y}, t) = \mathbb{E} \left( \mathbf{X} - \frac{t}{\sqrt{1-t^2}} \mathbf{W} \mid t\mathbf{X} + \sqrt{1-t^2} \mathbf{W} = \mathbf{x}, \mathbf{Y} = \mathbf{y} \right), \quad (4)$$

(ii)  $\mathbf{v}_F$  is the unique minimizer of the quadratic objective

$$\mathcal{L}(\mathbf{v}) := \frac{1}{T} \int_0^T \mathbb{E} \left\{ \left\| \mathbf{X} - \frac{t}{\sqrt{1-t^2}} \mathbf{W} - \mathbf{v}(t\mathbf{X} + \sqrt{1-t^2} \mathbf{W}, \mathbf{Y}, t) \right\|_2^2 \right\} dt. \quad (5)$$

Based on Proposition 1(ii), we can design a deep learning algorithm to estimate  $\mathbf{v}_F$  nonparametrically, where we are working with a set of independent and identically distributed (i.i.d.) samples  $\{(\mathbf{X}_i, \mathbf{Y}_i)\}_{i=1}^n \sim p_{x,y}(\mathbf{x}, \mathbf{y})$  and i.i.d. samples  $\{(t_j, \mathbf{W}_j)\}_{j=1}^m$  with  $t_j \sim \mathcal{U}(0, T)$  and  $\mathbf{W}_j \sim \mathcal{N}(\mathbf{0}, \mathbf{I}_{d_x})$  independently. To ensure effective learning, the employed deep network class should be expressive enough to approximate the true velocity field. More specifically, we can choose ReLU-based feed forward neural networks (FNN) defined as Definition 3.

**Definition 3** *Denote by  $\text{FNN}(L, M, J, K, \kappa, \gamma_1, \gamma_2, \gamma_3)$  the set of ReLU neural networks  $\mathbf{v}_\theta : \mathbb{R}^{d_x} \times \mathbb{R}^{d_y} \times \mathbb{R} \rightarrow \mathbb{R}^{d_x}$  with parameter  $\theta$ , depth  $L$ , width  $M$  and size  $J$  such that*

$$(a) \sup_{\mathbf{x}, \mathbf{y}, t} \|\mathbf{v}_\theta(\mathbf{x}, \mathbf{y}, t)\|_2 \leq K \text{ and } \|\theta\|_\infty \leq \kappa,$$

- (b)  $|\mathbf{v}(\mathbf{x}_1, \mathbf{y}, t) - \mathbf{v}(\mathbf{x}_2, \mathbf{y}, t)|_\infty \leq \gamma_1 |\mathbf{x}_1 - \mathbf{x}_2|_2$  for any  $t \in [0, T]$  and  $\mathbf{y} \in [0, B]^{d_y}$ ,
- (c)  $|\mathbf{v}(\mathbf{x}, \mathbf{y}_1, t) - \mathbf{v}(\mathbf{x}, \mathbf{y}_2, t)|_\infty \leq \gamma_2 |\mathbf{y}_1 - \mathbf{y}_2|_2$  for any  $t \in [0, T]$  and  $\mathbf{x} \in \mathbb{R}^{d_x}$ ,
- (d)  $|\mathbf{v}(\mathbf{x}, \mathbf{y}, t_1) - \mathbf{v}(\mathbf{x}, \mathbf{y}, t_2)|_\infty \leq \gamma_3 |t_1 - t_2|$  for any  $\mathbf{x} \in \mathbb{R}^{d_x}$  and  $\mathbf{y} \in [0, B]^{d_y}$ .

Here the depth  $L$  refers to the number of hidden layers, so the network has  $L + 1$  layers in total. A  $(L + 1)$ -vector  $(w_0, w_1, \dots, w_L)$  specifies the width of each layer, where  $w_0 = d_x + d_y + 1$  is the dimension of the input data and  $w_L = d_x$  is the dimension of the output. The width  $M = \max\{w_1, \dots, w_L\}$  is the maximum width of the hidden layers. The size  $J = \sum_{i=0}^L w_i(w_i + 1)$  is the total number of parameters in the network. A notable aspect of our construction is the ability to impose Lipschitz constraints  $(\gamma_1, \gamma_2, \gamma_3)$  on the neural network functions in the class FNN without undermining their approximation power. See Proposition P2 in the supplementary material for details. Such construction is crucial in bounding the sampling error of our proposed sampling method (Algorithm 1) mentioned later. Similar construction on the FNN class was also used in Chen et al. (2023b) to conduct a convergence analysis of the SDE-based diffusion models.

Given the empirical loss function

$$\widehat{\mathcal{L}}(\mathbf{v}) = \frac{1}{mn} \sum_{i=1}^n \sum_{j=1}^m \left| \mathbf{X}_i - \frac{t_j}{\sqrt{1-t_j^2}} \mathbf{W}_j - \mathbf{v}(t_j \mathbf{X}_i + \sqrt{1-t_j^2} \mathbf{W}_j, \mathbf{Y}_i, t_j) \right|_2^2, \quad (6)$$

we consider to estimate the conditional Föllmer velocity field  $\mathbf{v}_F$  as follows:

$$\widehat{\mathbf{v}} \in \arg \min_{\mathbf{v}_\theta \in \text{FNN}(L, M, J, K, \kappa, \gamma_1, \gamma_2, \gamma_3)} \widehat{\mathcal{L}}(\mathbf{v}_\theta). \quad (7)$$

In practice, we can employ the stochastic gradient descent algorithm to solve it.

When  $\mathbf{v}_F$  is known, Theorem 1 in Section 2.2 indicates that, to sample data from the conditional density  $p_{x|y}(\mathbf{x}|\mathbf{y})$ , we only need to generate  $\mathbf{z}$  from  $\mathcal{N}(\mathbf{0}, \mathbf{I}_{d_x})$  and run the ODE dynamics of the conditional Föllmer flow (1) with the time  $t$  near 1. In practice, based on  $\widehat{\mathbf{v}}$ , the estimate of  $\mathbf{v}_F$  given in (7), we can obtain the pseudo data via the following Algorithm 1.

---

**Algorithm 1:** Sampling pseudo data from  $p_{x|y}(\mathbf{x}|\mathbf{y})$ 

---

**Input:**  $\tilde{\mathbf{z}}_0 \sim \mathcal{N}(\mathbf{0}, \mathbf{I}_{d_x})$ , the estimated velocity field  $\hat{\mathbf{v}}$ , time steps  $N$  and stopping time  $T < 1$

**Output:**  $\tilde{\mathbf{Z}}_T^y$

```
1  $t_0 = 0$ ;  
2 for  $k = 0, 1, \dots, N - 1$  do  
3   Compute  $t_{k+1} = t_k + N^{-1}T$ ;  
4   Compute the velocity  $\hat{\mathbf{v}}(\tilde{\mathbf{z}}_{t_k}, \mathbf{y}, t_k)$ ;  
5   Update  $\tilde{\mathbf{z}}_{t_{k+1}} = \tilde{\mathbf{z}}_{t_k} + N^{-1}T\hat{\mathbf{v}}(\tilde{\mathbf{z}}_{t_k}, \mathbf{y}, t_k)$ ;  
6 end  
7  $\tilde{\mathbf{Z}}_T^y = \tilde{\mathbf{z}}_{t_N}$ ;
```

---

Mathematically, implementing such a sampling algorithm is equivalent to employing a fixed-step-size Euler’s method to discretize the continuous ODE flow with velocity field  $\hat{\mathbf{v}}(\mathbf{x}, \mathbf{y}, t)$  on  $[0, T]$ . With properly selected  $T$ , Theorem 2 in Section 4 shows that the Wasserstein-2 distance between  $p_{x|y}(\mathbf{x}|\mathbf{y})$  and the density of  $\tilde{\mathbf{Z}}_T^y$  converges to zero in probability as  $n \rightarrow \infty$ . Notice that estimating the conditional density  $p_{x|y}(\mathbf{x}|\mathbf{y})$  is highly challenging in practice when  $d_x$  and  $d_y$  are large. Our theoretical analysis shows that, in order to draw samples from  $p_{x|y}(\mathbf{x}|\mathbf{y})$ , we can just implement Algorithm 1 without estimating  $p_{x|y}(\mathbf{x}|\mathbf{y})$ . This is the first main advantage of our method.

Furthermore, since the trajectory of ODE flows is deterministic, Algorithm 1 also provides a deterministic sampling procedure. That is, a given starting point  $\tilde{\mathbf{z}}_0$  will lead to a unique ending point  $\tilde{\mathbf{z}}_T$ . In fact, when  $\hat{\mathbf{v}}$  sufficiently approximates  $\mathbf{v}_F$  and  $N$  is sufficiently large, we have  $\tilde{\mathbf{z}}_T \approx \mathbf{F}_T(\tilde{\mathbf{z}}_0, \mathbf{y})$ , where  $\mathbf{F}_t(\cdot, \mathbf{y})$  is the conditional Föllmer flow map defined in Definition 2. Hence, after repeatedly applying Algorithm 1 to obtain the corresponding

pseudo data  $\tilde{\mathbf{z}}_T^1, \dots, \tilde{\mathbf{z}}_T^{\tilde{N}}$  from a set of Gaussian noises  $\tilde{\mathbf{z}}_0^1, \dots, \tilde{\mathbf{z}}_0^{\tilde{N}} \sim_{\text{i.i.d.}} \mathcal{N}(\mathbf{0}, \mathbf{I}_{d_x})$ , we can use an additional deep neural network  $\mathbf{G}_\theta(\cdot)$  to directly fit the mapping relationship between noise-sample pairs  $\{(\tilde{\mathbf{z}}_0^i, \tilde{\mathbf{z}}_T^i)\}_{i=1}^{\tilde{N}}$ . This can be seen as effectively learning the flow map  $\mathbf{F}_T(\cdot, \mathbf{y})$ . It is important to note that, the sampling time of Algorithm 1 on a time grid with size  $N$  is of order  $\mathcal{O}(N)$ . However, once  $\mathbf{G}_\theta(\cdot)$  is trained, the time required to generate a new sample is significantly reduced to  $\mathcal{O}(1)$  since only one single network evaluation is needed. It is worth emphasizing that such end-to-end generator cannot be derived from the SDE-based method due to its inherent stochastic nature for each particle.

## 4 Theoretical Analysis

Our main interest lies in establishing the validity of Algorithm 1 in generating data from  $p_{x|y}(\mathbf{x}|\mathbf{y})$ . More specifically, we would like to investigate the convergence rate of the sampling error in Algorithm 1. To do this, we need the following regularity assumptions.

**Assumption 1 (Bounded condition)**  $p_y(\mathbf{y})$  is supported on  $[0, B]^{d_y}$ , where  $B > 0$  is a fixed constant.

**Assumption 2 (Bounded conditional distribution)**  $p_{x|y}(\mathbf{x}|\mathbf{y})$  is supported on  $[0, 1]^{d_x}$  for any  $\mathbf{y} \in [0, B]^{d_y}$ , resulting  $p_x(\mathbf{x})$  also supported on  $[0, 1]^{d_x}$ .

**Assumption 3 (Lipschitz velocity with respect to continuous condition)** The conditional Föllmer velocity Field  $\mathbf{v}_F(\mathbf{x}, \mathbf{y}, t)$  in Definition 1 is  $\omega$ -Lipschitz continuous with respect to  $\mathbf{y}$  on  $\mathbb{R}^{d_x} \times [0, B]^{d_y} \times [0, 1]$ , where  $\omega$  is a universal constant independent of  $(\mathbf{x}, \mathbf{y}, t)$ .

Assumptions 1 and 2 are natural requirements in the literature of generative learning, where the mainly focused data like texts, images and videos are usually treated as bounded vectors in Euclidean spaces (Austin et al., 2021; Esser et al., 2024; Liu et al., 2024). Under

Assumptions 1 and 2, we will obtain some satisfactory properties of the conditional Föllmer velocity field  $\mathbf{v}_F$ , such as the Lipschitz properties of  $\mathbf{v}_F(\mathbf{x}, \mathbf{y}, t)$  with respect to  $\mathbf{x}$  and  $t$ . See Proposition P1 in the supplementary material for details. Further, Assumption 3 is made to provide necessary technical groundwork for demonstrating the effectiveness of  $\hat{\mathbf{v}}$  in (7) as a neural network to estimate  $\mathbf{v}_F$ .

Proposition 2 presents the convergence rate of  $\hat{\mathbf{v}}$ , whose proof is given in Section D of the supplementary material.

**Proposition 2** *Let Assumptions 1-3 hold. Suppose we have i.i.d. samples  $\{(\mathbf{X}_i, \mathbf{Y}_i)\}_{i=1}^n \sim p_{x,y}(\mathbf{x}, \mathbf{y})$  and i.i.d. samples  $\{(t_j, \mathbf{W}_j)\}_{j=1}^m$  with  $t_j \sim \mathcal{U}(0, T)$  and  $\mathbf{W}_j \sim \mathcal{N}(\mathbf{0}, \mathbf{I}_{d_x})$  independently. We choose the hypothesis network class  $\text{FNN} = \text{FNN}(L, M, J, K, \kappa, \gamma_1, \gamma_2, \gamma_3)$  with*

$$\begin{aligned} L &\sim d_x + d_y + \log \frac{1}{\varepsilon}, & M &\sim \frac{d_x^{d_x+3/2} (B\omega)^{d_y} \log^{(d_x+1)/2} \{d_x \varepsilon^{-1} (1-T)^{-1}\}}{(1-T)^{2d_x+3} \varepsilon^{d_x+d_y+1}}, \\ J &\sim \frac{d_x^{d_x+3/2} (B\omega)^{d_y} \log^{(d_x+1)/2} \{d_x \varepsilon^{-1} (1-T)^{-1}\}}{(1-T)^{2d_x+3} \varepsilon^{d_x+d_y+1}} \left( d_x + d_y + \log \frac{1}{\varepsilon} \right), \\ \kappa &\sim 1 \vee B\omega \vee \frac{d_x \log^{1/2} \{d_x \varepsilon^{-1} (1-T)^{-1}\}}{(1-T)^2} \vee \frac{d_x^{3/2} \log^{1/2} \{d_x \varepsilon^{-1} (1-T)^{-1}\}}{(1-T)^3}, \\ K &\sim \frac{d_x^{1/2} \log^{1/2} \{d_x \varepsilon^{-1} (1-T)^{-1}\}}{1-T}, & \gamma_1 &= \frac{10d_x^2}{(1-T)^2}, \\ \gamma_2 &= 10d_y\omega, & \gamma_3 &\sim \frac{d_x^{3/2} \log^{1/2} \{d_x \varepsilon^{-1} (1-T)^{-1}\}}{(1-T)^3}. \end{aligned}$$

and choose  $\varepsilon = (1-T)^{-(2d_x+7)/(d_x+d_y+5)} n^{-1/(d_x+d_y+5)}$  with  $1-T \gg n^{-1/(2d_x+7)}$ . Denote by  $g_t(\cdot, \cdot)$  the joint density of  $(t\mathbf{X} + \sqrt{1-t^2}\mathbf{W}, \mathbf{Y})$ . Letting  $m = n$ , for any fixed  $(d_x, d_y)$ , we have

$$\frac{1}{T} \int_0^T \|\hat{\mathbf{v}}(\mathbf{x}, \mathbf{y}, t) - \mathbf{v}_F(\mathbf{x}, \mathbf{y}, t)\|_{L^2(g_t)}^2 dt = \tilde{\mathcal{O}} \left\{ \frac{(1-T)^{-(4d_x+14)/(d_x+d_y+5)}}{n^{2/(d_x+d_y+5)}} \right\}$$

with probability at least  $1 - n^{-2}$ , where  $\tilde{\mathcal{O}}(\cdot)$  omits the polynomial term of  $\log n$ .

Now, we begin to analyze the convergence rate of the sampling error in Algorithm 1.

Notice that the sampling error comes from the following three aspects:

- (Approximation Error) As stated in Theorem 1,  $f_t(\mathbf{x}|\mathbf{y})$  can arbitrarily approximate  $p_{x|y}(\mathbf{x}|\mathbf{y})$  when  $t \rightarrow 1$ . In practice, we would select an early stopping time  $T < 1$ , which introduces an error between  $f_T(\mathbf{x}|\mathbf{y})$  and  $p_{x|y}(\mathbf{x}|\mathbf{y})$ .
- (Perturbation Error) Recall that  $f_T(\mathbf{x}|\mathbf{y})$  is the density of the conditional Föllmer flow  $\mathbf{Z}_t^{\mathbf{y}} = \mathbf{Z}(t, \mathbf{y})$  at  $t = T$  in (1) with certain unknown velocity field  $\mathbf{v}_F$ . With the nonparametric estimation  $\hat{\mathbf{v}}$  in (7) for  $\mathbf{v}_F$ , we can define a new continuous ODE flow

$$d\hat{\mathbf{Z}}_t^{\mathbf{y}} = \hat{\mathbf{v}}(\hat{\mathbf{Z}}_t^{\mathbf{y}}, \mathbf{y}, t) dt, \quad \hat{\mathbf{Z}}_0^{\mathbf{y}} \sim \mathcal{N}(\mathbf{0}, \mathbf{I}_{d_x}), \quad 0 \leq t \leq T, \quad (8)$$

which provides an approximation to the original continuous ODE flow (1). Denote by  $\hat{p}_t(\mathbf{x}; \mathbf{y})$  the density of  $\hat{\mathbf{Z}}_t^{\mathbf{y}}$ . Hence, a perturbation error arises between  $f_T(\mathbf{x}|\mathbf{y})$  and  $\hat{p}_T(\mathbf{x}; \mathbf{y})$ .

- (Discretization Error) The solution of ODE flow (8) does not admit a closed form. Let  $t_0 = 0$  and  $t_k = t_{k-1} + N^{-1}T$  for  $k = 1, \dots, N$ . The pseudo data  $\tilde{\mathbf{Z}}_T^{\mathbf{y}}$  obtained via Algorithm 1 satisfies the following Euler discretization of (8):

$$d\tilde{\mathbf{Z}}_t^{\mathbf{y}} = \hat{\mathbf{v}}(\tilde{\mathbf{Z}}_{t_k}^{\mathbf{y}}, \mathbf{y}, t_k) dt, \quad \tilde{\mathbf{Z}}_0^{\mathbf{y}} \sim \mathcal{N}(\mathbf{0}, \mathbf{I}_{d_x}), \quad t_k \leq t \leq t_{k+1}, \quad 0 \leq k < N. \quad (9)$$

Denote by  $\tilde{p}_t(\mathbf{x}; \mathbf{y})$  the density of  $\tilde{\mathbf{Z}}_t^{\mathbf{y}}$ . The discretization error stems from the difference between  $\hat{p}_T(\mathbf{x}; \mathbf{y})$  and  $\tilde{p}_T(\mathbf{x}; \mathbf{y})$ .

We use  $W_2(\tilde{p}_T(\mathbf{x}; \mathbf{y}), p_{x|y}(\mathbf{x}|\mathbf{y}))$ , the Wasserstein-2 distance between  $\tilde{p}_T(\mathbf{x}; \mathbf{y})$  and the target  $p_{x|y}(\mathbf{x}|\mathbf{y})$ , to characterize the sampling error of Algorithm 1. By the triangle inequality, it can be decomposed into three terms:

$$W_2(\tilde{p}_T(\mathbf{x}; \mathbf{y}), p_{x|y}(\mathbf{x}|\mathbf{y})) \leq \underbrace{W_2(f_T(\mathbf{x}|\mathbf{y}), p_{x|y}(\mathbf{x}|\mathbf{y}))}_{\text{Approximation Error}} + \underbrace{W_2(\hat{p}_T(\mathbf{x}; \mathbf{y}), f_T(\mathbf{x}|\mathbf{y}))}_{\text{Perturbation Error}}$$

$$+ \underbrace{W_2(\tilde{p}_T(\mathbf{x}; \mathbf{y}), \hat{p}_T(\mathbf{x}|\mathbf{y}))}_{\text{Discretization Error}}.$$

Theorem 1 presents the convergence rate of Approximation Error, while Propositions 3 and 4 state the convergence rates of Perturbation Error and Discretization Error, respectively. The proofs of Propositions 3 and 4 are given in Sections E and F of the supplementary material, respectively.

**Proposition 3** *Let Assumptions 1–3 hold. Choose  $\hat{\mathbf{v}}(\mathbf{x}, \mathbf{y}, t)$  as in Proposition 2. For any fixed  $(d_x, d_y)$ , if  $1 - T \gg n^{-1/(2d_x+7)}$ , it holds that*

$$\int W_2^2(f_T(\mathbf{x}|\mathbf{y}), \hat{p}_T(\mathbf{x}; \mathbf{y}))p_y(\mathbf{y}) \, d\mathbf{y} = \tilde{\mathcal{O}} \left\{ \frac{e^{20d_x^{5/2}(1-T)^{-2}}}{(1-T)^{(4d_x+14)/(d_x+d_y+5)}\eta^{2/(d_x+d_y+5)}} \right\}$$

with probability at least  $1 - n^{-2}$ , where  $\tilde{\mathcal{O}}(\cdot)$  omits the polynomial term of  $\log n$ .

**Proposition 4** *Let Assumptions 1–3 hold. Choose  $\hat{\mathbf{v}}(\mathbf{x}, \mathbf{y}, t)$  as in Proposition 2. For any fixed  $(d_x, d_y)$ , if  $1 - T \gg n^{-1/(2d_x+7)}$ , it then holds that*

$$\sup_{\mathbf{y} \in [0, B]^{d_y}} W_2^2(\hat{p}_T(\mathbf{x}; \mathbf{y}), \tilde{p}_T(\mathbf{x}; \mathbf{y})) = \tilde{\mathcal{O}} \left\{ \frac{e^{20d_x^{5/2}(1-T)^{-2}}}{(1-T)^6 N^2} \right\},$$

where  $\tilde{\mathcal{O}}(\cdot)$  omits the polynomial term of  $\log n$ .

For any fixed  $(d_x, d_y)$ , by Theorem 1, Propositions 3 and 4, it holds with probability  $1 - n^{-2}$  that

$$\begin{aligned} & \int W_2^2(\tilde{p}_T(\mathbf{x}; \mathbf{y}), p_{x|\mathbf{y}}(\mathbf{x}|\mathbf{y}))p_y(\mathbf{y}) \, d\mathbf{y} \\ & \leq 3 \int W_2^2(f_T(\mathbf{x}|\mathbf{y}), p_{x|\mathbf{y}}(\mathbf{x}|\mathbf{y}))p_y(\mathbf{y}) \, d\mathbf{y} + 3 \int W_2^2(\hat{p}_T(\mathbf{x}; \mathbf{y}), f_T(\mathbf{x}|\mathbf{y}))p_y(\mathbf{y}) \, d\mathbf{y} \\ & \quad + 3 \int W_2^2(\tilde{p}_T(\mathbf{x}; \mathbf{y}), \hat{p}_T(\mathbf{x}|\mathbf{y}))p_y(\mathbf{y}) \, d\mathbf{y} \\ & = \underbrace{\mathcal{O}(1-T)}_{\text{Error I}} + \underbrace{\tilde{\mathcal{O}} \left\{ \frac{e^{20d_x^{5/2}(1-T)^{-2}}}{(1-T)^{(4d_x+14)/(d_x+d_y+5)}\eta^{2/(d_x+d_y+5)}} \right\}}_{\text{Error II}} + \underbrace{\tilde{\mathcal{O}} \left\{ \frac{e^{20d_x^{5/2}(1-T)^{-2}}}{(1-T)^6 N^2} \right\}}_{\text{Error III}} \end{aligned}$$

provided that  $1 - T \gg n^{-1/(2d_x+7)}$ , where  $\tilde{\mathcal{O}}(\cdot)$  omits the polynomial term of  $\log n$ . Set

$$T = 1 - C(\log n)^{-1/2}, \quad N \sim n^\xi, \quad (10)$$

with  $C > 10^{1/2}d_x^{5/4}(d_x + d_y + 5)^{1/2}$  and  $\xi \geq 1/(d_x + d_y + 5)$ . Then, for any given  $(d_x, d_y)$ , we have Error II + Error III =  $o_p\{(\log n)^{-1/2}\}$ , which is negligible in comparison to Error I =  $\mathcal{O}\{(\log n)^{-1/2}\}$ . This indicates that the sampling error of Algorithm 1 is mainly dominated by the error that using  $f_T(\mathbf{x}|\mathbf{y})$  to approximate  $p_{x|y}(\mathbf{x}|\mathbf{y})$ .

Theorem 2 summarizes our above discussion, which establishes the validity of Algorithm 1 in sampling data from  $p_{x|y}(\mathbf{x}|\mathbf{y})$ , and also highlights the effectiveness of the conditional Föllmer flow in sampling from the target conditional density.

**Theorem 2** *Let Assumptions 1–3 hold. Suppose we have i.i.d. samples  $\{(\mathbf{X}_i, \mathbf{Y}_i)\}_{i=1}^n \sim p_{x,y}(\mathbf{x}, \mathbf{y})$ . We choose the hypothesis network class  $\text{FNN} = \text{FNN}(L, M, J, K, \kappa, \gamma_1, \gamma_2, \gamma_3)$  as specified in Proposition 2 and then use  $\hat{\mathbf{v}}(\mathbf{x}, \mathbf{y}, t)$  in (7) to estimate the true velocity field  $\mathbf{v}_F(\mathbf{x}, \mathbf{y}, t)$ . For any fixed  $(d_x, d_y)$ , when implementing Algorithm 1 for sampling pseudo data with  $(T, N)$  satisfying (10), we have*

$$\int W_2^2(\tilde{p}_T(\mathbf{x}; \mathbf{y}), p_{x|y}(\mathbf{x}|\mathbf{y}))p_y(\mathbf{y}) \, d\mathbf{y} \rightarrow 0$$

*in probability as  $n \rightarrow \infty$ .*

## 5 Numerical Studies

In this section, we carry out numerical experiments to assess the performance of our proposed method. We conduct our method on both synthetic and real datasets. In simulation studies, we compare our ODE-based method with the SDE-based method and two popular conditional density estimation methods: Nearest Neighbor Conditional Density Estimation (NNKCDE) (Dalmasso et al., 2020) and Flexible Conditional Density

Estimator (FlexCode) (Izbicki and Lee, 2017). The experiments involving deep learning are computed on an NVIDIA 4xA800 device. Our code is available at the GitHub repository: <https://github.com/burning489/ConditionalFollmerFlow>. Our simulation studies demonstrate that though our proposed method and the SDE-based method do not directly provide the conditional density estimation, the samples generated by these two methods can be effectively utilized to estimate the conditional density and related statistical quantities, such as the conditional mean and the conditional standard deviation. See Sections 5.1 and 5.2 for details. We use two real data analyses in Sections 5.3 and 5.4 to demonstrate the advantages of the ODE-based method beyond the SDE-based method.

## 5.1 Simulation Study I

We consider several two-dimensional distributions with shapes of 4 squares, checkerboard, pinwheel, rings and Swiss roll, respectively. We display scatter plots of 5000 samples drawn from these target distributions in the first column of Figure 1. For these distributions, we take the  $x$ -axis variable as  $X$  and the  $y$ -axis variable as  $Y$ . We target on generating samples from conditional density  $p_{x|y}(x|y)$ . To do this, we first draw 5000 samples from target distributions for training, and denote by  $\mathcal{Y}$  the set including all the 5000  $y$ -axis variables of the samples shown in the first column of Figure 1.

For our proposed ODE-based method, we first train the velocity estimator by velocity matching on the training set, and then for each given  $y_i \in \mathcal{Y}$  we generate an  $\hat{X}_i$  by Algorithm 1 based on the trained velocity estimator. We display the scatter plots of the generated 5000 pairs of  $(\hat{X}_i, y_i)$  in the second column of Figure 1. For comparison, we also look into the SDE-based method for generating samples. As shown in (S.1) of the supplementary material, the ODE (1) related to our proposed method has a unique SDE

interpretation, where its time reversal shares the same marginal distribution as the ODE (1). Hence, we can also use the SDE-based method to generate samples from  $p_{x|y}(x|y)$ . More specifically, the trained velocity estimator from the ODE-based method can be used to compute the drift term of the time reversal of the associated SDE, and we can then generate samples by running the time reversal of the SDE using Euler-Maruyama method. Same as what we did in the ODE-based method, we display 5000 pairs of  $(\hat{X}_i, y_i)$  generated by SDE-based method in the third column of Figure 1. For NNKCDE and FlexCode, we first fit the conditional density on the training set, and then for each given  $y_i \in \mathcal{Y}$  we generate an  $\hat{X}_i$  from the estimated conditional density. The fourth and fifth columns of Figure 1 display the scatter plots of 5000 pairs of  $(\hat{X}_i, y_i)$  generated by NNKCDE and FlexCode. Figure 1 demonstrates that ODE-based method, SDE-based method and NNKCDE generate samples close to targets, while FlexCode is less stable for cases such as checkerboard and Swiss roll. Different from NNKCDE and FlexCode, the ODE-based method and the SDE-based method directly generate samples from the conditional density  $p_{x|y}(x|y)$  without estimating it. We are also interested in investigating the performance of the ODE-based method and the SDE-based method in estimating  $p_{x|y}(x|y)$ . To do this, for each  $y_i \in \mathcal{Y}$ , we first generate 200 samples  $\{\hat{X}_i^{(j)}\}_{j=1}^{200}$  associated with  $y_i$  by the ODE-based method (the SDE-based method), and then use kernel density estimation with Gaussian kernels to empirically estimate  $p_{x|y}(x|y_i)$ , denoted by  $\hat{p}_{x|y}(x|y_i)$ . For each  $y_i \in \mathcal{Y}$ , we compute the total variation distance between  $p_{x|y}(x|y_i)$  and  $\hat{p}_{x|y}(x|y_i)$ . We also consider the total variation distances between  $p_{x|y}(x|y_i)$  and its estimates based on NNKCDE and FlexCode, respectively. Table 1 reports the sample average (AVE) and standard deviation (STD) of 5000 obtained total variation distances based on different methods, which also includes the average sampling GPU machine time (GPU-T) of the ODE-based method and the SDE-based

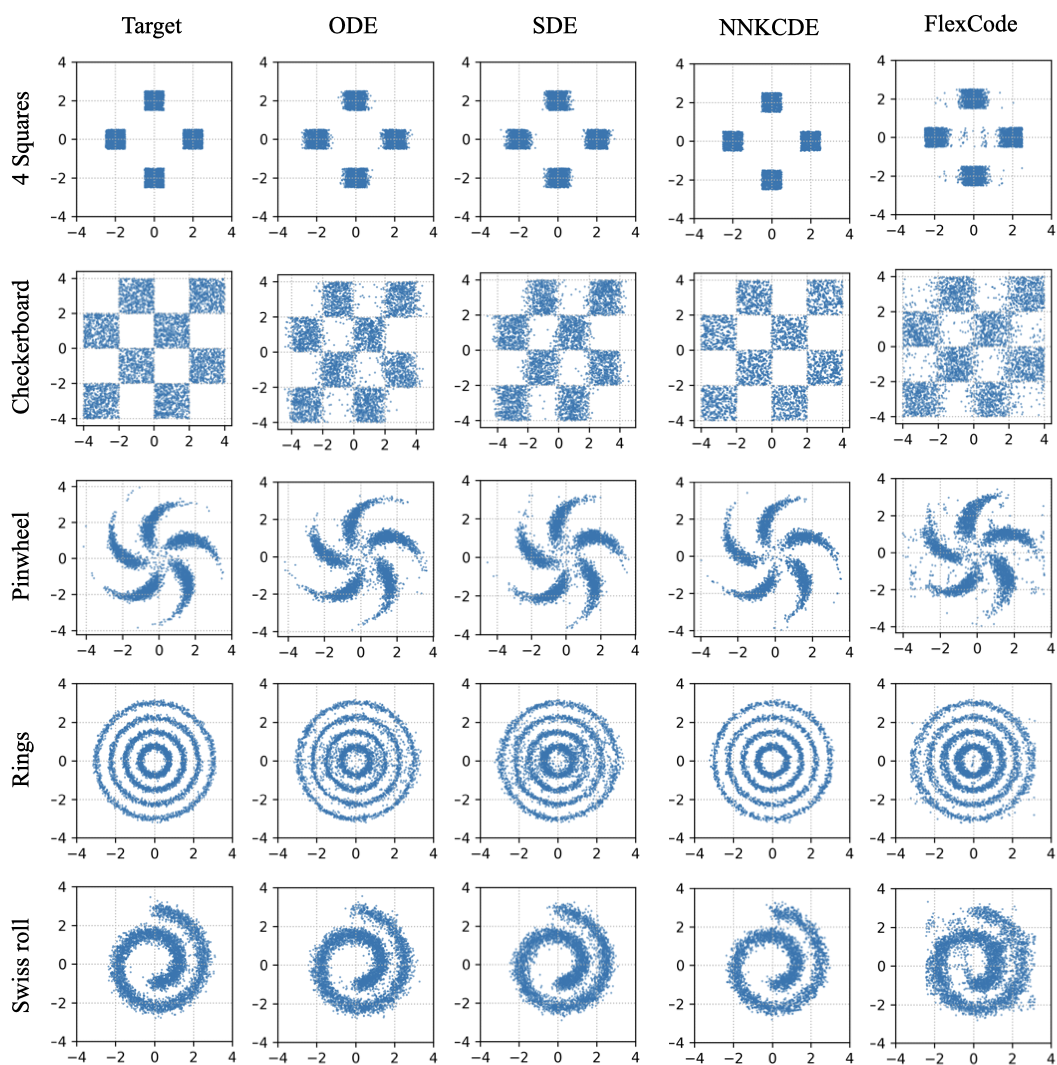


Figure 1: Scatter plots of joint distributions generated by different methods.

method. The sampling time of NNKCDE and FlexCode is omitted as they work on CPU. We can learn from Table 1 that (i) the ODE-based method and the SDE-based method uniformly outperform NNKCDE and FlexCode, (ii) the ODE-based method performs quite similar to the SDE-based method, and (iii) the ODE-based method is slightly faster than the SDE-based method.

Table 1: The sample average and standard deviation of 5000 obtained total variation distances based on different methods in simulation study I, and the average sampling GPU machine time of the ODE-based method and the SDE-based method.

	ODE			SDE			NNKCDE		FlexCode	
	AVE	STD	GPU-T	AVE	STD	GPU-T	AVE	STD	AVE	STD
4 Squares	0.134	0.091	1.005	0.126	0.099	1.201	0.825	0.021	0.448	0.067
Checkerboard	0.234	0.118	1.036	0.240	0.114	1.228	0.916	0.009	0.284	0.029
Pinwheel	0.255	0.116	1.056	0.256	0.113	1.215	0.908	0.012	0.543	0.068
Rings	0.082	0.041	0.973	0.093	0.039	1.203	0.911	0.012	0.519	0.074
Swiss roll	0.186	0.083	0.991	0.116	0.052	1.259	0.897	0.009	0.427	0.072

## 5.2 Simulation Study II

In this section, we investigate the performance of the ODE-based method and the SDE-based method in estimating the conditional mean  $\mathbb{E}(X|\mathbf{Y})$  and the conditional standard deviation  $\text{std}(X|\mathbf{Y})$  via the following three models.

(M1) A nonlinear model with an additive error term:

$$X = Y_1^2 + \exp(Y_2 + 0.25Y_3) + \cos(Y_4 + Y_5) + \varepsilon$$

with  $\varepsilon \sim \mathcal{N}(0, 1)$  and  $\mathbf{Y} = (Y_1, \dots, Y_5)^T \sim \mathcal{N}(\mathbf{0}, \mathbf{I}_5)$ .

(M2) A model with an additive error term whose variance depends on the predictors:

$$X = Y_1^2 + \exp(Y_2 + 0.25Y_3) + Y_4 - Y_5 + (0.5 + 0.5Y_2^2 + 0.5Y_5^2)\varepsilon$$

with  $\varepsilon \sim \mathcal{N}(0, 1)$  and  $\mathbf{Y} = (Y_1, \dots, Y_5)^T \sim \mathcal{N}(\mathbf{0}, \mathbf{I}_5)$ .

(M3) A mixture of two normal distributions:

$$X = \mathbb{I}_{\{U \leq 0.5\}} Z_1 + \mathbb{I}_{\{U > 0.5\}} Z_2$$

with  $U \sim \mathcal{U}(0, 1)$ ,  $Y \sim \mathcal{N}(0, 1)$ ,  $Z_1 \sim \mathcal{N}(-Y, 0.25^2)$  and  $Z_2 \sim \mathcal{N}(Y, 0.25^2)$ .

For each model, we first prepare a training set of  $(X, \mathbf{Y})$  with size 5000 drawn from this model, and let  $\mathcal{Y}$  be a set including 5000 additional samples of  $\mathbf{Y}$  generated from the associated marginal distribution of this model. For the ODE-based method and the SDE-based method, we only have access to generated samples. For each  $\mathbf{y}_i \in \mathcal{Y}$ , we generate 500 samples  $\{\hat{X}_i^{(j)}\}_{j=1}^{200}$  associated with  $\mathbf{y}_i$  by the ODE-based method (the SDE-based method), and then estimate  $\mathbb{E}(X | \mathbf{Y} = \mathbf{y}_i)$  and  $\text{std}(X | \mathbf{Y} = \mathbf{y}_i)$  by, respectively, the sample mean and sample standard deviation of  $\{\hat{X}_i^{(j)}\}_{j=1}^{200}$ . For NNKCDE and FlexCode, the estimated conditional density  $\hat{p}_{x|y}(X | \mathbf{Y} = \mathbf{y}_i)$  is already available after fitting, and we can then estimate  $\mathbb{E}(X | \mathbf{Y} = \mathbf{y}_i)$  and  $\text{std}(X | \mathbf{Y} = \mathbf{y}_i)$  by

$$\begin{aligned} \hat{\mathbb{E}}(X | \mathbf{Y} = \mathbf{y}_i) &= \int x \hat{p}_{x|y}(x | \mathbf{Y} = \mathbf{y}_i) dx, \\ \widehat{\text{std}}(X | \mathbf{Y} = \mathbf{y}_i) &= \sqrt{\int \{x - \hat{\mathbb{E}}(x | \mathbf{Y} = \mathbf{y}_i)\}^2 \hat{p}_{x|y}(x | \mathbf{Y} = \mathbf{y}_i) dx}. \end{aligned}$$

For the given estimates  $\hat{\mathbb{E}}(X | \mathbf{Y} = \mathbf{y}_i)$  and  $\widehat{\text{std}}(X | \mathbf{Y} = \mathbf{y}_i)$ , we compute

$$\begin{aligned} \text{MSE}_1 &= \frac{1}{5000} \sum_{i=1}^{5000} |\hat{\mathbb{E}}(X | \mathbf{Y} = \mathbf{y}_i) - \mathbb{E}(X | \mathbf{Y} = \mathbf{y}_i)|^2, \\ \text{MSE}_2 &= \frac{1}{5000} \sum_{i=1}^{5000} |\widehat{\text{std}}(X | \mathbf{Y} = \mathbf{y}_i) - \text{std}(X | \mathbf{Y} = \mathbf{y}_i)|^2. \end{aligned}$$

We report  $\text{MSE}_1$  and  $\text{MSE}_2$  for different methods in Table 2, along with the sampling GPU machine time (GPU-T) of the ODE-based method and the SDE-based method. The sampling time of NNKCDE and FlexCode is omitted as they work on CPU. Table 2 shows that (i) in terms of estimation error, the ODE-based and the SDE-based method uniformly outperform NNKCDE and FlexCode, (ii) the ODE-based method performs better than the SDE-based method, and (iii) the ODE-based method is slightly faster than the SDE-based method.

Table 2:  $\text{MSE}_1$  and  $\text{MSE}_2$  for different methods, and the average sampling GPU machine time of the ODE-based method and the SDE-based method.

	ODE			SDE			NNKCDE		FlexCode	
	$\text{MSE}_1$	$\text{MSE}_2$	GPU-T	$\text{MSE}_1$	$\text{MSE}_2$	GPU-T	$\text{MSE}_1$	$\text{MSE}_2$	$\text{MSE}_1$	$\text{MSE}_2$
M1	0.065	0.007	0.714	0.110	0.011	0.929	0.991	0.585	0.594	0.958
M2	0.327	0.007	0.143	0.783	0.242	0.929	1.232	0.586	0.729	0.865
M3	0.009	0.002	0.762	0.012	0.003	0.904	0.016	0.008	0.045	0.038

### 5.3 Real Data Analysis I

The wine quality dataset is available at UCI machine learning repository (Newman et al., 1998), which is a combination of two sub-datasets, related to red and white vinho verde wine samples, from the north of Portugal. The classes are ordered and not balanced (e.g. there are much more normal wines than excellent or poor ones). This dataset contains 11 continuous features: fixed acidity, volatile acidity, citric acid, residual sugar, chlorides, free sulfur dioxide, total sulfur dioxide, density, pH, sulphates, and alcohol. The main purpose of this dataset is to rank the wine quality (discrete score between 0 and 10) based

on the chemical analysis measurements (the 11 features mentioned above). The total sample size of this dataset is 6497. Denote by  $X$  the score of wine quality, and by  $\mathbf{Y}$  the vector of the chemical analysis measurements. We randomly use 90% of it for training and the rest 10% for testing. Denote by  $\mathcal{Y}$  the set including all the feature vectors of the testing set.

We compare the prediction intervals of wine quality for given features  $\mathbf{Y}$  constructed by the ODE-based method and the SDE-based method. For our proposed ODE-based method, we first train the velocity estimator on the training set, and then for each  $\mathbf{y}_i \in \mathcal{Y}$  we generate  $N_*$  predictions  $\{\hat{X}_i^{(j)}\}_{j=1}^{N_*}$  with  $N_* = 200$  associated with  $\mathbf{y}_i$  by Algorithm 1. Let  $\bar{X}_i$  and  $\hat{s}_i$  be the sample mean and sample standard deviation of  $\{\hat{X}_i^{(j)}\}_{j=1}^{200}$ , respectively. For each given  $i$ , we can approximate the distribution of the ancillary statistic  $(\hat{s}_i \sqrt{1 + N_*^{-1}})^{-1}(X - \bar{X}_i)$  by the Student's t-distribution with  $N_* - 1$  degrees of freedom. Let  $z_{1-\alpha/2}$  be the  $(1 - \alpha/2)$ -quantile of the Student's t-distribution with  $N_* - 1$  degrees of freedom. Then

$$\mathcal{C}_{i,1-\alpha}(\mathbf{y}_i) = \{x : \bar{X}_i - z_{1-\alpha/2} \hat{s}_i \sqrt{1 + N_*^{-1}} \leq x \leq \bar{X}_i + z_{1-\alpha/2} \hat{s}_i \sqrt{1 + N_*^{-1}}\}$$

provides an approximate of the  $100(1 - \alpha)\%$  prediction interval of  $X$  when  $\mathbf{Y} = \mathbf{y}_i$ . We compute

$$\text{CR}_{1-\alpha} = \frac{1}{650} \sum_{i=1}^{650} \mathbb{I}\{X_i \in \mathcal{C}_{i,1-\alpha}(\mathbf{Y}_i)\}$$

with the samples  $(X_i, \mathbf{Y}_i)$  from the testing set. For each given  $\alpha \in (0, 1)$ , the closer  $\text{CR}_{1-\alpha}$  is to  $1 - \alpha$ , the more accurate our constructed prediction interval is. Similar to what we did in Section 5.1, we can use the trained velocity estimator to estimate the drift term of the time reversal of the associated SDE involved in the SDE-based method, and then also generate  $N_*$  samples  $\{\hat{X}_i^{(j)}\}_{j=1}^{N_*}$  with  $N_* = 200$  associated with  $\mathbf{y}_i \in \mathcal{Y}$  by running the backward SDE using Euler-Maruyama method. Then we can compute the associated  $\text{CR}_{1-\alpha}$  for the SDE-based method in the same manner as that for the ODE-based method. With selecting  $\alpha = 10\%$ ,  $5\%$  and  $1\%$ , Table 3 reports the associated  $\text{CR}_{1-\alpha}$  for the ODE-based method

and the SDE-based method, which shows that the prediction intervals constructed by the ODE-based method are more accurate than those constructed by the SDE-based method.

Table 3: Associated  $CR_{1-\alpha}$  for the ODE-based method and the SDE-based method with different selections of  $\alpha$ .

	$\alpha = 10\%$	$\alpha = 5\%$	$\alpha = 1\%$
ODE	89.85%	94.00%	98.77%
SDE	86.92%	92.15%	98.00%

## 5.4 Real Data Analysis II

We apply our proposed ODE-based method to high-dimensional conditional generation problems. We work on the MNIST handwritten digits dataset, which contains 60000 images for training (LeCun, 1998). Each image is represented as a  $28 \times 28$  matrix with gray color intensity from 0 to 1, and paired with a label in  $\{0, 1, \dots, 9\}$  indicating the corresponding digit. We flatten the  $28 \times 28$  pixel matrix into a vector to represent  $\mathbf{X} \in \mathbb{R}^{784}$ . We perform on two tasks: generating images by classes and reconstructing missing parts of images from partial observations.

### 5.4.1 Class Conditional Generation

We target on generating images of handwritten digits given labels from  $\{0, 1, \dots, 9\}$ . In this problem, the condition is a categorical variable representing one of the ten digits, and we follow the common practice to use one-hot vectors to represent  $\mathbf{Y}$  with each label being represented by a binary vector in  $\mathbb{R}^{10}$  where only one element is hot (set to 1) and all others are cold (set to 0).

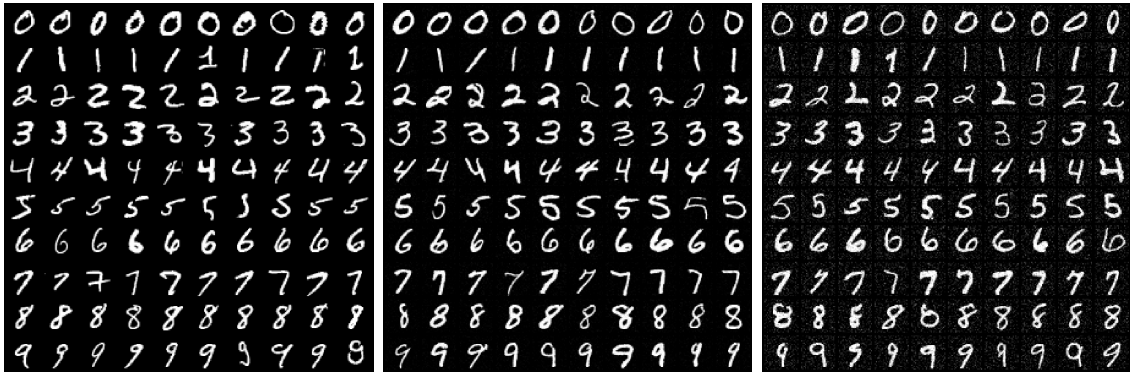


Figure 2: MNIST: real images (left panel) and generated images given labels by the ODE-based method (middle panel) and by the SDE-based method (right panel).

For our proposed ODE-based method, we train the velocity estimator by velocity matching on the training set, and then generate synthetic images by Algorithm 1. Figure 2 displays the real images randomly drawn from the training set (left panel) and synthetic images by our proposed ODE-based method (middle panel). Each row represents 10 images from the same label; and each column, from top to bottom, represents labels ranging from 0 to 9. We also compare our proposed ODE-based method with the SDE-based method. The right panel of Figure 2 displays the synthetic images by the SDE-based method. Generated images are similar to the real images and have differences across each row, indicating the random variations in the generating process, ensuring the richness of the generating capability.

In image generation tasks, the Fréchet inception distance (FID) is a common choice to measure difference between synthetic and real images (Heusel et al., 2017). To compute FID, we need to first use a pre-trained Inception network to extract the associated feature representations of real images  $\mathbf{X}$ 's and synthetic images  $\hat{\mathbf{X}}$ 's, respectively. Denote by  $\boldsymbol{\mu}_r$  and  $\boldsymbol{\Sigma}_r$  the sample mean and sample covariance matrix of the features of all real images  $\mathbf{X}$ 's from the training set, respectively. Parallely, let  $\boldsymbol{\mu}_g$  and  $\boldsymbol{\Sigma}_g$  be, respectively, the sample mean

and sample covariance matrix of features of the synthetic images  $\hat{\mathbf{X}}$ 's. The FID between synthetic and real images is defined as  $|\boldsymbol{\mu}_r - \boldsymbol{\mu}_g|_2^2 + \text{tr}\{\boldsymbol{\Sigma}_r + \boldsymbol{\Sigma}_g - 2(\boldsymbol{\Sigma}_r \boldsymbol{\Sigma}_g)^{1/2}\}$ . For the ODE-based method (SDE-based method), we generate 5000 images for each digit and compute the FID between the training set and the overall 50000 synthetic images. The FIDs of the ODE-based method and the SDE-based method are 1.87 and 12.83, respectively, indicating that the images generated by the ODE-based method are closer to the real images than those generated by the SDE-based method.

#### 5.4.2 Image Inpainting

We target on reconstructing an image when part of it is covered. In this problem,  $\mathbf{X} \in \mathbb{R}^{784}$  is the original intact image and  $\mathbf{Y}$  is the associated uncovered part of  $\mathbf{X}$ . Our goal is to reconstruct the image  $\mathbf{X}$  when just its partial observation  $\mathbf{Y}$  is given.

For each prescribed constant  $\delta \in \{3/4, 1/2, 1/4\}$ , we first prepare a new training set for inpainting by using the same images  $\mathbf{X}$ 's as those from the MNIST training set, and then manually cover  $\delta$  part of each original image  $\mathbf{X}$  to obtain the associated condition  $\mathbf{Y}$ . The MNIST dataset also contains a testing set with size 10000. We randomly draw 10 image  $\{\mathbf{X}_i\}_{i=1}^{10}$  in the testing set, with corresponding digit ranging from 0 to 9, and display them in the first column of each panel in Figure 3. The second column of each panel in Figure 3 displays the associated  $\{\mathbf{Y}_i\}_{i=1}^{10}$  of  $\{\mathbf{X}_i\}_{i=1}^{10}$ , with the covered parts shaded in red.

For our proposed ODE-based method, we first train the velocity estimator on the new training set, and then for each  $i = 1, \dots, 10$ , we generate 5 samples  $\{\hat{\mathbf{X}}_i^{(j)}\}_{j=1}^5$  associated with  $\mathbf{Y}_i$  by Algorithm 1. These 5 samples are displayed from the third to the seventh column of the top 3 panels in Figure 3. We also compare our proposed ODE-based method with the SDE-based method. The results reconstructed by the SDE-based method are displayed from the third to the seventh columns of the bottom 3 panels in Figure 3.

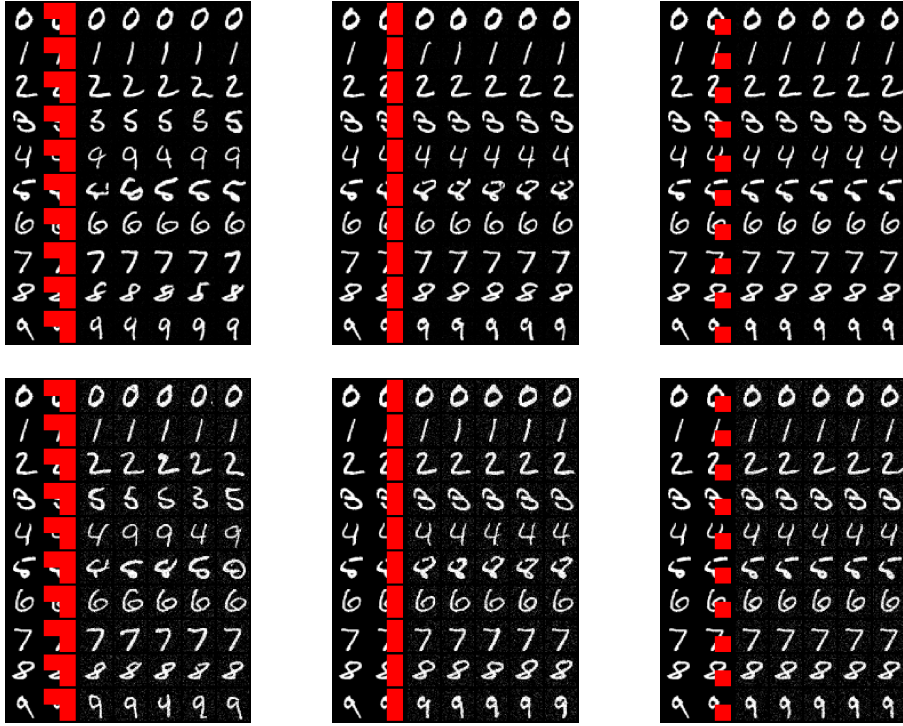


Figure 3: Original testing images  $\{\mathbf{X}_i\}_{i=1}^{10}$  (first columns), associated conditions  $\{\mathbf{Y}_i\}_{i=1}^{10}$  (second columns, with the covered parts shaded in red), and reconstructed images  $\{\mathbf{X}_i^{(j)}\}_{j=1}^5$  with  $i = 1, \dots, 10$  by the ODE-based method (top, third to seventh columns) and by the SDE-based method (bottom, third to seventh columns).

The reconstructed results show that (i) if 3/4 of the images is missing, the ODE-based method and the SDE-based method successfully reconstruct images for most digits and fail for some difficult cases, which confuse ‘3’ with ‘8’, ‘4’ with ‘9’, and ‘5’ with ‘8’, (ii) if 1/2 of the images is missing, the ODE-based method and the SDE-based method successfully reconstruct images for most digits except for ‘5’, which confuse it with ‘8’, and (iii) if 1/4 of the images is missing, the ODE-based method and the SDE-based method are able to reconstruct all images correctly.

We also compute the FID for the ODE-based method and the SDE-based method. For each prescribed constant  $\delta \in \{3/4, 1/2, 1/4\}$ , we generate a reconstructed image  $\hat{\mathbf{X}}$  for each original image  $\mathbf{X}$  in the training set by the ODE-based method (SDE-based method). Same as what we did in Section 5.4.1, we compute the FID between the 60000 original images and 60000 reconstructed images, and report the results in Table 4, which show that (i) the ODE-based method and the SDE-based method can reconstruct the images more accurately when there are fewer missing parts, and (ii) the images reconstructed by the ODE-based method are uniformly closer to the original images than those reconstructed by the SDE-based method.

Table 4: FIDs for the ODE-based method and the SDE-based method when 3/4, 1/2 and 1/4 of the images are covered.

	$\delta = 3/4$	$\delta = 1/2$	$\delta = 1/4$
ODE	1.85	1.83	1.75
SDE	12.91	12.79	12.69

## 6 Discussion

In this paper, we introduce an ODE-based generative method for sampling data from conditional distributions. Several issues deserve further investigation. First, we assume the Lipschitz property of  $\mathbf{v}_F(\mathbf{x}, \mathbf{y}, t)$  with respect to the conditional variable  $\mathbf{y}$  in Assumption 3, which is crucial for the effective construction of a neural network  $\hat{\mathbf{v}}(\mathbf{x}, \mathbf{y}, t)$  to approximate  $\mathbf{v}_F(\mathbf{x}, \mathbf{y}, t)$ . Thus, exploring the possibility of obtaining such property under some milder conditions becomes a topic worthy of in-depth scrutiny. Additionally, we have demonstrated the regularity of flow map  $\mathbf{F}_t(\cdot, \mathbf{y})$ ,  $t \in [0, T]$ , and explored the use of an additional neural network to facilitate one-step generation in Section 3, which can be regarded as directly fitting  $\mathbf{F}_T(\cdot, \mathbf{y})$ . In fact, we can also train a time-dependent neural network to approximate  $\mathbf{F}_t(\cdot, \mathbf{y})$  for all  $t \in [0, T]$ , i.e., predicting the trajectories or characteristic curves of the conditional Föllmer flow. Such research will aid in comprehending the mechanisms of generative models, laying foundation for more efficient and stable sampling methods. We plan to thoroughly investigate the aforementioned one-step generator and characteristic curve estimator in the future.

Reflecting on the methods we have employed and the problems we have tackled, it can be discovered that our conditional sampling methodology not only could be applied in modern generative learning settings, but also holds great potential in addressing traditional statistical predictive tasks. For instance, in various regression scenarios where estimating statistical quantities like conditional expectations is crucial, efficient conditional sampling would enable effective recovery of these quantities, such as through computing sample means. Furthermore, the conditional sampler contains rich information about the conditional distribution, enabling us to surpass traditional regression models by construct-

ing more precise prediction intervals instead of relying solely on a single point estimator, thereby providing more reliable decision-making foundations. Our numerical experiments with real datasets have fully demonstrated these advantages of the conditional Föllmer flow and further confirmed its capability to handle various types of responses and covariates, thus providing a generalized framework for solving predictive problems.

## References

- Albergo, M. S., Boffi, N. M. and Vanden-Eijnden, E. (2023a). Stochastic interpolants: A unifying framework for flows and diffusions, *arXiv:2303.08797*.
- Albergo, M. S., Goldstein, M., Boffi, N. M., Ranganath, R. and Vanden-Eijnden, E. (2023b). Stochastic interpolants with data-dependent couplings, *arXiv preprint arXiv:2310.03725*.
- Albergo, M. S. and Vanden-Eijnden, E. (2023). Building normalizing flows with stochastic interpolants, *The Eleventh International Conference on Learning Representations*.
- Austin, J., Johnson, D. D., Ho, J., Tarlow, D. and Van Den Berg, R. (2021). Structured denoising diffusion models in discrete state-spaces, *Advances in Neural Information Processing Systems* **34**: 17981–17993.
- Benton, J., De Bortoli, V., Doucet, A. and Deligiannidis, G. (2023). Linear convergence bounds for diffusion models via stochastic localization, *arXiv:2308.03686*.
- Butcher, J. C. (2016). *Numerical methods for ordinary differential equations*, John Wiley & Sons.

- Chen, H., Lee, H. and Lu, J. (2023a). Improved analysis of score-based generative modeling: User-friendly bounds under minimal smoothness assumptions, *International Conference on Machine Learning*, PMLR, pp. 4735–4763.
- Chen, M., Huang, K., Zhao, T. and Wang, M. (2023b). Score approximation, estimation and distribution recovery of diffusion models on low-dimensional data, *International Conference on Machine Learning*, PMLR, pp. 4672–4712.
- Chen, S., Chewi, S., Lee, H., Li, Y., Lu, J. and Salim, A. (2024). The probability flow ode is provably fast, *Advances in Neural Information Processing Systems* **36**.
- Chen, S., Chewi, S., Li, J., Li, Y., Salim, A. and Zhang, A. R. (2023c). Sampling is as easy as learning the score: theory for diffusion models with minimal data assumptions, *International Conference on Learning Representations*.
- Chen, S., Daras, G. and Dimakis, A. (2023d). Restoration-degradation beyond linear diffusions: A non-asymptotic analysis for ddim-type samplers, *International Conference on Machine Learning*, PMLR, pp. 4462–4484.
- Chen, X. and Linton, O. (2001). The estimation of conditional densities, *In Asymptotics in Statistics and Probability, Festschrift for George Roussas, ed. M.L. Puri.* .
- Dalmaso, N., Pospisil, T., Lee, A. B., Izbicki, R., Freeman, P. E. and Malz, A. I. (2020). Conditional density estimation tools in python and r with applications to photometric redshifts and likelihood-free cosmological inference, *Astronomy and Computing* **30**: 100362.
- De Bortoli, V. (2022). Convergence of denoising diffusion models under the manifold hypothesis, *Transactions on Machine Learning Research* .

- Esser, P., Kulal, S., Blattmann, A., Entezari, R., Müller, J., Saini, H., Levi, Y., Lorenz, D., Sauer, A., Boesel, F. et al. (2024). Scaling rectified flow transformers for high-resolution image synthesis, *arXiv preprint arXiv:2403.03206*.
- Fan, J., Yao, Q. and Tong, H. (1996). Estimation of conditional densities and sensitivity measures in nonlinear dynamical systems, *Biometrika* **83**(1): 189–206.
- Fan, J. and Yim, T. H. (2004). A crossvalidation method for estimating conditional densities, *Biometrika* **91**(4): 819–834.
- Gao, Y., Huang, J. and Jiao, Y. (2023). Gaussian interpolation flows, *arXiv:2311.11475*.
- Goodfellow, I. J., Pouget-Abadie, J., Mirza, M., Xu, B., Warde-Farley, D., Ozair, S., Courville, A. and Bengio, Y. (2014). Generative adversarial nets, *Proceedings of the 27th International Conference on Neural Information Processing Systems - Volume 2*, p. 2672–2680.
- Hall, P. and Yao, Q. (2005). Approximating conditional distribution functions using dimension reduction, *Annals of Statistics* **33**(3): 1404–1421.
- Heusel, M., Ramsauer, H., Unterthiner, T., Nessler, B. and Hochreiter, S. (2017). Gans trained by a two time-scale update rule converge to a local nash equilibrium, *Proceedings of the 31st International Conference on Neural Information Processing Systems*, pp. 6629–6640.
- Ho, J., Jain, A. and Abbeel, P. (2020). Denoising diffusion probabilistic models, *Proceedings of the 34th International Conference on Neural Information Processing Systems*, pp. 6840–6851.

- Huang, D., Huang, J., Li, T. and Shen, G. (2023). Conditional stochastic interpolation for generative learning, *arXiv:2312.05579*.
- Hyndman, R. J., Bashtannyk, D. M. and Grunwald, G. K. (1996). Estimating and visualizing conditional densities, *Journal of Computational and Graphical Statistics* **5**(4): 315–336.
- Izbicki, R. and Lee, A. B. (2016). Nonparametric conditional density estimation in a high-dimensional regression setting, *Journal of Computational and Graphical Statistics* **25**(4): 1297–1316.
- Izbicki, R. and Lee, A. B. (2017). Converting high-dimensional regression to high-dimensional conditional density estimation, *Electronic Journal of Statistics* **11**(2): 2800–2831.
- Karras, T., Laine, S. and Aila, T. (2019). A style-based generator architecture for generative adversarial networks, *Proceedings of the IEEE/CVF Conference on Computer Vision and Pattern Recognition*, pp. 4401–4410.
- LeCun, Y. (1998). The mnist database of handwritten digits, <http://yann.lecun.com/exdb/mnist/>.
- Lee, H., Lu, J. and Tan, Y. (2023). Convergence of score-based generative modeling for general data distributions, *International Conference on Algorithmic Learning Theory*, PMLR, pp. 946–985.
- Liu, X., Gong, C. and Liu, Q. (2023a). Flow straight and fast: Learning to generate and transfer data with rectified flow, *International conference on learning representations (ICLR)*.

- Liu, X., Wu, L., Zhang, S., Gong, C., Ping, W. and Liu, Q. (2023b). Flowgrad: Controlling the output of generative odes with gradients, *Proceedings of the IEEE/CVF Conference on Computer Vision and Pattern Recognition*, pp. 24335–24344.
- Liu, Y., Zhang, K., Li, Y., Yan, Z., Gao, C., Chen, R., Yuan, Z., Huang, Y., Sun, H., Gao, J. et al. (2024). Sora: A review on background, technology, limitations, and opportunities of large vision models, *arXiv preprint arXiv:2402.17177*.
- Meng, C., He, Y., Song, Y., Song, J., Wu, J., Zhu, J.-Y. and Ermon, S. (2021). Sdedit: Guided image synthesis and editing with stochastic differential equations, *International Conference on Learning Representations*.
- Newman, D., Hettich, S., Blake, C. and Merz, C. (1998). Uci repository of machine learning databases.
- URL:** <http://www.ics.uci.edu/mllearn/MLRepository.html>
- Oko, K., Akiyama, S. and Suzuki, T. (2023). Diffusion models are minimax optimal distribution estimators, *Proceedings of the 40th International Conference on Machine Learning*, pp. 26517–26582.
- Rosenblatt, M. (1969). Conditional probability density and regression estimators, in P. R. Krishnaiah (ed.), *Multivariate analysis, II*, Academic Press, New York, pp. 25–31.
- Shi, Y., De Bortoli, V., Deligiannidis, G. and Doucet, A. (2022). Conditional simulation using diffusion schrödinger bridges, *The 38th Conference on Uncertainty in Artificial Intelligence*.
- Song, Y., Sohl-Dickstein, J., Kingma, D. P., Kumar, A., Ermon, S. and Poole, B. (2021).

- Score-based generative modeling through stochastic differential equations, *International Conference on Learning Representations*.
- Sugiyama, M., Takeuchi, I., Suzuki, T., Kanamori, T., Hachiya, H. and Okanohara, D. (2010). Least-squares conditional density estimation, *IEICE Transactions on Information and Systems* **93**(3): 583–594.
- Wang, G., Jiao, Y., Xu, Q., Wang, Y. and Yang, C. (2021). Deep generative learning via schrödinger bridge, *International Conference on Machine Learning*, PMLR, pp. 10794–10804.
- Wildberger, J., Dax, M., Buchholz, S., Green, S., Macke, J. H. and Schölkopf, B. (2023). Flow matching for scalable simulation-based inference, *Advances in Neural Information Processing Systems*, Vol. 36, pp. 16837–16864.
- Xu, Y., Liu, Z., Tegmark, M. and Jaakkola, T. (2022). Poisson flow generative models, *Advances in Neural Information Processing Systems* **35**: 16782–16795.
- Zheng, Q., Le, M., Shaul, N., Lipman, Y., Grover, A. and Chen, R. T. (2023). Guided flows for generative modeling and decision making, *arXiv preprint arXiv:2311.13443*.
- Zhou, X., Jiao, Y., Liu, J. and Huang, J. (2023). A deep generative approach to conditional sampling, *Journal of the American Statistical Association* **118**: 1837–1848.

## SUPPLEMENTARY MATERIAL

We first provide some notation used in the supplementary material. For matrices  $\mathbf{A}$  and  $\mathbf{B}$ , we say  $\mathbf{A} \preceq \mathbf{B}$  if  $\mathbf{B} - \mathbf{A}$  is positive semi-definite. The  $d$ -dimensional identity matrix is denoted by  $\mathbf{I}_d$ . For a vector  $\mathbf{x} = (x_1, \dots, x_d)^\top \in \mathbb{R}^d$ , we define  $\mathbf{x}^{\otimes 2} := \mathbf{x}\mathbf{x}^\top$ . The  $\ell^2$ -norm and the  $\ell^\infty$ -norm of  $\mathbf{x}$  are, respectively, denoted by  $|\mathbf{x}|_2 := \sqrt{\sum_{i=1}^d x_i^2}$  and  $|\mathbf{x}|_\infty := \max_{1 \leq i \leq d} |x_i|$ . The operator norm of a matrix  $\mathbf{A}$  is defined as  $\|\mathbf{A}\|_{\text{op}} := \sup_{|\mathbf{x}|_2 \leq 1} |\mathbf{A}\mathbf{x}|_2$ . For a probability density function  $\pi$  and a measurable function  $f : \mathbb{R}^d \rightarrow \mathbb{R}$ , the  $L^2(\pi)$ -norm of  $f$  is defined as  $\|f\|_{L^2(\pi)} := \sqrt{\int f^2(\mathbf{x})\pi(\mathbf{x}) d\mathbf{x}}$ , and the  $L^\infty(K)$ -norm of  $f$  is defined as  $\|f\|_{L^\infty(K)} := \sup_{\mathbf{x} \in K} |f(\mathbf{x})|$ . For a vector function  $\mathbf{v} : \mathbb{R}^d \rightarrow \mathbb{R}^d$ , its  $L^2(\pi)$ -norm is denoted as  $\|\mathbf{v}\|_{L^2(\pi)} := \|\mathbf{v}|_2\|_{L^2(\pi)}$ , and its  $L^\infty(K)$ -norm is denoted as  $\|\mathbf{v}\|_{L^\infty(K)} := \|\mathbf{v}|_2\|_{L^\infty(K)}$ . We use  $\mathcal{U}(a, b)$  to denote the uniform distribution on interval  $(a, b)$ , and use  $\mathcal{N}(\mathbf{0}, \mathbf{I}_d)$  to denote the  $d$ -dimensional standard Gaussian distribution. For two positive sequences  $\{a_n\}_{n \geq 1}$  and  $\{b_n\}_{n \geq 1}$ , the asymptotic notation  $a_n = \mathcal{O}(b_n)$  denotes  $a_n \leq Cb_n$  for some constant  $C > 0$ . The notation  $\tilde{\mathcal{O}}(\cdot)$  is used to ignore logarithmic terms. Given two distributions  $\mu$  and  $\nu$ , the Wasserstein-2 distance is defined as  $W_2^2(\mu, \nu) := \inf_{\pi \in \Pi(\mu, \nu)} \mathbb{E}_{(\mathbf{x}, \mathbf{y}) \sim \pi} (|\mathbf{x} - \mathbf{y}|_2^2)$ , where  $\Pi(\mu, \nu)$  is the set of all couplings of  $\mu$  and  $\nu$ . A coupling is a joint distribution on  $\mathbb{R}^d \times \mathbb{R}^d$  whose marginals are  $\mu$  and  $\nu$  on the first and second factors, respectively.

Before delving into the proof of our theoretical results, we introduce an auxiliary proposition, which characterizes the regularity properties of the conditional Föllmer velocity field  $\mathbf{v}_F$ . The proof of Proposition P1 can be found in Section C.

**Proposition P1** *Let Assumptions 1 and 2 hold. The following two assertions are satisfied:*

- (i) *There exists some universal constant  $C > 1$  independent of  $(d_x, R, T)$  such that*

$$\sup_{t \in [0, T]} \sup_{\mathbf{x} \in [-R, R]^{d_x}} \sup_{\mathbf{y} \in [0, B]^{d_y}} |\mathbf{v}_F(\mathbf{x}, \mathbf{y}, t)|_\infty \leq \frac{1 + TR}{1 - T^2},$$

$$\sup_{t \in [0, T]} \sup_{\mathbf{x} \in [-R, R]^{d_x}} \sup_{\mathbf{y} \in [0, B]^{d_y}} |\partial_t \mathbf{v}_F(\mathbf{x}, \mathbf{y}, t)|_2 \leq \frac{C d_x^{3/2} (R + 1)}{(1 - T)^3},$$

for any  $R > 0$  and  $T \in (0, 1)$ .

(ii) For any  $\mathbf{y} \in [0, B]^{d_y}$  and  $t \in [0, T]$  with  $T \in (0, 1)$ ,  $\mathbf{v}_F(\mathbf{x}, \mathbf{y}, t)$  is  $d_x(1 - T)^{-2}$ -Lipschitz continuous w.r.t.  $\mathbf{x}$ , while  $\mathbf{F}_t(\mathbf{x}, \mathbf{y})$  is  $\exp\{d_x(1 - T)^{-2}\}$ -Lipschitz continuous w.r.t.  $\mathbf{x}$ .

## A Proof of Theorem 1

We will establish our proof of Theorem 1 through the following three steps.

**Step 1.** For any given  $\mathbf{y}$  and  $\varepsilon \in (0, 1)$ , we show the existence of a diffusion process  $(\bar{\mathbf{Z}}_t^{\mathbf{y}})_{t \in [0, 1 - \varepsilon]}$  determined by an Itô SDE, which can approximately transform the target conditional density  $p_{x|y}(\mathbf{x}|\mathbf{y})$  into the density of standard Gaussian distribution  $\mathcal{N}(\mathbf{0}, \mathbf{I}_{d_x})$ , and then there exists a process  $(\check{\mathbf{Z}}_t^{\mathbf{y}})_{t \in [\delta, 1 - \varepsilon]}$  determined by the associated ODE with any  $\delta \in (0, 1)$  satisfying  $\delta < 1 - \varepsilon$ , such that  $\check{\mathbf{Z}}_t^{\mathbf{y}}$  shares the same marginal density with  $\bar{\mathbf{Z}}_t^{\mathbf{y}}$  for any  $t \in [\delta, 1 - \varepsilon]$ .

**Step 2.** Under Assumption 2, we can extend the domain of the ODE involved in Step 1 to the interval  $[\delta, 1]$  by supplementing its definition at  $t = 1$ , ensuring an accurate transformation into the density of standard Gaussian distribution  $\mathcal{N}(\mathbf{0}, \mathbf{I}_{d_x})$ .

**Step 3.** Under Assumptions 2, we can prove that the ODE involved in Step 2 has a unique solution. Hence, we can time reverse it to obtain the conditional Föllmer flow (1) over  $[0, 1 - \delta]$  and further extend it to  $[0, 1)$  by letting  $\delta \rightarrow 0$ . This establishes the well-posedness of the conditional Föllmer flow and its ability to arbitrarily approach the target conditional density  $p_{x|y}(\mathbf{x}|\mathbf{y})$  from the density of the standard Gaussian distribution  $\mathcal{N}(\mathbf{0}, \mathbf{I}_{d_x})$ .

## A.1 Step 1

For any given  $\mathbf{y}$  and  $\varepsilon \in (0, 1)$ , we consider a diffusion process  $(\bar{\mathbf{Z}}_t^{\mathbf{y}})_{t \in [0, 1-\varepsilon]}$  defined by the following Itô SDE:

$$d\bar{\mathbf{Z}}_t^{\mathbf{y}} = -\frac{1}{1-t}\bar{\mathbf{Z}}_t^{\mathbf{y}} dt + \sqrt{\frac{2}{1-t}} d\mathbf{B}_t, \quad \bar{\mathbf{Z}}_0^{\mathbf{y}} \sim p_{x|y}(\mathbf{x}|\mathbf{y}), \quad t \in [0, 1-\varepsilon], \quad (\text{S.1})$$

where  $\mathbf{B}_t$  is a standard Brownian motion, and  $p_{x|y}(\mathbf{x}|\mathbf{y})$  is the conditional density of  $\mathbf{X}$  given  $\mathbf{Y} = \mathbf{y}$ . The diffusion process defined in (S.1) has a unique strong solution on  $[0, 1-\varepsilon]$ . The transition probability density of (S.1) from  $\bar{\mathbf{Z}}_0^{\mathbf{y}}$  to  $\bar{\mathbf{Z}}_t^{\mathbf{y}}$  is given by

$$\bar{\mathbf{Z}}_t^{\mathbf{y}} | \bar{\mathbf{Z}}_0^{\mathbf{y}} = \mathbf{x} \sim \mathcal{N}((1-t)\mathbf{x}, t(2-t)\mathbf{I}_{d_x}), \quad t \in [0, 1-\varepsilon].$$

Denote by  $\bar{p}_t(\mathbf{x}; \mathbf{y})$  the marginal density of  $\bar{\mathbf{Z}}_t^{\mathbf{y}}$  defined in (S.1).

Let  $f_t(\mathbf{x}|\mathbf{y})$  be the conditional density of  $t\mathbf{X} + \sqrt{1-t^2}\mathbf{W}$  given  $\mathbf{Y} = \mathbf{y}$ , where  $\mathbf{W} \sim \mathcal{N}(\mathbf{0}, \mathbf{I}_{d_x})$  is independent of  $(\mathbf{X}, \mathbf{Y})$ . Write  $\mathbf{W}_t = t\mathbf{X} + \sqrt{1-t^2}\mathbf{W}$ . Then

$$\begin{aligned} f_t(\mathbf{x}|\mathbf{y}) &= \int p_{x, w_t|y}(\mathbf{u}, \mathbf{x}|\mathbf{y}) d\mathbf{u} = \int p_{x|y}(\mathbf{u}|\mathbf{y}) p_{w_t|x, y}(\mathbf{x}|\mathbf{u}, \mathbf{y}) d\mathbf{u} \\ &= \int p_{x|y}(\mathbf{u}|\mathbf{y}) p_{w_t|x}(\mathbf{x}|\mathbf{u}) d\mathbf{u} = \int C \cdot p_{x|y}(\mathbf{u}|\mathbf{y}) \exp\left\{-\frac{|\mathbf{x} - t\mathbf{u}|_2^2}{2(1-t^2)}\right\} d\mathbf{u}, \end{aligned} \quad (\text{S.2})$$

where  $C = (2\pi)^{-d_x/2}(1-t^2)^{-d_x/2}$ . Hence,  $\bar{p}_t(\mathbf{x}; \mathbf{y}) = f_{1-t}(\mathbf{x}|\mathbf{y})$ . Further,  $\bar{p}_t(\mathbf{x}; \mathbf{y})$  satisfies the Fokker-Planck-Kolmogorov equation in an Eulerian framework over  $[\delta, 1-\varepsilon]$  with any  $\delta > 0$  satisfying  $\delta < 1-\varepsilon$  (Bogachev et al., 2022), which means on  $\mathbb{R}^{d_x} \times [0, B]^{d_y} \times [\delta, 1-\varepsilon]$ ,

$$\partial_t \bar{p}_t(\mathbf{x}; \mathbf{y}) = \nabla_{\mathbf{x}} \cdot \{\bar{p}_t(\mathbf{x}; \mathbf{y}) \mathbf{v}_F(\mathbf{x}, \mathbf{y}, 1-t)\}, \quad \bar{p}_\delta(\mathbf{x}; \mathbf{y}) = f_{1-\delta}(\mathbf{x}|\mathbf{y})$$

in the sense that  $\bar{p}_t(\mathbf{x}; \mathbf{y})$  is continuous in  $t$  under the weak topology, where the velocity field is defined by

$$\mathbf{v}_F(\mathbf{x}, \mathbf{y}, 1-t) := \frac{\mathbf{x} + \mathbf{s}(\mathbf{x}, \mathbf{y}, 1-t)}{1-t}, \quad t \in [\delta, 1-\varepsilon]$$

with

$$\mathbf{s}(\mathbf{x}, \mathbf{y}, t) := \nabla_{\mathbf{x}} \log \left[ \int C \cdot p_{x|y}(\mathbf{u} | \mathbf{y}) \exp \left\{ -\frac{|\mathbf{x} - t\mathbf{u}|_2^2}{2(1-t^2)} \right\} d\mathbf{u} \right] = \nabla_{\mathbf{x}} \log f_t(\mathbf{x} | \mathbf{y}),$$

for any  $t \in [\varepsilon, 1-\delta]$ , where  $C = (2\pi)^{-d_x/2}(1-t^2)^{-d_x/2}$ . Due to the classical Cauchy-Lipschitz theory (Ambrosio and Crippa, 2014) with a Lipschitz velocity field or the well-established Ambrosio-DiPerna-Lions theory with lower Sobolev regularity assumptions on the velocity fields (Ambrosio, 2004; DiPerna and Lions, 1989), we can define a flow  $(\check{\mathbf{Z}}_t^{\mathbf{y}})_{t \in [\delta, 1-\varepsilon]}$  in a Lagrangian formulation via the following ODE system

$$d\check{\mathbf{Z}}_t^{\mathbf{y}} = -\mathbf{v}_F(\check{\mathbf{Z}}_t^{\mathbf{y}}, \mathbf{y}, 1-t) dt, \quad \check{\mathbf{Z}}_{\delta}^{\mathbf{y}} \sim f_{1-\delta}(\mathbf{x} | \mathbf{y}), \quad t \in [\delta, 1-\varepsilon]. \quad (\text{S.3})$$

Denote by  $F(\mathbb{R}^{d_x}; \mathbb{R}^{d_x})$  the set of all functions  $f : \mathbb{R}^{d_x} \rightarrow \mathbb{R}^{d_x}$ , by  $W_{\text{loc}}^{1,\infty}(\mathbb{R}^{d_x}; \mathbb{R}^{d_x})$  the locally bounded Lipschitzian functions  $g : \mathbb{R}^{d_x} \rightarrow \mathbb{R}^{d_x}$ , and by  $L^1([a, b]; V)$  the set of all Bochner integrable functions  $h : [a, b] \rightarrow V$  with  $V$  being a Banach space. Based on Lemma 1 below, we can conclude that  $\check{\mathbf{Z}}_t^{\mathbf{y}}$  in (S.3) and  $\bar{\mathbf{Z}}_t^{\mathbf{y}}$  in (S.1) share the same marginal density over  $[\delta, 1-\varepsilon]$ , which can approximate the density of standard Gaussian distribution  $\mathcal{N}(\mathbf{0}, \mathbf{I}_{d_x})$  as  $t \rightarrow 1$ .

**Lemma 1** *For any fixed  $\mathbf{y}$ , treat the velocity field  $\mathbf{v}_F(\mathbf{x}, \mathbf{y}, t)$  as a map from  $[\varepsilon, 1-\delta]$  to  $F(\mathbb{R}^{d_x}; \mathbb{R}^{d_x})$  and assume that  $\mathbf{v}_F(\mathbf{x}, \mathbf{y}, t)$  satisfies*

$$\mathbf{v}_F(\mathbf{x}, \mathbf{y}, t) \in L^1([\varepsilon, 1-\delta]; W_{\text{loc}}^{1,\infty}(\mathbb{R}^{d_x}; \mathbb{R}^{d_x})), \quad \frac{|\mathbf{v}_F(\mathbf{x}, \mathbf{y}, t)|_2}{1 + |\mathbf{x}|_2} \in L^1([\varepsilon, 1-\delta]; L^\infty(\mathbb{R}^{d_x})).$$

*Then,  $\check{\mathbf{Z}}_t^{\mathbf{y}}$  in (S.3) also follows the marginal probability density  $\bar{p}_t(\mathbf{x}; \mathbf{y}) = f_{1-t}(\mathbf{x} | \mathbf{y})$  on  $[\delta, 1-\varepsilon]$ . Moreover, the distribution with density  $\bar{p}_{1-\varepsilon}(\mathbf{x}; \mathbf{y})$  converges to  $\mathcal{N}(\mathbf{0}, \mathbf{I}_{d_x})$  in the Wasserstein-2 distance as  $\varepsilon \rightarrow 0$ .*

Lemma 1 can be regarded as an application of Proposition 3.5 in Dai et al. (2023), so we omit the proof here. Under Assumption 2, the requirements of  $\mathbf{v}_F(\mathbf{x}, \mathbf{y}, t)$  in Lemma

1 are satisfied automatically. More specifically, as shown in Proposition P1(i) and P1(ii),  $\mathbf{v}_F(\mathbf{x}, \mathbf{y}, t)$  attains local boundedness and local Lipschitz constant uniformly over  $[\varepsilon, 1 - \delta]$  on any compact set  $\mathcal{K} \in \mathbb{R}^{d_x}$ . Further, by Assumption 2 and (S.9),  $|\mathbf{v}_F(\mathbf{x}, \mathbf{y}, t)|_2 / (1 + |\mathbf{x}|_2) \leq (d_x^{1/2} + 1) / \delta$  for any  $\mathbf{x} \in \mathbb{R}^{d_x}$  and  $t \in [\varepsilon, 1 - \delta]$ , thus achieving uniform  $L^\infty(\mathbb{R}^{d_x})$  norm over  $[\varepsilon, 1 - \delta]$ .

## A.2 Step 2

In Step 1, we have defined  $\mathbf{v}_F(\mathbf{x}, \mathbf{y}, t) := t^{-1}\{\mathbf{x} + \mathbf{s}(\mathbf{x}, \mathbf{y}, t)\}$  for any  $t \in [\varepsilon, 1 - \delta]$ . When  $t \in (0, \varepsilon)$ , we also define  $\mathbf{v}_F(\mathbf{x}, \mathbf{y}, t)$  in the same manner. Based on Lemma 2 below, we can define  $\mathbf{v}_F(\mathbf{x}, \mathbf{y}, 0) = \mathbb{E}(\mathbf{X} | \mathbf{Y} = \mathbf{y})$ .

**Lemma 2** *Let Assumption 2 hold. Then*

$$\lim_{t \rightarrow 0^+} \mathbf{v}_F(\mathbf{x}, \mathbf{y}, t) = \lim_{t \rightarrow 0^+} \partial_t \mathbf{s}(\mathbf{x}, \mathbf{y}, t) = \mathbb{E}(\mathbf{X} | \mathbf{Y} = \mathbf{y}).$$

Lemma 2 can be regarded as a natural extension of Lemma A.1 in Dai et al. (2023), so we omit the proof here. Now the process  $(\check{\mathbf{Z}}_t^{\mathbf{y}})_{t \in [\delta, 1]}$  can be extended to time  $t = 1$  such that  $\check{\mathbf{Z}}_1^{\mathbf{y}} \sim \mathcal{N}(\mathbf{0}, \mathbf{I}_{d_x})$ , which solves the initial value problem below

$$d\check{\mathbf{Z}}_t^{\mathbf{y}} = -\mathbf{v}_F(\check{\mathbf{Z}}_t^{\mathbf{y}}, \mathbf{y}, 1 - t)dt, \quad \check{\mathbf{Z}}_\delta^{\mathbf{y}} \sim f_{1-\delta}(\mathbf{x} | \mathbf{y}), \quad t \in [\delta, 1], \quad (\text{S.4})$$

and the marginal density of  $\check{\mathbf{Z}}_t^{\mathbf{y}}$  is  $\bar{p}_t(\mathbf{x}; \mathbf{y}) = f_{1-t}(\mathbf{x} | \mathbf{y})$  for any  $t \in [\delta, 1]$ .

## A.3 Step 3

To demonstrate that (S.4) has a unique solution, we also need the Lipschitz property of  $\mathbf{v}_F$ , which is provided in Proposition P1(ii) under Assumption 2. Now, a standard time reversal argument of (S.4) would yield the conditional Föllmer flow (1) over  $[0, 1 - \delta]$  as

given in Definition 1, i.e.

$$d\mathbf{Z}_t^y = \mathbf{v}_F(\mathbf{Z}_t^y, \mathbf{y}, t) dt, \quad \mathbf{Z}_0^y \sim \mathcal{N}(\mathbf{0}, \mathbf{I}_d), \quad t \in [0, 1 - \delta].$$

Thus, (1) is well-defined on  $[0, 1 - \delta]$  for any  $0 < \delta < 1$ , while letting  $\delta \rightarrow 0$  yields its well-posedness over  $[0, 1)$ . Moreover,  $\mathbf{Z}_t^y \sim f_t(\mathbf{x}|\mathbf{y})$ . Recall that  $\mathbf{W}_t = t\mathbf{X} + \sqrt{1 - t^2}\mathbf{W}$  and  $\mathbf{W} \sim \mathcal{N}(\mathbf{0}, \mathbf{I}_{d_x})$  is independent of  $(\mathbf{X}, \mathbf{Y})$ . Given  $\mathbf{Y} = \mathbf{y}$ , the conditional densities of  $\mathbf{W}_{1-\delta}$  and  $\mathbf{X}$  are, respectively,  $f_{1-\delta}(\mathbf{x}|\mathbf{y})$  and  $p_{x|y}(\mathbf{x}|\mathbf{y})$ . By the definition of Wasserstein-2 distance, we have

$$\begin{aligned} W_2^2(f_{1-\delta}(\mathbf{x}|\mathbf{y}), p_{x|y}(\mathbf{x}|\mathbf{y})) &\leq \mathbb{E}(|\mathbf{W}_{1-\delta} - \mathbf{X}|_2^2 | \mathbf{Y} = \mathbf{y}) \\ &= \mathbb{E}\{|\delta\mathbf{X} - \delta^{1/2}(2 - \delta)^{1/2}\mathbf{W}|_2^2 | \mathbf{Y} = \mathbf{y}\}. \end{aligned}$$

By Assumption 2,  $|\mathbf{X}|_\infty \leq 1$ . It holds that

$$W_2^2(f_{1-\delta}(\mathbf{x}|\mathbf{y}), p_{x|y}(\mathbf{x}|\mathbf{y})) \leq 4d_x\delta \rightarrow 0$$

as  $\delta \rightarrow 0$ . We then complete the proof of Theorem 1.  $\square$

## B Proof of Proposition 1

### B.1 Proof of Proposition 1(i)

Since  $\mathbf{W} \sim \mathcal{N}(\mathbf{0}, \mathbf{I}_{d_x})$  is independent of  $(\mathbf{X}, \mathbf{Y})$  and  $\mathbf{v}_F(\mathbf{x}, \mathbf{y}, 0) = \mathbb{E}(\mathbf{X}|\mathbf{Y} = \mathbf{y})$ , then  $\mathbf{v}_F(\mathbf{x}, \mathbf{y}, 0) = \mathbb{E}(\mathbf{X}|\mathbf{Y} = \mathbf{y}) = \mathbb{E}(\mathbf{X}|\mathbf{W} = \mathbf{x}, \mathbf{Y} = \mathbf{y})$ , which implies (4) holds for  $t = 0$ .

Write  $\mathbf{W}_t = t\mathbf{X} + \sqrt{1 - t^2}\mathbf{W}$ . For any  $t \in (0, T]$ , we have

$$\begin{aligned} &\mathbb{E}\left(\mathbf{X} - \frac{t}{\sqrt{1 - t^2}}\mathbf{W} \middle| \mathbf{W}_t = \mathbf{x}, \mathbf{Y} = \mathbf{y}\right) \\ &= \mathbb{E}\left\{\frac{1}{1 - t^2}\mathbf{X} - \frac{t}{1 - t^2}(t\mathbf{X} + \sqrt{1 - t^2}\mathbf{W}) \middle| \mathbf{W}_t = \mathbf{x}, \mathbf{Y} = \mathbf{y}\right\} \quad (\text{S.5}) \\ &= \frac{1}{1 - t^2}\mathbb{E}(\mathbf{X}|\mathbf{W}_t = \mathbf{x}, \mathbf{Y} = \mathbf{y}) - \frac{t}{1 - t^2}\mathbf{x}. \end{aligned}$$

Recall that  $f_t(\mathbf{x}|\mathbf{y})$  is the conditional density of  $\mathbf{W}_t$  given  $\mathbf{Y} = \mathbf{y}$ . Write  $C = (2\pi)^{-d_x/2}(1 - t^2)^{-d_x/2}$ . For any  $t \in (0, T]$ , by (S.2), it holds that

$$\begin{aligned}
\mathbb{E}(\mathbf{X}|\mathbf{W}_t = \mathbf{x}, \mathbf{Y} = \mathbf{y}) &= \int \mathbf{u} \cdot \frac{p_{x, w_t, y}(\mathbf{u}, \mathbf{x}, \mathbf{y})}{p_{w_t, y}(\mathbf{x}, \mathbf{y})} d\mathbf{u} = \int \mathbf{u} \cdot \frac{p_{w_t|x, y}(\mathbf{x}|\mathbf{u}, \mathbf{y})p_{x, y}(\mathbf{u}, \mathbf{y})}{p_{w_t, y}(\mathbf{x}, \mathbf{y})} d\mathbf{u} \\
&= \int C \mathbf{u} \cdot \frac{p_{x|y}(\mathbf{u}|\mathbf{y})}{f_t(\mathbf{x}|\mathbf{y})} \exp\left\{-\frac{|\mathbf{x} - t\mathbf{u}|_2^2}{2(1-t^2)}\right\} d\mathbf{u} \\
&= \frac{1-t^2}{t} \int C \cdot \frac{p_{x|y}(\mathbf{u}|\mathbf{y})}{f_t(\mathbf{x}|\mathbf{y})} \left(\frac{t\mathbf{u} - \mathbf{x}}{1-t^2} + \frac{\mathbf{x}}{1-t^2}\right) \exp\left\{-\frac{|\mathbf{x} - t\mathbf{u}|_2^2}{2(1-t^2)}\right\} d\mathbf{u} \\
&= \frac{1-t^2}{t} \int C \cdot \frac{p_{x|y}(\mathbf{u}|\mathbf{y})}{f_t(\mathbf{x}|\mathbf{y})} \nabla_{\mathbf{x}} \exp\left\{-\frac{|\mathbf{x} - t\mathbf{u}|_2^2}{2(1-t^2)}\right\} d\mathbf{u} + \frac{1}{t}\mathbf{x} \\
&= \frac{1-t^2}{t} \frac{\nabla_{\mathbf{x}} f_t(\mathbf{x}|\mathbf{y})}{f_t(\mathbf{x}|\mathbf{y})} + \frac{1}{t}\mathbf{x} = \frac{1-t^2}{t} \nabla_{\mathbf{x}} \log f_t(\mathbf{x}|\mathbf{y}) + \frac{1}{t}\mathbf{x},
\end{aligned} \tag{S.6}$$

which implies

$$\mathbb{E}\left(\mathbf{X} - \frac{t}{\sqrt{1-t^2}}\mathbf{W} \middle| \mathbf{W}_t = \mathbf{x}, \mathbf{Y} = \mathbf{y}\right) = \frac{\nabla_{\mathbf{x}} \log f_t(\mathbf{x}|\mathbf{y})}{t} + \frac{1}{t}\mathbf{x} = \mathbf{v}_F(\mathbf{x}, \mathbf{y}, t)$$

for any  $t \in (0, T]$ . We complete the proof of Proof of Proposition 1(i).  $\square$

## B.2 Proof of Proposition 1(ii)

Recall that  $\mathbf{W}_t = t\mathbf{X} + \sqrt{1-t^2}\mathbf{W}$ . For any vector-valued function  $\mathbf{v}(\mathbf{x}, \mathbf{y}, t) : \mathbb{R}^{d_x} \times \mathbb{R}^{d_y} \times [0, T] \rightarrow \mathbb{R}^{d_x}$ , we have

$$\begin{aligned}
&\mathbb{E}\left\{\left|\mathbf{X} - \frac{t}{\sqrt{1-t^2}}\mathbf{W} - \mathbf{v}(\mathbf{W}_t, \mathbf{Y}, t)\right|_2^2\right\} \\
&= \mathbb{E}\left\{\left|\mathbf{X} - \frac{t}{\sqrt{1-t^2}}\mathbf{W} - \mathbf{v}_F(\mathbf{W}_t, \mathbf{Y}, t) + \mathbf{v}_F(\mathbf{W}_t, \mathbf{Y}, t) - \mathbf{v}(\mathbf{W}_t, \mathbf{Y}, t)\right|_2^2\right\} \\
&= \mathbb{E}\left\{\left|\mathbf{X} - \frac{t}{\sqrt{1-t^2}}\mathbf{W} - \mathbf{v}_F(\mathbf{W}_t, \mathbf{Y}, t)\right|_2^2\right\} + \mathbb{E}\{|\mathbf{v}_F(\mathbf{W}_t, \mathbf{Y}, t) - \mathbf{v}(\mathbf{W}_t, \mathbf{Y}, t)|_2^2\} \\
&\quad + 2\mathbb{E}\left\{\left\langle \mathbf{v}_F(\mathbf{W}_t, \mathbf{Y}, t) - \mathbf{v}(\mathbf{W}_t, \mathbf{Y}, t), \mathbf{X} - \frac{t}{\sqrt{1-t^2}}\mathbf{W} - \mathbf{v}_F(\mathbf{W}_t, \mathbf{Y}, t) \right\rangle\right\}
\end{aligned} \tag{S.7}$$

for any  $t \in [0, T]$ . Due to

$$\mathbb{E}\left\{\left\langle \mathbf{v}_F(\mathbf{W}_t, \mathbf{Y}, t) - \mathbf{v}(\mathbf{W}_t, \mathbf{Y}, t), \mathbf{X} - \frac{t}{\sqrt{1-t^2}}\mathbf{W} - \mathbf{v}_F(\mathbf{W}_t, \mathbf{Y}, t) \right\rangle\right\}$$

$$\begin{aligned}
&= \mathbb{E} \left[ \mathbb{E} \left\{ \left\langle \mathbf{v}_F(\mathbf{W}_t, \mathbf{Y}, t) - \mathbf{v}(\mathbf{W}_t, \mathbf{Y}, t), \mathbf{X} - \frac{t}{\sqrt{1-t^2}} \mathbf{W} - \mathbf{v}_F(\mathbf{W}_t, \mathbf{Y}, t) \right\rangle \middle| \mathbf{W}_t, \mathbf{Y} \right\} \right] \\
&= \mathbb{E} \left\{ \left\langle \mathbf{v}_F(\mathbf{W}_t, \mathbf{Y}, t) - \mathbf{v}(\mathbf{W}_t, \mathbf{Y}, t), \mathbb{E} \left( \mathbf{X} - \frac{t}{\sqrt{1-t^2}} \mathbf{W} \middle| \mathbf{W}_t, \mathbf{Y} \right) - \mathbf{v}_F(\mathbf{W}_t, \mathbf{Y}, t) \right\rangle \right\} \\
&= \mathbb{E} \{ \langle \mathbf{v}_F(\mathbf{W}_t, \mathbf{Y}, t) - \mathbf{v}(\mathbf{W}_t, \mathbf{Y}, t), \mathbf{0} \rangle \} = 0
\end{aligned} \tag{S.8}$$

for any  $t \in [0, T]$ , by (S.7), we have

$$\mathbb{E} \left\{ \left| \mathbf{X} - \frac{t}{\sqrt{1-t^2}} \mathbf{W} - \mathbf{v}(\mathbf{W}_t, \mathbf{Y}, t) \right|_2^2 \right\} \geq \mathbb{E} \left\{ \left| \mathbf{X} - \frac{t}{\sqrt{1-t^2}} \mathbf{W} - \mathbf{v}_F(\mathbf{W}_t, \mathbf{Y}, t) \right|_2^2 \right\}$$

for any  $t \in [0, T]$ , where the equation holds if and only if  $\mathbf{v} = \mathbf{v}_F$ . Thus, we complete the proof of Proposition 1(ii).  $\square$

## C Proof of Proposition P1

To prove Proposition P1, we need the following Grönwall's inequality, whose proof can be found in Lemma 1.1 of Bainov and Simeonov (1992).

**Lemma 3 (Grönwall's inequality)** *Let  $\beta(t)$ ,  $\lambda(t)$  and  $v(t)$  be real-valued continuous functions defined on  $[a, b]$  with  $a < b$ . If  $v(t)$  is differentiable over the interval  $(a, b)$  and satisfies  $v'(t) \leq \beta(t)v(t) + \lambda(t)$  for any  $t \in (a, b)$ , then*

$$v(t) \leq v(a) \exp \left\{ \int_a^t \beta(s) ds \right\} + \int_a^t \lambda(s) \exp \left\{ \int_s^t \beta(\tau) d\tau \right\} ds$$

for any  $t \in (a, b)$ .

### C.1 Proof of Proposition P1(i)

By Proposition 1(i) and (S.5), it holds that

$$\mathbf{v}_F(\mathbf{x}, \mathbf{y}, t) = \frac{1}{1-t^2} \mathbb{E}(\mathbf{X} | \mathbf{W}_t = \mathbf{x}, \mathbf{Y} = \mathbf{y}) - \frac{t}{1-t^2} \mathbf{x}. \tag{S.9}$$

By Assumption 2, we have  $|\mathbf{X}|_\infty \leq 1$ , which implies

$$\sup_{t \in [0, T]} \sup_{\mathbf{x} \in [-R, R]^{d_x}} \sup_{\mathbf{y} \in [0, B]^{d_y}} |\mathbf{v}_F(\mathbf{x}, \mathbf{y}, t)|_\infty \leq \frac{1 + TR}{1 - T^2}.$$

Recall that  $f_t(\mathbf{x}|\mathbf{y})$  is the conditional density of  $\mathbf{W}_t$  given  $\mathbf{Y} = \mathbf{y}$  and  $\mathbf{W}_t = t\mathbf{X} + \sqrt{1 - t^2}\mathbf{W}$ . Write

$$\phi_t^{\mathbf{y}}(\mathbf{x}) := \int p_{x|y}(\mathbf{u}|\mathbf{y}) \exp \left\{ -\frac{|\mathbf{x} - t\mathbf{u}|_2^2}{2(1 - t^2)} \right\} d\mathbf{u}.$$

As we have shown in (S.2) in Section B.1,  $\phi_t^{\mathbf{y}}(\mathbf{x}) = C^{-1}f_t(\mathbf{x}|\mathbf{y})$  with  $C = (2\pi)^{-d_x/2}(1 - t^2)^{-d_x/2}$ . Then  $\nabla_{\mathbf{x}} \log \phi_t^{\mathbf{y}}(\mathbf{x}) = \nabla_{\mathbf{x}} \log f_t(\mathbf{x}|\mathbf{y})$ . By the definition of  $\mathbf{v}_F(\mathbf{x}, \mathbf{y}, t)$  given in Definition 1 and (S.9), we have

$$\nabla_{\mathbf{x}} \log f_t(\mathbf{x}|\mathbf{y}) = \frac{t}{1 - t^2} \mathbb{E}(\mathbf{X} | \mathbf{W}_t = \mathbf{x}, \mathbf{Y} = \mathbf{y}) - \frac{1}{1 - t^2} \mathbf{x}.$$

Furthermore, it holds that

$$\begin{aligned} \partial_t \mathbf{v}_F(\mathbf{x}, \mathbf{y}, t) &= -\frac{\nabla_{\mathbf{x}} \log f_t(\mathbf{x}|\mathbf{y})}{t^2} + \frac{\partial_t \nabla_{\mathbf{x}} \log f_t(\mathbf{x}|\mathbf{y})}{t} - \frac{\mathbf{x}}{t^2} \\ &= \frac{\mathbf{x}}{1 - t^2} - \frac{\mathbb{E}(\mathbf{X} | \mathbf{W}_t = \mathbf{x}, \mathbf{Y} = \mathbf{y})}{t(1 - t^2)} + \frac{1}{t} \left[ \frac{\partial_t \nabla_{\mathbf{x}} \phi_t^{\mathbf{y}}(\mathbf{x})}{\phi_t^{\mathbf{y}}(\mathbf{x})} - \frac{\partial_t \phi_t^{\mathbf{y}}(\mathbf{x}) \nabla_{\mathbf{x}} \phi_t^{\mathbf{y}}(\mathbf{x})}{\{\phi_t^{\mathbf{y}}(\mathbf{x})\}^2} \right]. \end{aligned} \quad (\text{S.10})$$

Notice that

$$\begin{aligned} \frac{\partial_t \nabla_{\mathbf{x}} \phi_t^{\mathbf{y}}(\mathbf{x})}{\phi_t^{\mathbf{y}}(\mathbf{x})} &= \int \frac{(1 + t^2)\mathbf{u} - 2t\mathbf{x}}{(1 - t^2)^2} \frac{p_{x|y}(\mathbf{u}|\mathbf{y})}{\phi_t^{\mathbf{y}}(\mathbf{x})} \exp \left\{ -\frac{|\mathbf{x} - t\mathbf{u}|_2^2}{2(1 - t^2)} \right\} d\mathbf{u} \\ &\quad + \int \frac{(\mathbf{u}^T \mathbf{x} - t|\mathbf{u}|_2^2)(t\mathbf{u} - \mathbf{x})}{(1 - t^2)^2} \frac{p_{x|y}(\mathbf{u}|\mathbf{y})}{\phi_t^{\mathbf{y}}(\mathbf{x})} \exp \left\{ -\frac{|\mathbf{x} - t\mathbf{u}|_2^2}{2(1 - t^2)} \right\} d\mathbf{u} \\ &\quad + \int \frac{t|\mathbf{x} - t\mathbf{u}|_2^2(\mathbf{x} - t\mathbf{u})}{(1 - t^2)^3} \frac{p_{x|y}(\mathbf{u}|\mathbf{y})}{\phi_t^{\mathbf{y}}(\mathbf{x})} \exp \left\{ -\frac{|\mathbf{x} - t\mathbf{u}|_2^2}{2(1 - t^2)} \right\} d\mathbf{u}. \end{aligned}$$

As we have shown in (S.6) in Section B.1, the conditional density of  $\mathbf{X}$  given  $(\mathbf{W}_t, \mathbf{Y}) = (\mathbf{x}, \mathbf{y})$  is given by

$$p_{x|w_t, y}(\mathbf{u}|\mathbf{x}, \mathbf{y}) = C \cdot \frac{p_{x|y}(\mathbf{u}|\mathbf{y})}{f_t(\mathbf{x}|\mathbf{y})} \exp \left\{ -\frac{|\mathbf{x} - t\mathbf{u}|_2^2}{2(1 - t^2)} \right\} \quad (\text{S.11})$$

with  $C = (2\pi)^{-d_x/2}(1 - t^2)^{-d_x/2}$ . Due to  $\phi_t^{\mathbf{y}}(\mathbf{x}) = C^{-1}f_t(\mathbf{x}|\mathbf{y})$ , then

$$\frac{\partial_t \nabla_{\mathbf{x}} \phi_t^{\mathbf{y}}(\mathbf{x})}{\phi_t^{\mathbf{y}}(\mathbf{x})} = \frac{-2t\mathbf{x}}{(1 - t^2)^2} + \frac{1 + t^2}{(1 - t^2)^2} \mathbb{E}(\mathbf{X} | \mathbf{W}_t = \mathbf{x}, \mathbf{Y} = \mathbf{y}) + \frac{t|\mathbf{x}|_2^2 \mathbf{x}}{(1 - t^2)^3}$$

$$\begin{aligned}
& - \frac{t^2}{(1-t^2)^3} \mathbb{E}(|\mathbf{X}|_2^2 \mathbf{X} | \mathbf{W}_t = \mathbf{x}, \mathbf{Y} = \mathbf{y}) + \frac{t(1+t^2)}{(1-t^2)^3} \mathbb{E}(\mathbf{X}\mathbf{X}^\top | \mathbf{W}_t = \mathbf{x}, \mathbf{Y} = \mathbf{y}) \mathbf{x} \\
& - \frac{1+t^2}{(1-t^2)^3} \mathbb{E}(\mathbf{X}^\top \mathbf{x} | \mathbf{W}_t = \mathbf{x}, \mathbf{Y} = \mathbf{y}) \mathbf{x} + \frac{t}{(1-t^2)^3} \mathbb{E}(|\mathbf{X}|_2^2 | \mathbf{W}_t = \mathbf{x}, \mathbf{Y} = \mathbf{y}) \mathbf{x} \\
& - \frac{t^2}{(1-t^2)^3} \mathbb{E}(\mathbf{X} | \mathbf{W}_t = \mathbf{x}, \mathbf{Y} = \mathbf{y}) |\mathbf{x}|_2^2.
\end{aligned} \tag{S.12}$$

Analogously, we also have

$$\begin{aligned}
\frac{\partial_t \phi_t^{\mathbf{y}}(\mathbf{x})}{\phi_t^{\mathbf{y}}(\mathbf{x})} &= \frac{1}{\phi_t^{\mathbf{y}}(\mathbf{x})} \int \frac{(\mathbf{u}^\top \mathbf{x} - t|\mathbf{u}|_2^2)}{1-t^2} \exp \left\{ -\frac{|\mathbf{x} - t\mathbf{u}|_2^2}{2(1-t^2)} \right\} p_{x|y}(\mathbf{u} | \mathbf{y}) \, d\mathbf{u} \\
& - \frac{1}{\phi_t^{\mathbf{y}}(\mathbf{x})} \int \frac{t|\mathbf{x} - t\mathbf{u}|_2^2}{(1-t^2)^2} \exp \left\{ -\frac{|\mathbf{x} - t\mathbf{u}|_2^2}{2(1-t^2)} \right\} p_{x|y}(\mathbf{u} | \mathbf{y}) \, d\mathbf{u} \\
& = \frac{-t|\mathbf{x}|_2^2}{(1-t^2)^2} + \frac{1+t^2}{(1-t^2)^2} \mathbb{E}(\mathbf{X}^\top \mathbf{x} | \mathbf{W}_t = \mathbf{x}, \mathbf{Y} = \mathbf{y}) \\
& - \frac{t}{(1-t^2)^2} \mathbb{E}(|\mathbf{X}|_2^2 | \mathbf{W}_t = \mathbf{x}, \mathbf{Y} = \mathbf{y}),
\end{aligned} \tag{S.13}$$

$$\begin{aligned}
\frac{\nabla_{\mathbf{x}} \phi_t^{\mathbf{y}}(\mathbf{x})}{\phi_t^{\mathbf{y}}(\mathbf{x})} &= \frac{1}{\phi_t^{\mathbf{y}}(\mathbf{x})} \int \frac{t\mathbf{u} - \mathbf{x}}{1-t^2} \exp \left\{ -\frac{|\mathbf{x} - t\mathbf{u}|_2^2}{2(1-t^2)} \right\} p_{x|y}(\mathbf{u} | \mathbf{y}) \, d\mathbf{u} \\
& = \frac{-\mathbf{x}}{1-t^2} + \frac{t}{1-t^2} \mathbb{E}(\mathbf{X} | \mathbf{W}_t = \mathbf{x}, \mathbf{Y} = \mathbf{y}).
\end{aligned} \tag{S.14}$$

Combining (S.10), (S.12), (S.13) and (S.14), we obtain

$$\begin{aligned}
\partial_t \mathbf{v}_F(\mathbf{x}, \mathbf{y}, t) &= \frac{1+t^2}{(1-t^2)^3} \text{Cov}(\mathbf{X} | \mathbf{W}_t = \mathbf{x}, \mathbf{Y} = \mathbf{y}) \mathbf{x} + \frac{2t}{(1-t^2)^2} \mathbb{E}(\mathbf{X} | \mathbf{W}_t = \mathbf{x}, \mathbf{Y} = \mathbf{y}) \\
& - \frac{t}{(1-t^2)^3} \mathbb{E}(\mathbf{X} | \mathbf{X}|_2^2 | \mathbf{W}_t = \mathbf{x}, \mathbf{Y} = \mathbf{y}) - \frac{1+t^2}{(1-t^2)^2} \mathbf{x} \\
& + \frac{t}{(1-t^2)^3} \mathbb{E}(\mathbf{X} | \mathbf{W}_t = \mathbf{x}, \mathbf{Y} = \mathbf{y}) \mathbb{E}(|\mathbf{X}|_2^2 | \mathbf{W}_t = \mathbf{x}, \mathbf{Y} = \mathbf{y}),
\end{aligned}$$

which implies

$$\begin{aligned}
|\partial_t \mathbf{v}_F(\mathbf{x}, \mathbf{y}, t)|_2 &\leq \frac{1+t^2}{(1-t^2)^3} \|\text{Cov}(\mathbf{X} | \mathbf{W}_t = \mathbf{x}, \mathbf{Y} = \mathbf{y})\|_{\text{op}} |\mathbf{x}|_2 \\
& + \frac{2t}{(1-t^2)^2} |\mathbb{E}(\mathbf{X} | \mathbf{W}_t = \mathbf{x}, \mathbf{Y} = \mathbf{y})|_2 + \frac{1+t^2}{(1-t^2)^2} |\mathbf{x}|_2 \\
& + \frac{t}{(1-t^2)^3} |\mathbb{E}(\mathbf{X} | \mathbf{X}|_2^2 | \mathbf{W}_t = \mathbf{x}, \mathbf{Y} = \mathbf{y})|_2 \\
& + \frac{t}{(1-t^2)^3} |\mathbb{E}(\mathbf{X} | \mathbf{W}_t = \mathbf{x}, \mathbf{Y} = \mathbf{y})|_2 \mathbb{E}(|\mathbf{X}|_2^2 | \mathbf{W}_t = \mathbf{x}, \mathbf{Y} = \mathbf{y}).
\end{aligned} \tag{S.15}$$

By Assumption 2, we have  $\|\mathbf{X}\|_\infty \leq 1$ , so  $|\mathbb{E}(\mathbf{X} | \mathbf{W}_t = \mathbf{x}, \mathbf{Y} = \mathbf{y})|_2 \leq d_x^{1/2}$ ,  $|\mathbb{E}(\|\mathbf{X}\|_2^2 | \mathbf{W}_t = \mathbf{x}, \mathbf{Y} = \mathbf{y})|_2 \leq d_x$  and  $|\mathbb{E}(\mathbf{X}\|\mathbf{X}\|_2^2 | \mathbf{W}_t = \mathbf{x}, \mathbf{Y} = \mathbf{y})|_2 \leq d_x^{3/2}$ . For any  $\mathbf{u} \in \mathbb{R}^{d_x}$ , due to

$$\mathbf{u}^\top \text{Cov}(\mathbf{X} | \mathbf{W}_t = \mathbf{x}, \mathbf{Y} = \mathbf{y}) \mathbf{u} \leq \mathbb{E}\{(\mathbf{u}^\top \mathbf{X})^2 | \mathbf{W}_t = \mathbf{x}, \mathbf{Y} = \mathbf{y}\} \leq d_x \|\mathbf{u}\|_2^2,$$

we have  $\|\text{Cov}(\mathbf{X} | \mathbf{W}_t = \mathbf{x}, \mathbf{Y} = \mathbf{y})\|_{\text{op}} \leq d_x$ . Hence, due to  $T < 1$ , by (S.15), it holds that

$$\begin{aligned} & \sup_{t \in [0, T]} \sup_{\mathbf{x} \in [-R, R]^{d_x}} \sup_{\mathbf{y} \in [0, B]^{d_y}} |\partial_t \mathbf{v}_F(\mathbf{x}, \mathbf{y}, t)|_2 \\ & \leq \frac{1 + T^2}{(1 - T^2)^3} d_x^{3/2} R + \frac{2T d_x^{1/2}}{(1 - T^2)^2} + \frac{2T d_x^{3/2}}{(1 - T^2)^3} + \frac{1 + T^2}{(1 - T^2)^2} R d_x^{1/2} \\ & \leq \frac{C_* d_x^{3/2} (R + 1)}{(1 - T)^3}, \end{aligned}$$

where  $C_* > 1$  is some universal constant independent of  $(d_x, R, T)$ . We complete the proof of Proposition P1(i).  $\square$

## C.2 Proof of Proposition P1(ii)

Recall that  $\mathbf{v}_F(\mathbf{x}, \mathbf{y}, t) = t^{-1} \nabla_{\mathbf{x}} \log f_t(\mathbf{x} | \mathbf{y}) + t^{-1} \mathbf{x}$ . Then we have

$$\nabla_{\mathbf{x}} \mathbf{v}_F(\mathbf{x}, \mathbf{y}, t) = \frac{1}{t} \nabla_{\mathbf{x}}^2 \log f_t(\mathbf{x} | \mathbf{y}) + \frac{1}{t} \mathbf{I}_{d_x}.$$

As we have shown in (S.2) in Section B.1,

$$f_t(\mathbf{x} | \mathbf{y}) = C \int p_{x|y}(\mathbf{u} | \mathbf{y}) \exp \left\{ -\frac{\|\mathbf{x} - t\mathbf{u}\|_2^2}{2(1 - t^2)} \right\} d\mathbf{u},$$

where  $C = (2\pi)^{-d_x/2} (1 - t^2)^{-d_x/2}$ . Then it holds that

$$\begin{aligned} \nabla_{\mathbf{x}}^2 \log f_t(\mathbf{x} | \mathbf{y}) &= - \int \frac{\mathbf{x} - t\mathbf{u}}{1 - t^2} \frac{p_{x|y}(\mathbf{u} | \mathbf{y})}{C^{-1} f_t(\mathbf{x} | \mathbf{y})} \exp \left\{ -\frac{\|\mathbf{x} - t\mathbf{u}\|_2^2}{2(1 - t^2)} \right\} d\mathbf{u} \\ &\quad \times \left[ \int \frac{\mathbf{x} - t\mathbf{u}}{1 - t^2} \frac{p_{x|y}(\mathbf{u} | \mathbf{y})}{C^{-1} f_t(\mathbf{x} | \mathbf{y})} \exp \left\{ -\frac{\|\mathbf{x} - t\mathbf{u}\|_2^2}{2(1 - t^2)} \right\} d\mathbf{u} \right]^\top \\ &\quad - \int \frac{\mathbf{x} - t\mathbf{u}}{1 - t^2} \frac{(\mathbf{x} - t\mathbf{u})^\top}{1 - t^2} \frac{p_{x|y}(\mathbf{u} | \mathbf{y})}{C^{-1} f_t(\mathbf{x} | \mathbf{y})} \exp \left\{ -\frac{\|\mathbf{x} - t\mathbf{u}\|_2^2}{2(1 - t^2)} \right\} d\mathbf{u} \\ &\quad - \mathbf{I}_{d_x} \int \frac{1}{1 - t^2} \frac{p_{x|y}(\mathbf{u} | \mathbf{y})}{C^{-1} f_t(\mathbf{x} | \mathbf{y})} \exp \left\{ -\frac{\|\mathbf{x} - t\mathbf{u}\|_2^2}{2(1 - t^2)} \right\} d\mathbf{u} \end{aligned}$$

$$\begin{aligned}
&= - \int \frac{\mathbf{x} - t\mathbf{u}}{1 - t^2} p_{x|w_t,y}(\mathbf{u}|\mathbf{x}, \mathbf{y}) \, d\mathbf{u} \times \left[ \int \frac{\mathbf{x} - t\mathbf{u}}{1 - t^2} p_{x|w_t,y}(\mathbf{u}|\mathbf{x}, \mathbf{y}) \, d\mathbf{u} \right]^T \\
&\quad + \int \frac{\mathbf{x} - t\mathbf{u}}{1 - t^2} \frac{(\mathbf{x} - t\mathbf{u})^T}{1 - t^2} p_{x|w_t,y}(\mathbf{u}|\mathbf{x}, \mathbf{y}) \, d\mathbf{u} - \mathbf{I}_{d_x} \int \frac{p_{x|w_t,y}(\mathbf{u}|\mathbf{x}, \mathbf{y})}{1 - t^2} \, d\mathbf{u},
\end{aligned}$$

where the last step is based on the identity (S.11) and  $p_{x|w_t,y}(\mathbf{u}|\mathbf{x}, \mathbf{y})$  is the conditional density of  $\mathbf{X}$  given  $(\mathbf{W}_t, \mathbf{Y}) = (\mathbf{x}, \mathbf{y})$ . Hence,

$$\nabla_{\mathbf{x}}^2 \log f_t(\mathbf{x}|\mathbf{y}) = \frac{-1}{1 - t^2} \mathbf{I}_{d_x} + \frac{t^2}{(1 - t^2)^2} \text{Cov}(\mathbf{X}|\mathbf{W}_t = \mathbf{x}, \mathbf{Y} = \mathbf{y}),$$

which implies that

$$\nabla_{\mathbf{x}} \mathbf{v}_F(\mathbf{x}, \mathbf{y}, t) = \frac{-t}{1 - t^2} \mathbf{I}_{d_x} + \frac{t}{(1 - t^2)^2} \text{Cov}(\mathbf{X}|\mathbf{W}_t = \mathbf{x}, \mathbf{Y} = \mathbf{y}). \quad (\text{S.16})$$

As we have shown in Section C.1,  $\|\text{Cov}(\mathbf{X}|\mathbf{W}_t = \mathbf{x}, \mathbf{Y} = \mathbf{y})\|_{\text{op}} \leq d_x$ , which implies  $0 \preceq \text{Cov}(\mathbf{X}|\mathbf{W}_t = \mathbf{x}, \mathbf{Y} = \mathbf{y}) \preceq d_x \mathbf{I}_{d_x}$ . Hence,

$$-\frac{t}{1 - t^2} \mathbf{I}_{d_x} \preceq \nabla_{\mathbf{x}} \mathbf{v}_F(\mathbf{x}, \mathbf{y}, t) \preceq \left\{ \frac{td_x}{(1 - t^2)^2} - \frac{t}{1 - t^2} \right\} \mathbf{I}_{d_x}. \quad (\text{S.17})$$

Then it holds that

$$\|\nabla_{\mathbf{x}} \mathbf{v}_F(\mathbf{x}, \mathbf{y}, t)\|_{\text{op}} \leq \left| \frac{t}{1 - t^2} \right| \vee \left| \frac{t(d_x - 1) + t^2}{(1 - t^2)^2} \right| \leq \frac{d_x}{(1 - T)^2}. \quad (\text{S.18})$$

This means  $\mathbf{v}_F(\mathbf{x}, \mathbf{y}, t)$  is  $d_x(1 - T)^{-2}$ -Lipschitz w.r.t.  $\mathbf{x}$  over  $[0, T]$ .

In the sequel, we demonstrate that for any  $t \in [0, T]$ ,  $\mathbf{F}_t(\mathbf{x}, \mathbf{y})$  exhibits Lipschitz property. Recall that the conditional Föllmer flow map  $\mathbf{F}_t(\mathbf{x}, \mathbf{y})$  defined in Definition 2 represents the ODE solution of  $d\mathbf{x}_t = \mathbf{v}_F(\mathbf{x}_t, \mathbf{y}, t) dt$  at time  $t$ , given initial value  $\mathbf{x}_0 = \mathbf{x}$ .

Thus, it holds that

$$\mathbf{F}_t(\mathbf{x}, \mathbf{y}) - \mathbf{F}_0(\mathbf{x}, \mathbf{y}) = \int_0^t \mathbf{v}_F(\mathbf{F}_s(\mathbf{x}, \mathbf{y}), \mathbf{y}, s) \, ds, \quad \mathbf{F}_0(\mathbf{x}, \mathbf{y}) = \mathbf{x}.$$

Taking the gradient w.r.t.  $\mathbf{x}$  on both sides of above equation, we obtain

$$\nabla_{\mathbf{x}} \mathbf{F}_t(\mathbf{x}, \mathbf{y}) - \nabla_{\mathbf{x}} \mathbf{F}_0(\mathbf{x}, \mathbf{y}) = \int_0^t \left\{ \nabla_{\mathbf{u}} \mathbf{v}_F(\mathbf{u}, \mathbf{y}, s) \right\} \Big|_{\mathbf{u}=\mathbf{F}_s(\mathbf{x}, \mathbf{y})} \nabla_{\mathbf{x}} \mathbf{F}_s(\mathbf{x}, \mathbf{y}) \, ds,$$

which implies

$$\partial_t \nabla_{\mathbf{x}} \mathbf{F}_t(\mathbf{x}, \mathbf{y}) = \left\{ \nabla_{\mathbf{u}} \mathbf{v}_F(\mathbf{u}, \mathbf{y}, t) \right\} \Big|_{\mathbf{u}=\mathbf{F}_t(\mathbf{x}, \mathbf{y})} \nabla_{\mathbf{x}} \mathbf{F}_t(\mathbf{x}, \mathbf{y}).$$

For any given  $\mathbf{r} \in \mathbb{R}^{d_x}$  with  $|\mathbf{r}|_2 = 1$ , let  $u_{\mathbf{r}}(\mathbf{x}, \mathbf{y}, t) = |\nabla_{\mathbf{x}} \mathbf{F}_t(\mathbf{x}, \mathbf{y}) \mathbf{r}|_2^2$ . Then we further have

$$\begin{aligned} \partial_t u_{\mathbf{r}}(\mathbf{x}, \mathbf{y}, t) &= 2 \langle \nabla_{\mathbf{x}} \mathbf{F}_t(\mathbf{x}, \mathbf{y}) \mathbf{r}, \partial_t \nabla_{\mathbf{x}} \mathbf{F}_t(\mathbf{x}, \mathbf{y}) \mathbf{r} \rangle \\ &= 2 \langle \nabla_{\mathbf{x}} \mathbf{F}_t(\mathbf{x}, \mathbf{y}) \mathbf{r}, \left\{ \nabla_{\mathbf{u}} \mathbf{v}_F(\mathbf{u}, \mathbf{y}, t) \right\} \Big|_{\mathbf{u}=\mathbf{F}_t(\mathbf{x}, \mathbf{y})} \nabla_{\mathbf{x}} \mathbf{F}_t(\mathbf{x}, \mathbf{y}) \mathbf{r} \rangle \\ &\leq 2 |\nabla_{\mathbf{x}} \mathbf{F}_t(\mathbf{x}, \mathbf{y}) \mathbf{r}|_2 \left| \left\{ \nabla_{\mathbf{u}} \mathbf{v}_F(\mathbf{u}, \mathbf{y}, t) \right\} \Big|_{\mathbf{u}=\mathbf{F}_t(\mathbf{x}, \mathbf{y})} \nabla_{\mathbf{x}} \mathbf{F}_t(\mathbf{x}, \mathbf{y}) \mathbf{r} \right|_2 \\ &\leq 2 \|\nabla_{\mathbf{x}} \mathbf{v}_F(\mathbf{x}, \mathbf{y}, t)\|_{\text{op}} u_{\mathbf{r}}(\mathbf{x}, \mathbf{y}, t) \leq \frac{2d_x}{(1-T)^2} u_{\mathbf{r}}(\mathbf{x}, \mathbf{y}, t), \end{aligned}$$

where the first inequality follows from the Cauchy-Schwarz inequality. By Lemma 3, it holds that

$$\begin{aligned} \|\nabla_{\mathbf{x}} \mathbf{F}_t(\mathbf{x}, \mathbf{y})\|_{\text{op}} &= \sup_{|\mathbf{r}|_2=1} \sqrt{u_{\mathbf{r}}(\mathbf{x}, \mathbf{y}, t)} \\ &\leq \sup_{|\mathbf{r}|_2=1} \sqrt{u_{\mathbf{r}}(\mathbf{x}, \mathbf{y}, 0)} \exp\{d_x(1-T)^{-2}\} = \exp\{d_x(1-T)^{-2}\}. \end{aligned}$$

which concludes the proof.  $\square$

## D Proof of Proposition 2

Denote by  $g_t(\mathbf{x}, \mathbf{y})$  the joint density of  $t\mathbf{X} + \sqrt{1-t^2}\mathbf{W}$  and  $\mathbf{Y}$ . For simplicity, we will use  $\mathbf{W}_t$  to represent  $t\mathbf{X} + \sqrt{1-t^2}\mathbf{W}$  and abbreviate  $L^2(g_t(\mathbf{x}, \mathbf{y}))$  as  $L^2(g_t)$  in the remaining part of this section. For any velocity field  $\mathbf{v} : \mathbb{R}^{d_x} \times \mathbb{R}^{d_y} \times [0, T] \rightarrow \mathbb{R}^{d_x}$ , by (S.7) and (S.8), we have

$$\begin{aligned} &\mathbb{E} \left\{ \left| \mathbf{X} - \frac{t}{\sqrt{1-t^2}} \mathbf{W} - \mathbf{v}(\mathbf{W}_t, \mathbf{Y}, t) \right|_2^2 \right\} \\ &= \mathbb{E} \left\{ \left| \mathbf{X} - \frac{t}{\sqrt{1-t^2}} \mathbf{W} - \mathbf{v}_F(\mathbf{W}_t, \mathbf{Y}, t) \right|_2^2 \right\} + \mathbb{E} \left\{ |\mathbf{v}_F(\mathbf{W}_t, \mathbf{Y}, t) - \mathbf{v}(\mathbf{W}_t, \mathbf{Y}, t)|_2^2 \right\} \end{aligned} \tag{S.19}$$

for any  $t \in [0, T]$ . By the definition of  $\mathcal{L}(\cdot)$  given in Proposition 1(ii), it holds that

$$\mathcal{L}(\mathbf{v}) - \mathcal{L}(\mathbf{v}_F) = \frac{1}{T} \int_0^T \|\mathbf{v}(\mathbf{x}, \mathbf{y}, t) - \mathbf{v}_F(\mathbf{x}, \mathbf{y}, t)\|_{L^2(g_t)}^2 dt. \quad (\text{S.20})$$

Thus, to construct Proposition 2, we only need to consider  $\mathcal{L}(\hat{\mathbf{v}}) - \mathcal{L}(\mathbf{v}_F)$ , which can be further decomposed as:

$$\mathcal{L}(\hat{\mathbf{v}}) - \mathcal{L}(\mathbf{v}_F) = \underbrace{\mathcal{L}(\hat{\mathbf{v}}) - \inf_{\mathbf{v} \in \text{FNN}} \mathcal{L}(\mathbf{v})}_{\text{Generalization Error}} + \underbrace{\inf_{\mathbf{v} \in \text{FNN}} \{\mathcal{L}(\mathbf{v}) - \mathcal{L}(\mathbf{v}_F)\}}_{\text{Approximation Error}}. \quad (\text{S.21})$$

To handle the Approximation Error in (S.21), we need the following proposition, whose proof is given in Section D.1.

**Proposition P2** *Let Assumptions 1–3 hold and  $\varepsilon_* > 0$  be a sufficiently small universal constant. Given an approximation error  $\varepsilon \in (0, \varepsilon_*)$ , we choose the hypothesis network class  $\text{FNN} = \text{FNN}(L, M, J, K, \kappa, \gamma_1, \gamma_2, \gamma_3)$  with*

$$\begin{aligned} L &\sim d_x + d_y + \log \frac{1}{\varepsilon}, & M &\sim \frac{d_x^{d_x+3/2} (B\omega)^{d_y} \log^{(d_x+1)/2} \{d_x \varepsilon^{-1} (1-T)^{-1}\}}{(1-T)^{2d_x+3} \varepsilon^{d_x+d_y+1}}, \\ J &\sim \frac{d_x^{d_x+3/2} (B\omega)^{d_y} \log^{(d_x+1)/2} \{d_x \varepsilon^{-1} (1-T)^{-1}\}}{(1-T)^{2d_x+3} \varepsilon^{d_x+d_y+1}} \left( d_x + d_y + \log \frac{1}{\varepsilon} \right), \\ \kappa &\sim 1 \vee B\omega \vee \frac{d_x \log^{1/2} \{d_x \varepsilon^{-1} (1-T)^{-1}\}}{(1-T)^2} \vee \frac{d_x^{3/2} \log^{1/2} \{d_x \varepsilon^{-1} (1-T)^{-1}\}}{(1-T)^3}, \\ K &\sim \frac{d_x^{1/2} \log^{1/2} \{d_x \varepsilon^{-1} (1-T)^{-1}\}}{1-T}, & \gamma_1 &= \frac{10d_x^2}{(1-T)^2}, \\ \gamma_2 &= 10d_y\omega, & \gamma_3 &\sim \frac{d_x^{3/2} \log^{1/2} \{d_x \varepsilon^{-1} (1-T)^{-1}\}}{(1-T)^3}. \end{aligned}$$

There exists some  $\tilde{\mathbf{v}}(\mathbf{x}, \mathbf{y}, t) \in \text{FNN}(L, M, J, K, \kappa, \gamma_1, \gamma_2, \gamma_3)$  such that

$$\|\tilde{\mathbf{v}}(\mathbf{x}, \mathbf{y}, t) - \mathbf{v}_F(\mathbf{x}, \mathbf{y}, t)\|_{L^2(g_t)} \leq \varepsilon \sqrt{d_x + 1}$$

for any  $t \in [0, T]$  with  $T < 1$ .

In the sequel, we select  $\text{FNN} = \text{FNN}(L, M, J, K, \kappa, \gamma_1, \gamma_2, \gamma_3)$  in Proposition P2. By (S.20), we have

$$\inf_{\mathbf{v} \in \text{FNN}} \{\mathcal{L}(\mathbf{v}) - \mathcal{L}(\mathbf{v}_F)\} \leq \frac{1}{T} \int_0^T \|\tilde{\mathbf{v}}(\mathbf{x}, \mathbf{y}, t) - \mathbf{v}_F(\mathbf{x}, \mathbf{y}, t)\|_{L^2(g_t)}^2 dt \leq (d_x + 1)\varepsilon^2. \quad (\text{S.22})$$

Now we begin to control the Generalization Error in (S.21). Since  $\hat{\mathbf{v}} \in \arg \min_{\mathbf{v} \in \text{FNN}} \widehat{\mathcal{L}}(\mathbf{v})$ , then

$$\begin{aligned} \mathcal{L}(\hat{\mathbf{v}}) - \inf_{\mathbf{v} \in \text{FNN}} \mathcal{L}(\mathbf{v}) &= \mathcal{L}(\hat{\mathbf{v}}) - \widehat{\mathcal{L}}(\hat{\mathbf{v}}) + \widehat{\mathcal{L}}(\hat{\mathbf{v}}) - \widehat{\mathcal{L}}(\check{\mathbf{v}}) + \widehat{\mathcal{L}}(\check{\mathbf{v}}) - \mathcal{L}(\check{\mathbf{v}}) \\ &\leq \mathcal{L}(\hat{\mathbf{v}}) - \widehat{\mathcal{L}}(\hat{\mathbf{v}}) + \widehat{\mathcal{L}}(\check{\mathbf{v}}) - \mathcal{L}(\check{\mathbf{v}}) \leq 2 \sup_{\mathbf{v} \in \text{FNN}} |\mathcal{L}(\mathbf{v}) - \widehat{\mathcal{L}}(\mathbf{v})|, \end{aligned} \quad (\text{S.23})$$

where  $\check{\mathbf{v}} \in \arg \min_{\mathbf{v} \in \text{FNN}} \mathcal{L}(\mathbf{v})$ . Hence, to control the Generalization Error in (S.21), it suffices to control  $\sup_{\mathbf{v} \in \text{FNN}} |\mathcal{L}(\mathbf{v}) - \widehat{\mathcal{L}}(\mathbf{v})|$ . Define

$$\begin{aligned} \ell(\mathbf{x}, \mathbf{y}, \mathbf{v}) &:= \frac{1}{T} \int_0^T \mathbb{E}_{\mathbf{W}} \left\{ \left| \mathbf{x} - \frac{t}{\sqrt{1-t^2}} \mathbf{W} - \mathbf{v}(t\mathbf{x} + \sqrt{1-t^2} \mathbf{W}, \mathbf{y}, t) \right|_2^2 \right\} dt, \\ \hat{\ell}(\mathbf{x}, \mathbf{y}, \mathbf{v}) &:= \frac{1}{m} \sum_{j=1}^m \left| \mathbf{x} - \frac{t_j}{\sqrt{1-t_j^2}} \mathbf{W}_j - \mathbf{v}(t_j \mathbf{x} + \sqrt{1-t_j^2} \mathbf{W}_j, \mathbf{y}, t_j) \right|_2^2. \end{aligned} \quad (\text{S.24})$$

By (5) and (6), we have  $\mathcal{L}(\mathbf{v}) = \mathbb{E}_{\mathbf{X}, \mathbf{Y}} \{\ell(\mathbf{X}, \mathbf{Y}, \mathbf{v})\}$  and  $\widehat{\mathcal{L}}(\mathbf{v}) = n^{-1} \sum_{i=1}^n \hat{\ell}(\mathbf{X}_i, \mathbf{Y}_i, \mathbf{v})$ .

Introducing  $\bar{\mathcal{L}}(\mathbf{v}) := n^{-1} \sum_{i=1}^n \ell(\mathbf{X}_i, \mathbf{Y}_i, \mathbf{v})$ , we have

$$\begin{aligned} \sup_{\mathbf{v} \in \text{FNN}} |\mathcal{L}(\mathbf{v}) - \widehat{\mathcal{L}}(\mathbf{v})| &\leq \sup_{\mathbf{v} \in \text{FNN}} |\mathcal{L}(\mathbf{v}) - \bar{\mathcal{L}}(\mathbf{v}) + \bar{\mathcal{L}}(\mathbf{v}) - \widehat{\mathcal{L}}(\mathbf{v})| \\ &\leq \underbrace{\frac{1}{n} \sup_{\mathbf{v} \in \text{FNN}} \left| \sum_{i=1}^n [\mathbb{E}_{\mathbf{X}, \mathbf{Y}} \{\ell(\mathbf{X}, \mathbf{Y}, \mathbf{v})\} - \ell(\mathbf{X}_i, \mathbf{Y}_i, \mathbf{v})] \right|}_{\text{term 1}} \\ &\quad + \underbrace{\frac{1}{n} \sup_{\mathbf{v} \in \text{FNN}} \left| \sum_{i=1}^n [\ell(\mathbf{X}_i, \mathbf{Y}_i, \mathbf{v}) - \hat{\ell}(\mathbf{X}_i, \mathbf{Y}_i, \mathbf{v})] \right|}_{\text{term 2}}. \end{aligned} \quad (\text{S.25})$$

Define  $\mathcal{H} := \{\ell(\cdot, \cdot, \mathbf{v}) : \mathbf{v} \in \text{FNN}(L, M, J, K, \kappa, \gamma_1, \gamma_2, \gamma_3)\}$ . Since  $\|\mathbf{x}\|_\infty \leq 1$  and  $\mathbf{W} \sim \mathcal{N}(\mathbf{0}, \mathbf{I}_{d_x})$ , we have

$$\begin{aligned} \ell(\mathbf{x}, \mathbf{y}, \mathbf{v}) &= \frac{1}{T} \int_0^T \mathbb{E}_{\mathbf{W}} \left\{ \left| \mathbf{x} - \frac{t}{\sqrt{1-t^2}} \mathbf{W} - \mathbf{v}(t\mathbf{x} + \sqrt{1-t^2} \mathbf{W}, \mathbf{y}, t) \right|_2^2 \right\} dt \\ &\leq \frac{2}{T} \int_0^T \left[ \mathbb{E}_{\mathbf{W}} \left( \left| \mathbf{x} - \frac{t}{\sqrt{1-t^2}} \mathbf{W} \right|_2^2 \right) + \mathbb{E}_{\mathbf{W}} \left\{ \left| \mathbf{v}(t\mathbf{x} + \sqrt{1-t^2} \mathbf{W}, \mathbf{y}, t) \right|_2^2 \right\} \right] dt \\ &\leq \frac{2d_x}{T} \int_0^T \frac{dt}{1-t^2} + 2 \sup_{\mathbf{x}, \mathbf{y}, t} \|\mathbf{v}(\mathbf{x}, \mathbf{y}, t)\|_2^2 \leq \frac{2d_x}{1-T} + 2K^2 \end{aligned} \quad (\text{S.26})$$

for any function  $\ell(\cdot, \cdot, \mathbf{v}) \in \mathcal{H}$  and  $(\mathbf{x}, \mathbf{y}) \in [0, 1]^{d_x} \times [0, B]^{d_y}$ .

We first bound term 1 in (S.25). To do this, we need the following two lemmas.

**Lemma 4** Write  $\mathcal{V} = \text{FNN}(L, M, J, K, \kappa, \gamma_1, \gamma_2, \gamma_3)$ . The covering numbers of  $\mathcal{V}$  and  $\mathcal{H}$  satisfy

$$\begin{aligned} \log \mathcal{N}(\delta, \mathcal{V}, \|\cdot\|_{L^\infty([-R, R]^{d_x} \times [0, B]^{d_y} \times [0, 1])}) &\leq C_1 J L \log\{LM(R \vee B \vee 1)\kappa\delta^{-1}\}, \\ \log \mathcal{N}(\delta, \mathcal{H}, \|\cdot\|_{L^\infty([0, 1]^{d_x} \times [0, B]^{d_y})}) &\leq C_2 J L \log\left(\{K + (1 - T)^{-1/2}d_x^{1/2}\}LM\kappa\delta^{-1}\right. \\ &\quad \left.\times \log^{1/2}[Kd_x^{1/2}\delta^{-1}\{K + (1 - T)^{-1/2}d_x^{1/2}\}]\right) \end{aligned}$$

for some universal constants  $C_1, C_2 > 0$ , where  $B > 0$  is specified in Assumption 1.

**Lemma 5** Let  $\mathcal{F}$  be a bounded function class, i.e., there exists a constant  $B$  such that for any  $f \in \mathcal{F}$  and any  $\mathbf{x}$  in its domain,  $0 \leq f(\mathbf{x}) \leq B$ . Let  $\mathbf{X}, \dots, \mathbf{X}_n \in \mathbb{R}^{d_x}$  be i.i.d. random variables. For any  $\varepsilon \in (0, 1)$  and  $f \in \mathcal{F}$ , we have

$$\mathbb{P}\left(\frac{1}{n}\left|\sum_{i=1}^n [f(\mathbf{X}_i) - \mathbb{E}\{f(\mathbf{X})\}]\right| > \varepsilon\right) \leq 2 \exp\left(-\frac{2n\varepsilon^2}{B^2}\right).$$

The proof of Lemma 4 is given in Section G.1, while Lemma 5 is stated as Theorem 1 of Boucheron et al. (2003). Let  $\{\ell(\cdot, \cdot, \mathbf{v}_k)\}_{k=1}^{N_1}$  be a  $\delta$ -covering of  $\mathcal{H}$ , i.e. for each  $\ell(\cdot, \cdot, \mathbf{v}) \in \mathcal{H}$ , there exists a corresponding index  $k$ , s.t.  $\|\ell(\cdot, \cdot, \mathbf{v}) - \ell(\cdot, \cdot, \mathbf{v}_k)\|_{L^\infty([0, 1]^{d_x} \times [0, B]^{d_y})} \leq \delta$ . Consequently, for any  $\mathbf{v} \in \text{FNN}$ , we can assert

$$\begin{aligned} &\frac{1}{n}\left|\sum_{i=1}^n [\mathbb{E}_{\mathbf{X}, \mathbf{Y}}\{\ell(\mathbf{X}, \mathbf{Y}, \mathbf{v})\} - \ell(\mathbf{X}_i, \mathbf{Y}_i, \mathbf{v})]\right| \\ &\leq \max_{1 \leq k \leq N_1} \frac{1}{n}\left|\sum_{i=1}^n [\mathbb{E}_{\mathbf{X}, \mathbf{Y}}\{\ell(\mathbf{X}, \mathbf{Y}, \mathbf{v}_k)\} - \ell(\mathbf{X}_i, \mathbf{Y}_i, \mathbf{v}_k)]\right| + 2\delta. \end{aligned}$$

Taking supremum over  $\mathcal{H}$  on both sides, we have

$$\begin{aligned} &\sup_{\ell \in \mathcal{H}} \frac{1}{n}\left|\sum_{i=1}^n [\mathbb{E}_{\mathbf{X}, \mathbf{Y}}\{\ell(\mathbf{X}, \mathbf{Y}, \mathbf{v})\} - \ell(\mathbf{X}_i, \mathbf{Y}_i, \mathbf{v})]\right| \\ &\leq \max_{1 \leq k \leq N_1} \frac{1}{n}\left|\sum_{i=1}^n [\mathbb{E}_{\mathbf{X}, \mathbf{Y}}\{\ell(\mathbf{X}, \mathbf{Y}, \mathbf{v}_k)\} - \ell(\mathbf{X}_i, \mathbf{Y}_i, \mathbf{v}_k)]\right| + 2\delta. \end{aligned}$$

Thus, it holds that

$$\begin{aligned}
& \mathbb{P} \left( \sup_{\ell \in \mathcal{H}} \frac{1}{n} \left| \sum_{i=1}^n [\mathbb{E}_{\mathbf{X}, \mathbf{Y}} \{\ell(\mathbf{X}, \mathbf{Y}, \mathbf{v})\} - \ell(\mathbf{X}_i, \mathbf{Y}_i, \mathbf{v})] \right| > \varepsilon_1 + 2\delta \right) \\
& \leq \mathbb{P} \left( \max_{1 \leq k \leq N_1} \frac{1}{n} \left| \sum_{i=1}^n [\mathbb{E}_{\mathbf{X}, \mathbf{Y}} \{\ell(\mathbf{X}, \mathbf{Y}, \mathbf{v}_k)\} - \ell(\mathbf{X}_i, \mathbf{Y}_i, \mathbf{v}_k)] \right| > \varepsilon_1 \right) \\
& \leq \sum_{k=1}^{N_1} \mathbb{P} \left( \frac{1}{n} \left| \sum_{i=1}^n [\mathbb{E}_{\mathbf{X}, \mathbf{Y}} \{\ell(\mathbf{X}, \mathbf{Y}, \mathbf{v}_k)\} - \ell(\mathbf{X}_i, \mathbf{Y}_i, \mathbf{v}_k)] \right| > \varepsilon_1 \right).
\end{aligned}$$

By (S.26),  $\mathcal{H}$  is a bounded function class with boundedness constant  $B_{\mathcal{H}} = 2d_x(1-T)^{-1} + 2K^2$ . Invoking Lemma 5, we have

$$\mathbb{P} \left( \sup_{\ell \in \mathcal{H}} \left| \frac{1}{n} \sum_{i=1}^n [\mathbb{E}_{\mathbf{X}, \mathbf{Y}} \{\ell(\mathbf{X}, \mathbf{Y}, \mathbf{v})\} - \ell(\mathbf{X}_i, \mathbf{Y}_i, \mathbf{v})] \right| > \varepsilon_1 + 2\delta \right) \leq 2N_1 \exp \left( -\frac{2n\varepsilon_1^2}{B_{\mathcal{H}}^2} \right),$$

Letting  $\varepsilon_1 = [2^{-1}n^{-1}B_{\mathcal{H}}^2 \log(2\delta^{-1}N_1)]^{1/2}$ , we get with probability at most  $\delta$ ,

$$\sup_{\ell \in \mathcal{H}} \left| \frac{1}{n} \sum_{i=1}^n [\mathbb{E}_{\mathbf{X}, \mathbf{Y}} \{\ell(\mathbf{X}, \mathbf{Y}, \mathbf{v})\} - \ell(\mathbf{X}_i, \mathbf{Y}_i, \mathbf{v})] \right| > \sqrt{\frac{B_{\mathcal{H}}^2 \log(2N_1/\delta)}{2n}} + 2\delta. \quad (\text{S.27})$$

Then we complete the analysis of term 1 in (S.25).

To bound term 2 in (S.25), we need some additional truncation arguments. More specifically, we define

$$\begin{aligned}
r_D(\mathbf{w}, t, \mathbf{x}, \mathbf{y}, \mathbf{v}) & := \left| \mathbf{x} - \frac{t}{\sqrt{1-t^2}} \mathbf{w} - \mathbf{v}(t\mathbf{x} + \sqrt{1-t^2} \mathbf{w}, \mathbf{y}, t) \right|_2^2 \mathbb{I}(|\mathbf{w}|_{\infty} \leq D), \\
\ell_D(\mathbf{x}, \mathbf{y}, \mathbf{v}) & := \mathbb{E}_{t, \mathbf{W}} \{r_D(\mathbf{W}, t, \mathbf{x}, \mathbf{y}, \mathbf{v})\}, \quad \hat{\ell}_D(\mathbf{x}, \mathbf{y}, \mathbf{v}) := \frac{1}{m} \sum_{j=1}^m r_D(\mathbf{W}_j, t_j, \mathbf{x}, \mathbf{y}, \mathbf{v}) \quad (\text{S.28})
\end{aligned}$$

with some  $D > 0$  determined later. Setting  $\Delta = \Delta_1 + \Delta_2 + \Delta_3$ , term 2 has the following decomposition:

$$\begin{aligned}
& \mathbb{P} \left[ \frac{1}{n} \sup_{\mathbf{v} \in \text{FNN}} \left| \sum_{i=1}^n \{\ell(\mathbf{X}_i, \mathbf{Y}_i, \mathbf{v}) - \hat{\ell}(\mathbf{X}_i, \mathbf{Y}_i, \mathbf{v})\} \right| > \Delta \right] \\
& \leq \underbrace{\mathbb{P} \left\{ \frac{1}{n} \sum_{i=1}^n \sup_{\mathbf{v} \in \text{FNN}} |\ell(\mathbf{X}_i, \mathbf{Y}_i, \mathbf{v}) - \ell_D(\mathbf{X}_i, \mathbf{Y}_i, \mathbf{v})| > \Delta_1 \right\}}_{\text{Truncation Error (I)}}
\end{aligned}$$

$$\begin{aligned}
& + \underbrace{\sum_{i=1}^n \mathbb{P} \left\{ \sup_{\mathbf{v} \in \text{FNN}} |\ell_D(\mathbf{X}_i, \mathbf{Y}_i, \mathbf{v}) - \hat{\ell}_D(\mathbf{X}_i, \mathbf{Y}_i, \mathbf{v})| > \Delta_2 \right\}}_{\text{Statistical Error}} \\
& + \underbrace{\sum_{i=1}^n \mathbb{P} \left\{ \sup_{\mathbf{v} \in \text{FNN}} |\hat{\ell}(\mathbf{X}_i, \mathbf{Y}_i, \mathbf{v}) - \hat{\ell}_D(\mathbf{X}_i, \mathbf{Y}_i, \mathbf{v})| > \Delta_3 \right\}}_{\text{Truncation Error (II)}}. \tag{S.29}
\end{aligned}$$

We first control Truncation Error (I) in (S.29). By (S.24) and (S.28), we have

$$\begin{aligned}
& \ell(\mathbf{X}_i, \mathbf{Y}_i, \mathbf{v}) - \ell_D(\mathbf{X}_i, \mathbf{Y}_i, \mathbf{v}) \\
& = \mathbb{E}_{t, \mathbf{W}} \left\{ \left| \mathbf{X}_i - \frac{t}{\sqrt{1-t^2}} \mathbf{W} - \mathbf{v}(t\mathbf{X}_i + \sqrt{1-t^2}\mathbf{W}, \mathbf{Y}_i, t) \right|_2^2 \mathbb{I}(|\mathbf{W}|_\infty > D) \right\} \\
& \leq \mathbb{E}_t \left[ \mathbb{E}_{\mathbf{W}}^{1/2} \left\{ \left| \mathbf{X}_i - \frac{t}{\sqrt{1-t^2}} \mathbf{W} - \mathbf{v}(t\mathbf{X}_i + \sqrt{1-t^2}\mathbf{W}, \mathbf{Y}_i, t) \right|_2^4 \right\} \mathbb{P}^{1/2}(|\mathbf{W}|_\infty > D) \right].
\end{aligned}$$

Since  $|\mathbf{v}(\mathbf{x}, \mathbf{y}, t)|_2 \leq K$  for any  $\mathbf{v} \in \text{FNN}(L, M, J, K, \kappa, \gamma_1, \gamma_2, \gamma_3)$ ,  $\mathbf{W} \sim \mathcal{N}(\mathbf{0}, \mathbf{I}_{d_x})$  and  $|\mathbf{X}_i|_\infty \leq 1$  by Assumption 2, it holds that

$$\begin{aligned}
& \mathbb{E}_{\mathbf{W}}^{1/2} \left\{ \left| \mathbf{X}_i - \frac{t}{\sqrt{1-t^2}} \mathbf{W} - \mathbf{v}(t\mathbf{X}_i + \sqrt{1-t^2}\mathbf{W}, \mathbf{Y}_i, t) \right|_2^4 \right\} \\
& \leq 2 \left\{ \mathbb{E}_{\mathbf{W}} \left( \left| \mathbf{X}_i - \frac{t}{\sqrt{1-t^2}} \mathbf{W} \right|_2^4 \right) + \mathbb{E} \left( \left| \mathbf{v}(t\mathbf{X}_i + \sqrt{1-t^2}\mathbf{W}, t) \right|_2^4 \right) \right\}^{1/2} \\
& \leq 2 \left\{ 4|\mathbf{X}_i|_2^4 + \frac{4t^4}{(1-t^2)^2} \mathbb{E}(|\mathbf{W}|_2^4) + K^4 \right\}^{1/2} \leq 2 \left\{ 4d_x^2 + \frac{4t^4}{(1-t^2)^2} d_x(d_x + 2) + K^4 \right\}^{1/2} \\
& \leq 2 \left\{ \frac{8(d_x + 2)^2}{(1-t^2)^2} + K^4 \right\}^{1/2} \leq \frac{4\sqrt{2}(d_x + 2)}{1-t^2} + 2K^2.
\end{aligned}$$

Write  $\mathbf{W} = (W_1, \dots, W_{d_x})^\top$ . It holds that

$$\mathbb{P}(|\mathbf{W}|_\infty > D) \leq \sum_{k=1}^{d_x} \mathbb{P}(|W_k| > D) \leq 2d_x \exp\left(-\frac{D^2}{2}\right).$$

Combining above estimations and notice  $t \leq T < 1$ , we have

$$\ell(\mathbf{X}_i, \mathbf{Y}_i, \mathbf{v}) - \ell_D(\mathbf{X}_i, \mathbf{Y}_i, \mathbf{v}) \leq \left\{ \frac{8(d_x + 2)^{3/2}}{1-T} + 4d_x^{1/2}K^2 \right\} \exp\left(-\frac{D^2}{4}\right).$$

Letting  $\Delta_1 = \{8(d_x + 2)^{3/2}(1-T)^{-1} + 4d_x^{1/2}K^2\} \exp(-D^2/4)$ , it then holds that

$$\mathbb{P} \left\{ \frac{1}{n} \sum_{i=1}^n \sup_{\mathbf{v} \in \text{FNN}} |\ell(\mathbf{X}_i, \mathbf{Y}_i, \mathbf{v}) - \ell_D(\mathbf{X}_i, \mathbf{Y}_i, \mathbf{v})| > \Delta_1 \right\} = 0. \tag{S.30}$$

Next, we deal with Truncation Error (II) in (S.29). We have

$$\begin{aligned}
& \sum_{i=1}^n \mathbb{P} \left\{ \sup_{\mathbf{v} \in \text{FNN}} |\hat{\ell}(\mathbf{X}_i, \mathbf{Y}_i, \mathbf{v}) - \hat{\ell}_D(\mathbf{X}_i, \mathbf{Y}_i, \mathbf{v})| > \Delta_3 \right\} \\
&= \sum_{i=1}^n \mathbb{E}_{\mathbf{X}_i, \mathbf{Y}_i} \left[ \mathbb{P} \left\{ \sup_{\mathbf{v} \in \text{FNN}} |\hat{\ell}(\mathbf{X}_i, \mathbf{Y}_i, \mathbf{v}) - \hat{\ell}_D(\mathbf{X}_i, \mathbf{Y}_i, \mathbf{v})| > \Delta_3 \mid \mathbf{X}_i, \mathbf{Y}_i \right\} \right] \\
&= \sum_{i=1}^n \mathbb{E}_{\mathbf{X}_i, \mathbf{Y}_i} \left[ \mathbb{P} \left\{ \sup_{\mathbf{v} \in \text{FNN}} |\hat{\ell}(\mathbf{x}, \mathbf{y}, \mathbf{v}) - \hat{\ell}_D(\mathbf{x}, \mathbf{y}, \mathbf{v})| > \Delta_3 \right\} \Big|_{(\mathbf{x}, \mathbf{y}) = (\mathbf{X}_i, \mathbf{Y}_i)} \right]. \tag{S.31}
\end{aligned}$$

By (S.24) and (S.28), it holds that

$$\begin{aligned}
& \hat{\ell}(\mathbf{x}, \mathbf{y}, \mathbf{v}) - \hat{\ell}_D(\mathbf{x}, \mathbf{y}, \mathbf{v}) \\
&= \frac{1}{m} \sum_{j=1}^m \left| \mathbf{x} - \frac{t}{\sqrt{1-t^2}} \mathbf{W}_j - \mathbf{v}(t\mathbf{x} + \sqrt{1-t^2} \mathbf{W}_j, \mathbf{y}, t) \right|_2^2 \mathbb{I}(|\mathbf{W}_j|_\infty > D).
\end{aligned}$$

Thus, if  $|\mathbf{W}_j|_\infty \leq D$  for all  $j = 1, \dots, m$ , we have

$$\sup_{\mathbf{v} \in \text{FNN}} |\hat{\ell}(\mathbf{x}, \mathbf{y}, \mathbf{v}) - \hat{\ell}_D(\mathbf{x}, \mathbf{y}, \mathbf{v})| = 0.$$

Since  $\mathbf{W}_j \sim \mathcal{N}(\mathbf{0}, \mathbf{I}_{d_x})$ , this implies

$$\begin{aligned}
& \mathbb{P} \left\{ \sup_{\mathbf{v} \in \text{FNN}} |\hat{\ell}(\mathbf{x}, \mathbf{y}, \mathbf{v}) - \hat{\ell}_D(\mathbf{x}, \mathbf{y}, \mathbf{v})| > 0 \right\} \\
&\leq \sum_{j=1}^m \mathbb{P}(|\mathbf{W}_j|_\infty > D) \leq 2md_x \exp\left(-\frac{D^2}{2}\right). \tag{S.32}
\end{aligned}$$

Combining (S.31) and (S.32), and letting  $\Delta_3 = 0$ , it holds that

$$\sum_{i=1}^n \mathbb{P} \left\{ \sup_{\mathbf{v} \in \text{FNN}} |\hat{\ell}(\mathbf{X}_i, \mathbf{Y}_i, \mathbf{v}) - \hat{\ell}_D(\mathbf{X}_i, \mathbf{Y}_i, \mathbf{v})| > \Delta_3 \right\} \leq 2nmd_x \exp\left(-\frac{D^2}{2}\right). \tag{S.33}$$

Finally, we control the Statistical Error in (S.29). We have

$$\begin{aligned}
& \sum_{i=1}^n \mathbb{P} \left\{ \sup_{\mathbf{v} \in \text{FNN}} |\ell_D(\mathbf{X}_i, \mathbf{Y}_i, \mathbf{v}) - \hat{\ell}_D(\mathbf{X}_i, \mathbf{Y}_i, \mathbf{v})| > \Delta_2 \right\} \\
&= \sum_{i=1}^n \mathbb{E}_{\mathbf{X}_i, \mathbf{Y}_i} \left[ \mathbb{P} \left\{ \sup_{\mathbf{v} \in \text{FNN}} |\ell_D(\mathbf{X}_i, \mathbf{Y}_i, \mathbf{v}) - \hat{\ell}_D(\mathbf{X}_i, \mathbf{Y}_i, \mathbf{v})| > \Delta_2 \mid \mathbf{X}_i, \mathbf{Y}_i \right\} \right] \\
&= \sum_{i=1}^n \mathbb{E}_{\mathbf{X}_i, \mathbf{Y}_i} \left[ \mathbb{P} \left\{ \sup_{\mathbf{v} \in \text{FNN}} |\ell_D(\mathbf{x}, \mathbf{y}, \mathbf{v}) - \hat{\ell}_D(\mathbf{x}, \mathbf{y}, \mathbf{v})| > \Delta_2 \right\} \Big|_{(\mathbf{x}, \mathbf{y}) = (\mathbf{X}_i, \mathbf{Y}_i)} \right]. \tag{S.34}
\end{aligned}$$

By (S.28), it holds that

$$\begin{aligned} \ell_D(\mathbf{x}, \mathbf{y}, \mathbf{v}) - \hat{\ell}_D(\mathbf{x}, \mathbf{y}, \mathbf{v}) & \\ &= \mathbb{E}_{t, \mathbf{W}} \{r_D(\mathbf{W}, t, \mathbf{x}, \mathbf{y}, \mathbf{v})\} - \frac{1}{m} \sum_{j=1}^m r_D(\mathbf{W}_j, t_j, \mathbf{x}, \mathbf{y}, \mathbf{v}). \end{aligned} \quad (\text{S.35})$$

For any fixed  $(\mathbf{x}, \mathbf{y}) \in [0, 1]^{d_x} \times [0, B]^{d_y}$ , we define

$$\mathcal{R}_{\mathbf{x}, \mathbf{y}}^D := \{r_D(\cdot, \cdot, \mathbf{x}, \mathbf{y}, \mathbf{v}) : \mathbf{v} \in \text{FNN}(L, M, J, K, \kappa, \gamma_1, \gamma_2, \gamma_3)\}.$$

Denote by  $\mathbb{I}_D(\mathbf{w}) := \mathbb{I}(|\mathbf{w}|_\infty \leq D)$ . Since  $0 \leq t \leq T < 1$ , we have

$$\begin{aligned} r_D(\mathbf{w}, t, \mathbf{x}, \mathbf{y}, \mathbf{v}) &= \left| \mathbf{x} - \frac{t}{\sqrt{1-t^2}} \mathbf{w} - \mathbf{v}(t\mathbf{x} + \sqrt{1-t^2} \mathbf{w}, \mathbf{y}, t) \right|_2^2 \mathbb{I}_D(\mathbf{w}) \\ &\leq 4|\mathbf{x}|_2^2 + \frac{4}{1-T} |\mathbf{w}|_2^2 \mathbb{I}_D(\mathbf{w}) + 2 \sup_{\mathbf{x}, \mathbf{y}, t} |\mathbf{v}(\mathbf{x}, \mathbf{y}, t)|_2^2 \leq \frac{4d_x(D+1)^2}{1-T} + 2K^2 \end{aligned} \quad (\text{S.36})$$

for any  $r_D(\cdot, \cdot, \mathbf{x}, \mathbf{y}, \mathbf{v}) \in \mathcal{R}_{\mathbf{x}, \mathbf{y}}^D$  and  $(\mathbf{w}, t) \in \mathbb{R}^{d_x} \times [0, T]$ .

Note when  $|\mathbf{w}|_\infty \leq D$  and  $|\mathbf{x}|_\infty \leq 1$ , we have  $t\mathbf{x} + \sqrt{1-t^2} \mathbf{w} \in [-D-1, D+1]^{d_x}$ . Denote by  $\mathbf{w}_t = t\mathbf{x} + \sqrt{1-t^2} \mathbf{w}$  and  $\mathcal{K}_D = [-D-1, D+1]^{d_x} \times [0, B]^{d_y} \times [0, T]$ . Let  $\{\mathbf{v}_i\}_{i=1}^{N_2}$  be a  $G(\delta)$ -covering of FNN w.r.t.  $\|\cdot\|_{L^\infty(\mathcal{K}_D)}$ , i.e. for any  $\mathbf{v} \in \text{FNN}$ , there exists a corresponding index  $k$ , s.t.  $\|\mathbf{v} - \mathbf{v}_k\|_{L^\infty(\mathcal{K}_D)} \leq G(\delta)$ . For any fixed  $(\mathbf{x}, \mathbf{y}) \in [0, 1]^{d_x} \times [0, B]^{d_y}$ , it holds that

$$\begin{aligned} &|r_D(\mathbf{w}, t, \mathbf{x}, \mathbf{y}, \mathbf{v}_k) - r_D(\mathbf{w}, t, \mathbf{x}, \mathbf{y}, \mathbf{v})| \\ &= \left| \left\langle \left\{ 2\mathbf{x} - \frac{2t}{\sqrt{1-t^2}} \mathbf{w} - \mathbf{v}_k(\mathbf{w}_t, \mathbf{y}, t) - \mathbf{v}(\mathbf{w}_t, \mathbf{y}, t) \right\} \mathbb{I}_D(\mathbf{w}), \right. \right. \\ &\quad \left. \left. \left\{ \mathbf{v}_k(\mathbf{w}_t, \mathbf{y}, t) - \mathbf{v}(\mathbf{w}_t, \mathbf{y}, t) \right\} \mathbb{I}_D(\mathbf{w}) \right\rangle \right| \\ &\leq \left| \left\{ 2\mathbf{x} - \frac{2t}{\sqrt{1-t^2}} \mathbf{w} - \mathbf{v}_k(\mathbf{w}_t, \mathbf{y}, t) - \mathbf{v}(\mathbf{w}_t, \mathbf{y}, t) \right\} \mathbb{I}_D(\mathbf{w}) \right|_2 \\ &\quad \cdot \left| \left\{ \mathbf{v}_k(\mathbf{w}_t, \mathbf{y}, t) - \mathbf{v}(\mathbf{w}_t, \mathbf{y}, t) \right\} \mathbb{I}_D(\mathbf{w}) \right|_2 \\ &\leq \left\{ 2|\mathbf{x}|_2 + \frac{2t}{\sqrt{1-t^2}} |\mathbf{w}|_2 \mathbb{I}_D(\mathbf{w}) + |\mathbf{v}(\mathbf{w}_t, \mathbf{y}, t)|_2 + |\mathbf{v}_k(\mathbf{w}_t, \mathbf{y}, t)|_2 \right\} \|\mathbf{v} - \mathbf{v}_k\|_{L^\infty(\mathcal{K}_D)} \end{aligned} \quad (\text{S.37})$$

$$\leq \{2(1-T)^{-1/2}d_x^{1/2}(D+1) + 2K\} \cdot G(\delta).$$

for any  $(\mathbf{w}, t) \in \mathbb{R}^{d_x} \times [0, T]$ . Set  $G(\delta) = \{2(1-T)^{-1/2}d_x^{1/2}(D+1) + 2K\}^{-1}\delta$ . By (S.37), we can assert that a  $G(\delta)$ -covering of FNN w.r.t.  $\|\cdot\|_{L^\infty(\mathcal{K}_D)}$  induces a  $\delta$ -covering of  $\mathcal{R}_{\mathbf{x}, \mathbf{y}}^D$  w.r.t.  $\|\cdot\|_{L^\infty(\mathbb{R}^{d_x} \times [0, T])}$ .

By (S.35), for any  $\mathbf{v} \in \text{FNN}$ , we have

$$\begin{aligned} & |\ell_D(\mathbf{x}, \mathbf{y}, \mathbf{v}) - \hat{\ell}_D(\mathbf{x}, \mathbf{y}, \mathbf{v})| \\ &= \left| \mathbb{E}_{t, \mathbf{W}} \{r_D(\mathbf{W}, t, \mathbf{x}, \mathbf{y}, \mathbf{v})\} - \frac{1}{m} \sum_{j=1}^m r_D(\mathbf{W}_j, t_j, \mathbf{x}, \mathbf{y}, \mathbf{v}) \right| \\ &\leq \max_{1 \leq k \leq N_2} \left| \mathbb{E}_{t, \mathbf{W}} \{r_D(\mathbf{W}, t, \mathbf{x}, \mathbf{y}, \mathbf{v}_k)\} - \frac{1}{m} \sum_{j=1}^m r_D(\mathbf{W}_j, t_j, \mathbf{x}, \mathbf{y}, \mathbf{v}_k) \right| + 2\delta. \end{aligned}$$

Taking supremum on both sides, it holds that

$$\begin{aligned} & \sup_{\mathbf{v} \in \text{FNN}} |\ell_D(\mathbf{x}, \mathbf{y}, \mathbf{v}) - \hat{\ell}_D(\mathbf{x}, \mathbf{y}, \mathbf{v})| \\ &\leq 2\delta + \max_{1 \leq k \leq N_2} \left| \mathbb{E}_{t, \mathbf{W}} \{r_D(\mathbf{W}, t, \mathbf{x}, \mathbf{y}, \mathbf{v}_k)\} - \frac{1}{m} \sum_{j=1}^m r_D(\mathbf{W}_j, t_j, \mathbf{x}, \mathbf{y}, \mathbf{v}_k) \right|. \end{aligned}$$

Thus, we have

$$\begin{aligned} & \mathbb{P} \left\{ \sup_{\mathbf{v} \in \text{FNN}} |\ell_D(\mathbf{x}, \mathbf{y}, \mathbf{v}) - \hat{\ell}_D(\mathbf{x}, \mathbf{y}, \mathbf{v})| > \varepsilon_2 + 2\delta \right\} \tag{S.38} \\ &= \mathbb{P} \left[ \max_{1 \leq k \leq N_2} \left| \mathbb{E}_{t, \mathbf{W}} \{r_D(\mathbf{W}, t, \mathbf{x}, \mathbf{y}, \mathbf{v}_k)\} - \frac{1}{m} \sum_{j=1}^m r_D(\mathbf{W}_j, t_j, \mathbf{x}, \mathbf{y}, \mathbf{v}_k) \right| > \varepsilon_2 \right] \\ &\leq \sum_{k=1}^{N_2} \mathbb{P} \left[ \left| \mathbb{E}_{t, \mathbf{W}} \{r_D(\mathbf{W}, t, \mathbf{x}, \mathbf{y}, \mathbf{v}_k)\} - \frac{1}{m} \sum_{j=1}^m r_D(\mathbf{W}_j, t_j, \mathbf{x}, \mathbf{y}, \mathbf{v}_k) \right| > \varepsilon_2 \right]. \end{aligned}$$

By (S.36), for any fixed  $(\mathbf{x}, \mathbf{y}) \in [0, 1]^{d_x} \times [0, B]^{d_y}$ ,  $\mathcal{R}_{\mathbf{x}, \mathbf{y}}^D$  is a bounded function class with boundedness constant  $B_D = 4d_x(D+1)^2(1-T)^{-1} + 2K^2$ . Invoking Lemma 5, we obtain

$$\begin{aligned} & \mathbb{P} \left[ \left| \mathbb{E}_{t, \mathbf{W}} \{r_D(\mathbf{W}, t, \mathbf{x}, \mathbf{y}, \mathbf{v}_k)\} - \frac{1}{m} \sum_{j=1}^m r_D(\mathbf{W}_j, t_j, \mathbf{x}, \mathbf{y}, \mathbf{v}_k) \right| > \varepsilon_2 \right] \\ &\leq 2 \exp \left( -\frac{2m\varepsilon_2^2}{B_D^2} \right). \tag{S.39} \end{aligned}$$

Let  $\Delta_2 = \varepsilon_2 + 2\delta$ . Combining (S.34), (S.38) and (S.39), we have

$$\sum_{i=1}^n \mathbb{P} \left\{ \sup_{\mathbf{v} \in \text{FNN}} |\ell_D(\mathbf{X}_i, \mathbf{Y}_i, \mathbf{v}) - \hat{\ell}_D(\mathbf{X}_i, \mathbf{Y}_i, \mathbf{v})| > \Delta_2 \right\} \leq 2nN_2 \exp \left( -\frac{2m\varepsilon_2^2}{B_D^2} \right). \quad (\text{S.40})$$

Now return to (S.29). Combining (S.30), (S.33) and (S.40), by (S.29), it holds that, with probability at most  $2nmd_x \exp(-2^{-1}D^2) + 2nN_2 \exp(-2m\varepsilon_2^2 B_D^{-2})$ ,

$$\begin{aligned} & \frac{1}{n} \sup_{\mathbf{v} \in \text{FNN}} \left| \sum_{i=1}^n \{ \ell(\mathbf{X}_i, \mathbf{Y}_i, \mathbf{v}) - \hat{\ell}(\mathbf{X}_i, \mathbf{Y}_i, \mathbf{v}) \} \right| \\ & > \varepsilon_2 + 2\delta + \left\{ \frac{8(d_x + 2)^{3/2}}{1 - T} + 4d_x^{1/2}K^2 \right\} \exp \left( -\frac{D^2}{4} \right). \end{aligned} \quad (\text{S.41})$$

Recall  $B_D = 4d_x(D + 1)^2(1 - T)^{-1} + 2K^2$ . Letting

$$2nmd_x \exp \left( -\frac{D^2}{2} \right) = \delta, \quad 2nN_2 \exp \left( -\frac{2m\varepsilon_2^2}{B_D^2} \right) = \delta,$$

we have that, with probability at most  $2\delta$ ,

$$\begin{aligned} & \frac{1}{n} \sup_{\mathbf{v} \in \text{FNN}} \left| \sum_{i=1}^n \{ \ell(\mathbf{X}_i, \mathbf{Y}_i, \mathbf{v}) - \hat{\ell}(\mathbf{X}_i, \mathbf{Y}_i, \mathbf{v}) \} \right| \\ & > \left[ \frac{4d_x \{ \sqrt{2} \log^{1/2}(2nmd_x \delta^{-1}) + 1 \}^2}{1 - T} + 2K^2 \right] \sqrt{\frac{\log(2n\delta^{-1}N_2)}{2m}} + 2\delta \\ & \quad + \left\{ \frac{8(d_x + 2)^{3/2}}{1 - T} + 4d_x^{1/2}K^2 \right\} \cdot \sqrt{\frac{\delta}{2nmd_x}}. \end{aligned} \quad (\text{S.42})$$

Combining (S.27) and (S.42), by (S.25) and (S.23), it holds that, with probability at least  $1 - 3\delta$ ,

$$\begin{aligned} \mathcal{L}(\hat{\mathbf{v}}) - \inf_{\mathbf{v} \in \text{FNN}} \mathcal{L}(\mathbf{v}) & \leq \left[ \frac{2d_x \{ \sqrt{2} \log^{1/2}(2nmd_x \delta^{-1}) + 1 \}^2}{1 - T} + K^2 \right] \sqrt{\frac{8 \log(2n\delta^{-1}N_2)}{m}} \\ & \quad + \left\{ \frac{2(d_x + 2)^{3/2}}{1 - T} + d_x^{1/2}K^2 \right\} \cdot \sqrt{\frac{32\delta}{mnd_x}} \\ & \quad + \sqrt{\frac{2B_{\mathcal{H}}^2 \log(2N_1\delta^{-1})}{n}} + 8\delta. \end{aligned} \quad (\text{S.43})$$

Recall that  $\{ \ell(\cdot, \cdot, \mathbf{v}_i) \}_{i=1}^{N_1}$  is a  $\delta$ -covering of  $\mathcal{H}$  w.r.t.  $\| \cdot \|_{L^\infty([0,1]^{d_x} \times [0,B]^{d_y})}$ ,  $\{ \mathbf{v}_j \}_{j=1}^{N_2}$  is a  $\{ 2(1 - T)^{-1/2}d_x^{1/2}(D + 1) + 2K \}^{-1}\delta$ -covering of FNN w.r.t.  $\| \cdot \|_{L^\infty(\mathcal{K}_D)}$  where  $\mathcal{K}_D = [-D -$

$1, D+1]^{d_x} \times [0, B]^{d_y} \times [0, T]$  and  $2nmd_x \exp(-2^{-1}D^2) = \delta$ . By Proposition P2 and Lemma 4, it holds that

$$\begin{aligned} \log N_1 &\leq \frac{C_3 d_x^{d_x+3/2} (B\omega)^{d_y} \log^{(d_x+1)/2} \{d_x \varepsilon^{-1} (1-T)^{-1}\}}{(1-T)^{2d_x+3} \varepsilon^{d_x+d_y+1}} \left( d_x + d_y + \log \frac{1}{\varepsilon} \right)^2 \\ &\quad \times \left\{ \log \frac{1}{\delta} + d_x \log d_x - d_x \log(1-T) + (d_x + d_y) \log \frac{1}{\varepsilon} \right\}, \\ \log N_2 &\leq \frac{C_4 d_x^{d_x+3/2} (B\omega)^{d_y} \log^{(d_x+1)/2} \{d_x \varepsilon^{-1} (1-T)^{-1}\}}{(1-T)^{2d_x+3} \varepsilon^{d_x+d_y+1}} \left( d_x + d_y + \log \frac{1}{\varepsilon} \right)^2 \\ &\quad \times \left\{ \log \frac{1}{\delta} + d_x \log d_x - d_x \log(1-T) + (d_x + d_y) \log \frac{1}{\varepsilon} + \log \log(nm) \right\} \end{aligned}$$

when  $\delta, \varepsilon \rightarrow 0$  and  $T \rightarrow 1$ . Here,  $C_3, C_4 > 0$  are two universal constants.

Letting  $m = n$  and  $\delta = 3^{-1}n^{-2}$ , (S.43) implies that, with probability at least  $1 - n^{-2}$ ,

$$\begin{aligned} \mathcal{L}(\hat{\mathbf{v}}) - \inf_{\mathbf{v} \in \text{FNN}} \mathcal{L}(\mathbf{v}) & \tag{S.44} \\ &\leq \frac{C_5 d_x^{(2d_x+7)/4} (B\omega)^{d_y/2} \log^{(d_x+5)/4} \{d_x \varepsilon^{-1} (1-T)^{-1}\}}{(1-T)^{(2d_x+7)/2} \varepsilon^{(d_x+d_y+1)/2} n^{1/2}} \left( d_x + d_y + \log \frac{1}{\varepsilon} \right) \\ &\quad \times \left\{ \log^{1/2} n + d_x^{1/2} \log^{1/2} d_x + d_x^{1/2} \log^{1/2} \left( \frac{1}{1-T} \right) + (d_x^{1/2} + d_y^{1/2}) \log^{1/2} \left( \frac{1}{\varepsilon} \right) \right\}, \end{aligned}$$

where  $C_5 > 0$  is a universal constants. Combining (S.22) and (S.44), by (S.20) and (S.21), we have that, with probability at least  $1 - n^{-2}$ ,

$$\begin{aligned} &\frac{1}{T} \int_0^T \|\hat{\mathbf{v}}(\mathbf{x}, \mathbf{y}, t) - \mathbf{v}_F(\mathbf{x}, \mathbf{y}, t)\|_{L^2(g_t)}^2 dt \\ &\leq 2d_x \varepsilon^2 + \frac{C_5 d_x^{(2d_x+7)/4} (B\omega)^{d_y/2} \log^{(d_x+5)/4} \{d_x \varepsilon^{-1} (1-T)^{-1}\}}{(1-T)^{(2d_x+7)/2} \varepsilon^{(d_x+d_y+1)/2} n^{1/2}} \left( d_x + d_y + \log \frac{1}{\varepsilon} \right) \\ &\quad \times \left\{ \log^{1/2} n + d_x^{1/2} \log^{1/2} d_x + d_x^{1/2} \log^{1/2} \left( \frac{1}{1-T} \right) + (d_x^{1/2} + d_y^{1/2}) \log^{1/2} \left( \frac{1}{\varepsilon} \right) \right\}. \end{aligned}$$

Let  $\varepsilon = (1-T)^{-(2d_x+7)/(d_x+d_y+5)} n^{-1/(d_x+d_y+5)}$  with  $1-T \gg n^{-1/(2d_x+7)}$ . Therefore, for given  $(d_x, d_y)$ , it holds that

$$\frac{1}{T} \int_0^T \|\hat{\mathbf{v}}(\mathbf{x}, \mathbf{y}, t) - \mathbf{v}_F(\mathbf{x}, \mathbf{y}, t)\|_{L^2(g_t)}^2 dt = \tilde{\mathcal{O}} \left\{ \frac{(1-T)^{-(4d_x+14)/(d_x+d_y+5)}}{n^{2/(d_x+d_y+5)}} \right\}$$

with probability at least  $1 - n^{-2}$ . Here,  $\tilde{\mathcal{O}}(\cdot)$  omits the polynomial term of  $\log n$ . We complete the proof of Proposition 2.  $\square$

## D.1 Proof of Proposition P2

The goal is to find a network  $\tilde{\mathbf{v}}(\mathbf{x}, \mathbf{y}, t)$  in  $\text{FNN} = \text{FNN}(L, M, J, K, \kappa, \gamma_1, \gamma_2, \gamma_3)$  to approximate the true vector field  $\mathbf{v}_F(\mathbf{x}, \mathbf{y}, t)$ , where a major difficulty is that the input space  $\mathbb{R}^{d_x} \times [0, B]^{d_y} \times [0, T]$  is unbounded. To address this difficulty, we partition  $\mathbb{R}^{d_x}$  into a compact subset  $\mathcal{K}$  and its complement  $\mathcal{K}^c$ .

We first consider the approximation on  $\mathcal{K} \times [0, B]^{d_y} \times [0, T]$ . Let  $\mathcal{K} = \{\mathbf{x} \in \mathbb{R}^{d_x} : |\mathbf{x}|_\infty \leq R\}$  to be a  $d_x$ -dimensional hypercube with edge length  $2R > 0$ , where  $R$  will be determined later. Write  $\mathbf{v}_F(\mathbf{x}, \mathbf{y}, t) = (v_F^1(\mathbf{x}, \mathbf{y}, t), \dots, v_F^{d_x}(\mathbf{x}, \mathbf{y}, t))^T$ . On  $\mathcal{K} \times [0, B]^{d_y} \times [0, T]$ , we approximate each coordinate map  $v_F^k(\mathbf{x}, \mathbf{y}, t)$  separately.

We first rescale the input by  $\mathbf{x}' = (\mathbf{x} + R\mathbf{1})/(2R)$ ,  $\mathbf{y}' = \mathbf{y}/B$  and  $t' = t/T$ , where  $\mathbf{1} := (1, \dots, 1)^T$ , so that the transformed space is  $[0, 1]^{d_x+d_y+1}$ . Such a transformation can be exactly implemented by a single ReLU layer. By Proposition P1(ii),  $\mathbf{v}_F(\mathbf{x}, \mathbf{y}, t)$  is  $d_x(1-T)^{-2}$ -Lipschitz w.r.t.  $\mathbf{x}$ . For simplicity, we write  $d_x(1-T)^{-2}$  as  $\zeta_T$  in the rest of this section. We now define the rescaled function on the transformed input space as  $\mathbf{v}(\mathbf{x}', \mathbf{y}', t') := \mathbf{v}_F(2R\mathbf{x}' - R\mathbf{1}, B\mathbf{y}', Tt')$ . Such defined  $\mathbf{v}$  is  $(2R\zeta_T)$ -Lipschitz w.r.t.  $\mathbf{x}'$ . Further by Assumption 3,  $\mathbf{v}$  is  $(B\omega)$ -Lipschitz w.r.t.  $\mathbf{y}'$ . By Proposition P1(i), we know that  $\mathbf{v}(\mathbf{x}', \mathbf{y}', t')$  is  $(T\tau_R)$ -Lipschitz w.r.t.  $t'$ , where  $\tau_R := \sup_{t \in [0, T]} \sup_{\mathbf{y} \in [0, B]^{d_y}} \sup_{\mathbf{x} \in [-R, R]^{d_x}} |\partial_t \mathbf{v}_F(\mathbf{x}, \mathbf{y}, t)|_2 \leq C_1 d_x^{3/2} (R+1)(1-T)^{-3}$  for some universal constant  $C_1 > 1$ . Now the goal becomes approximating  $\mathbf{v}(\mathbf{x}', \mathbf{y}', t')$  on  $[0, 1]^{d_x+d_y+1}$ . We partition  $[0, 1]^{d_x}$  into non-overlapping hypercubes with equal edge length  $e_1$ , and  $[0, 1]^{d_y}$  into equal edge length  $e_2$ . We also partition the time interval  $[0, 1]$  into non-overlapping sub-intervals of length  $e_3$ . We will choose  $e_1$ ,  $e_2$  and  $e_3$  later depending on the desired approximation level. Write  $N_1 = \lceil e_1^{-1} \rceil$ ,  $N_2 = \lceil e_2^{-1} \rceil$  and  $N_3 = \lceil e_3^{-1} \rceil$ .

We denote  $[N] := \{0, \dots, N-1\}$  for any positive integer  $N$ . Let  $\mathbf{p} = (p_1, \dots, p_{d_x})^T \in$

$[N_1]^{d_x}$ ,  $\mathbf{q} = (q_1, \dots, q_{d_y})^\top \in [N_2]^{d_y}$  be multi-indexes. Consider vector-valued function

$$\bar{\mathbf{v}}(\mathbf{x}', \mathbf{y}', t') = (\bar{v}_1(\mathbf{x}', \mathbf{y}', t'), \dots, \bar{v}_{d_x}(\mathbf{x}', \mathbf{y}', t'))^\top$$

with

$$\bar{v}_i(\mathbf{x}', \mathbf{y}', t') := \sum_{\mathbf{p} \in [N_1]^{d_x}, \mathbf{q} \in [N_2]^{d_y}, j \in [N_3]} v_F^i \left( 2R \frac{\mathbf{p}}{N_1} - R\mathbf{1}, B \frac{\mathbf{q}}{N_2}, T \frac{j}{N_3} \right) \Psi_{\mathbf{p}, \mathbf{q}, j}(\mathbf{x}', \mathbf{y}', t'),$$

where  $\Psi_{\mathbf{p}, \mathbf{q}, j}(\mathbf{x}', \mathbf{y}', t')$  is a partition of unity function, that is

$$\sum_{\mathbf{p} \in [N_1]^{d_x}, \mathbf{q} \in [N_2]^{d_y}, j \in [N_3]} \Psi_{\mathbf{p}, \mathbf{q}, j}(\mathbf{x}', \mathbf{y}', t') \equiv 1$$

for any  $(\mathbf{x}', \mathbf{y}', t') \in [0, 1]^{d_x} \times [0, 1]^{d_y} \times [0, 1]$ . More specifically,  $\Psi_{\mathbf{p}, \mathbf{q}, j}$  can be selected as a

product of coordinate-wise trapezoid functions:

$$\Psi_{\mathbf{p}, \mathbf{q}, j}(\mathbf{x}', \mathbf{y}', t') := \psi \left( 3N_3 \left( t' - \frac{j}{N_3} \right) \right) \prod_{i=1}^{d_y} \psi \left( 3N_2 \left( x'_i - \frac{q_i}{N_2} \right) \right) \prod_{i=1}^{d_x} \psi \left( 3N_1 \left( x'_i - \frac{p_i}{N_1} \right) \right)$$

with  $\mathbf{x}' = (x'_1, \dots, x'_{d_x})^\top$  and  $\mathbf{y}' = (y'_1, \dots, y'_{d_y})^\top$ , where  $\psi$  is a trapezoid function

$$\psi(a) := \begin{cases} 1, & \text{if } |a| < 1, \\ 2 - |a|, & \text{if } |a| \in [1, 2], \\ 0, & \text{if } |a| > 2. \end{cases}$$

We claim that  $\bar{v}_i(\mathbf{x}', \mathbf{y}', t')$  is an approximation of  $v_i(\mathbf{x}', \mathbf{y}', t')$  and  $\bar{\mathbf{v}}(\mathbf{x}', \mathbf{y}', t')$  can be implemented by a ReLU neural network  $\tilde{v}_i^*(\mathbf{x}', \mathbf{y}', t')$  with small error. Both claims can be considered as extensions of Theorem 1 in [Chen et al. \(2023b\)](#). Here, we draw upon their conclusion, while extending the input dimension of the neural network from  $\mathbb{R}^{d_x+1}$  in [Chen et al. \(2023b\)](#) to  $\mathbb{R}^{d_x+d_y+1}$ . By concatenating all  $\tilde{v}_i^*(\mathbf{x}', \mathbf{y}', t')$ 's together, we construct

$$\tilde{\mathbf{v}}^*(\mathbf{x}', \mathbf{y}', t') = (\tilde{v}_1^*(\mathbf{x}', \mathbf{y}', t'), \dots, \tilde{v}_d^*(\mathbf{x}', \mathbf{y}', t'))^\top.$$

Recall  $\varepsilon_* > 0$  is a sufficiently small universal constant. Given an approximation error  $\varepsilon \in (0, \varepsilon_*)$ , we select  $e_1 = \mathcal{O}(\varepsilon R^{-1} \zeta_T^{-1})$ ,  $e_2 = \mathcal{O}(\varepsilon T^{-1} \tau_R^{-1})$  and  $e_3 = \mathcal{O}(\varepsilon B^{-1} \omega^{-1})$ . In order

to make

$$\sup_{(\mathbf{x}', \mathbf{y}', t') \in [0,1]^{d_x} \times [0,1]^{d_y} \times [0,1]} |\tilde{\mathbf{v}}^*(\mathbf{x}', \mathbf{y}', t') - \mathbf{v}(\mathbf{x}', \mathbf{y}', t')|_\infty \leq \varepsilon,$$

the neural network configuration of FNN( $L, M, J, K, \kappa, \gamma_1, \gamma_2, \gamma_3$ ) is

$$\begin{aligned} L &\sim d_x + d_y + \log \frac{1}{\varepsilon}, & M &\sim T\tau_R(R\zeta_T)^{d_x} (B\omega)^{d_y} \varepsilon^{-d_x - d_y - 1}, \\ J &\sim T\tau_R(R\zeta_T)^{d_x} (B\omega)^{d_y} \varepsilon^{-d_x - d_y - 1} \left( d_x + d_y + \log \frac{1}{\varepsilon} \right), \\ K &\sim \frac{d_x^{1/2} R}{1 - T}, & \kappa &= 1 \vee R\zeta_T \vee T\tau_R \vee B\omega, \end{aligned} \tag{S.45}$$

where the output range  $K$  is computed by Proposition P1(i) as

$$\sup_{(\mathbf{x}, \mathbf{y}, t) \in \mathcal{K} \times [0, B]^{d_y} \times [0, T]} |\mathbf{v}_F(\mathbf{x}, \mathbf{y}, t)|_2 \leq \frac{d_x^{1/2} (1 + TR)}{1 - T^2}. \tag{S.46}$$

Let  $\mathring{\mathbf{v}}(\mathbf{x}, \mathbf{y}, t) = \tilde{\mathbf{v}}^*(\mathbf{x}', \mathbf{y}', t')$  with  $\mathbf{x}' = (\mathbf{x} + R\mathbf{1})/(2R)$ ,  $\mathbf{y}' = \mathbf{y}/B$  and  $t' = t/T$ . Referring to the proof of Theorem 1 in [Chen et al. \(2023b\)](#), we have that  $\mathring{\mathbf{v}}(\mathbf{x}, \mathbf{y}, t)$  is locally Lipschitz continuous w.r.t.  $\mathbf{x}$ , that is,

$$|\mathring{\mathbf{v}}(\mathbf{x}_1, \mathbf{y}, t) - \mathring{\mathbf{v}}(\mathbf{x}_2, \mathbf{y}, t)|_\infty \leq 10d_x\zeta_T |\mathbf{x}_1 - \mathbf{x}_2|_2$$

for any  $\mathbf{x}_1, \mathbf{x}_2 \in \mathcal{K}$ ,  $\mathbf{y} \in [0, B]^{d_y}$  and  $t \in [0, T]$ . Furthermore, the network is also Lipschitz in  $\mathbf{y}$  and  $t$ :

$$|\mathring{\mathbf{v}}(\mathbf{x}, \mathbf{y}_1, t) - \mathring{\mathbf{v}}(\mathbf{x}, \mathbf{y}_2, t)|_\infty \leq 10d_y\omega |\mathbf{y}_1 - \mathbf{y}_2|_2$$

for any  $\mathbf{y}_1, \mathbf{y}_2 \in [0, B]^{d_y}$ ,  $|\mathbf{x}|_\infty \leq R$  and  $t \in [0, T]$ , and

$$|\mathring{\mathbf{v}}(\mathbf{x}, \mathbf{y}, t_1) - \mathring{\mathbf{v}}(\mathbf{x}, \mathbf{y}, t_2)|_\infty \leq 10\tau_R |t_1 - t_2|$$

for any  $t_1, t_2 \in [0, T]$  and  $|\mathbf{x}|_\infty \leq R$  and  $\mathbf{y} \in [0, B]^{d_y}$ . Consider the following univariate real-valued function

$$T_R(x) := \begin{cases} R, & \text{if } x > R, \\ x, & \text{if } x \in [-R, R], \\ -R, & \text{if } x < -R. \end{cases}$$

Define  $\mathcal{T}_{\mathcal{K}}(\mathbf{x}) = (T_R(x_1), \dots, T_R(x_{d_x}))^T$  with  $\mathbf{x} = (x_1, \dots, x_{d_x})^T$ . Immediately, it yields that  $\mathcal{T}_{\mathcal{K}}(\mathbf{x}) = \mathbf{x}$  for any  $\mathbf{x} \in \mathcal{K}$ , and  $\mathcal{T}_{\mathcal{K}}(\mathbf{x}) \in \partial\mathcal{K}$  for any  $\mathbf{x} \in \mathcal{K}^c$ . Simple calculation tells us

$$\begin{aligned} |\mathcal{T}_{\mathcal{K}}(\mathbf{x}) - \mathcal{T}_{\mathcal{K}}(\mathbf{y})|_2 &= \left\{ \sum_{i=1}^{d_x} |T_R(x_i) - T_R(y_i)|^2 \right\}^{1/2} \\ &\leq \left( \sum_{i=1}^{d_x} |x_i - y_i|^2 \right)^{1/2} = |\mathbf{x} - \mathbf{y}|_2. \end{aligned}$$

Also, it's easy to check  $T_R(x) = \text{ReLU}(x) - \text{ReLU}(-x) + \text{ReLU}(-x - R) - \text{ReLU}(x - R)$ .

Due to

$$\begin{aligned} &\sup_{(\mathbf{x}, \mathbf{y}, t) \in \mathcal{K} \times [0, B]^{d_y} \times [0, T]} |\mathring{\mathbf{v}}(\mathcal{T}_{\mathcal{K}}(\mathbf{x}), \mathbf{y}, t) - \mathbf{v}_{\mathbb{F}}(\mathbf{x}, \mathbf{y}, t)|_{\infty} \\ &= \sup_{(\mathbf{x}, \mathbf{y}, t) \in \mathcal{K} \times [0, B]^{d_y} \times [0, T]} |\mathring{\mathbf{v}}(\mathbf{x}, \mathbf{y}, t) - \mathbf{v}_{\mathbb{F}}(\mathbf{x}, \mathbf{y}, t)|_{\infty} \leq \varepsilon, \end{aligned}$$

we know that  $\mathring{\mathbf{v}}(\mathcal{T}_{\mathcal{K}}(\mathbf{x}), \mathbf{y}, t)$  preserves the approximation capability of  $\mathring{\mathbf{v}}(\mathbf{x}, \mathbf{y}, t)$ . Meanwhile,

$$\begin{aligned} \sup_{(\mathbf{x}, \mathbf{y}, t) \in \mathbb{R}^{d_x} \times [0, B]^{d_y} \times [0, T]} |\mathring{\mathbf{v}}(\mathcal{T}_{\mathcal{K}}(\mathbf{x}), \mathbf{y}, t)|_2 &= \sup_{(\mathbf{x}, \mathbf{y}, t) \in \mathcal{K} \times [0, B]^{d_y} \times [0, T]} |\mathring{\mathbf{v}}(\mathbf{x}, \mathbf{y}, t)|_2 \\ &\leq K \leq \frac{\bar{C} d_x^{1/2} R}{1 - T} \end{aligned} \tag{S.47}$$

for some universal constant  $\bar{C} > 1$ . Furthermore, for any  $\mathbf{x}_1, \mathbf{x}_2 \in \mathbb{R}^{d_x}$ ,  $\mathbf{y} \in [0, B]^{d_y}$  and  $t \in [0, T]$ , it holds that

$$|\mathring{\mathbf{v}}(\mathcal{T}_{\mathcal{K}}(\mathbf{x}_1), \mathbf{y}, t) - \mathring{\mathbf{v}}(\mathcal{T}_{\mathcal{K}}(\mathbf{x}_2), \mathbf{y}, t)|_{\infty} \leq 10d_x \zeta_T |\mathcal{T}_{\mathcal{K}}(\mathbf{x}_1) - \mathcal{T}_{\mathcal{K}}(\mathbf{x}_2)|_2 \leq 10d_x \zeta_T |\mathbf{x}_1 - \mathbf{x}_2|_2.$$

So  $\mathring{\mathbf{v}}(\mathcal{T}_{\mathcal{K}}(\mathbf{x}), \mathbf{y}, t)$  acquires global Lipschitz continuity w.r.t.  $\mathbf{x}$ . Let

$$\tilde{\mathbf{v}}(\mathbf{x}, \mathbf{y}, t) = \mathring{\mathbf{v}}(\mathcal{T}_{\mathcal{K}}(\mathbf{x}), \mathbf{y}, t). \tag{S.48}$$

The  $L^2$  approximation error of  $\tilde{\mathbf{v}}$  now can be decomposed into two terms,

$$\begin{aligned} \|\mathbf{v}_{\mathbb{F}}(\mathbf{x}, \mathbf{y}, t) - \tilde{\mathbf{v}}(\mathbf{x}, \mathbf{y}, t)\|_{L^2(g_t)}^2 &= \|\{\mathbf{v}_{\mathbb{F}}(\mathbf{x}, \mathbf{y}, t) - \tilde{\mathbf{v}}(\mathbf{x}, \mathbf{y}, t)\} \mathbb{I}(|\mathbf{x}|_{\infty} \leq R)\|_{L^2(g_t)}^2 \\ &\quad + \|\{\mathbf{v}_{\mathbb{F}}(\mathbf{x}, \mathbf{y}, t) - \tilde{\mathbf{v}}(\mathbf{x}, \mathbf{y}, t)\} \mathbb{I}(|\mathbf{x}|_{\infty} > R)\|_{L^2(g_t)}^2. \end{aligned}$$

The first term on the right-hand side of the last display is bounded by

$$\begin{aligned} & \|\{\mathbf{v}_F(\mathbf{x}, \mathbf{y}, t) - \tilde{\mathbf{v}}(\mathbf{x}, \mathbf{y}, t)\}\mathbb{I}(|\mathbf{x}|_\infty \leq R)\|_{L^2(g_t)}^2 \\ & \leq d_x \sup_{(\mathbf{x}, \mathbf{y}, t) \in \mathcal{K} \times [0, B]^{d_y} \times [0, T]} |\mathbf{v}_F(\mathbf{x}, \mathbf{y}, t) - \tilde{\mathbf{v}}(\mathbf{x}, \mathbf{y}, t)|_\infty^2 \leq d_x \varepsilon^2. \end{aligned}$$

The following lemma gives an upper bound for the second term whose proof is presented in Section [G.2](#).

**Lemma 6** *Let Assumptions [1](#) and [2](#) hold. There exists some universal constant  $C > 0$  such that*

$$\|\{\mathbf{v}_F(\mathbf{x}, \mathbf{y}, t) - \tilde{\mathbf{v}}(\mathbf{x}, \mathbf{y}, t)\}\mathbb{I}(|\mathbf{x}|_\infty > R)\|_{L^2(g_t)}^2 \leq \varepsilon^2$$

for any  $\varepsilon \in (0, \varepsilon_*)$  and  $t \in [0, T]$  with selecting  $R \geq C[\log\{d_x \varepsilon^{-1}(1-T)^{-1}\}]^{1/2}$ , where  $\varepsilon_*$  is specified in Proposition [P2](#).

With selecting  $R \geq C[\log\{d_x \varepsilon^{-1}(1-T)^{-1}\}]^{1/2}$ , it holds that

$$\|\mathbf{v}_F(\mathbf{x}, \mathbf{y}, t) - \tilde{\mathbf{v}}(\mathbf{x}, \mathbf{y}, t)\|_{L^2(g_t)} \leq \varepsilon \sqrt{d_x + 1}.$$

Substituting  $R$  into the network configuration in ([S.45](#)) together with the Lipschitz constraints derived above, we obtain

$$\begin{aligned} L & \sim d_x + d_y + \log \frac{1}{\varepsilon}, \quad M \sim \frac{d_x^{d_x+3/2} (B\omega)^{d_y} \log^{(d_x+1)/2} \{d_x \varepsilon^{-1}(1-T)^{-1}\}}{(1-T)^{2d_x+3} \varepsilon^{d_x+d_y+1}}, \\ J & \sim \frac{d_x^{d_x+3/2} (B\omega)^{d_y} \log^{(d_x+1)/2} \{d_x \varepsilon^{-1}(1-T)^{-1}\}}{(1-T)^{2d_x+3} \varepsilon^{d_x+d_y+1}} \left( d_x + d_y + \log \frac{1}{\varepsilon} \right), \\ \kappa & \sim 1 \vee B\omega \vee \frac{d_x \log^{1/2} \{d_x \varepsilon^{-1}(1-T)^{-1}\}}{(1-T)^2} \vee \frac{d_x^{3/2} \log^{1/2} \{d_x \varepsilon^{-1}(1-T)^{-1}\}}{(1-T)^3}, \\ K & \sim \frac{d_x^{1/2} \log^{1/2} \{d_x \varepsilon^{-1}(1-T)^{-1}\}}{1-T}, \quad \gamma_1 = \frac{10d_x^2}{(1-T)^2}, \\ \gamma_2 & = 10d_y\omega, \quad \gamma_3 \sim \frac{d_x^{3/2} \log^{1/2} \{d_x \varepsilon^{-1}(1-T)^{-1}\}}{(1-T)^3}. \end{aligned}$$

We complete the proof of Proposition [P2](#). □

## E Proof of Proposition 3

Recall that the flow map related to  $\mathbf{Z}_t^{\mathbf{y}}$  is  $\mathbf{F}_t(\cdot, \mathbf{y})$ . Denote by  $\hat{\mathbf{F}}_t(\cdot, \mathbf{y})$  the flow map related to  $\hat{\mathbf{Z}}_t^{\mathbf{y}}$  in (8). Then, given  $\mathbf{Z}_0 \sim \mathcal{N}(\mathbf{0}, \mathbf{I}_{d_x})$ , we have  $\mathbf{F}_t(\mathbf{Z}_0, \mathbf{y}) \sim f_t(\mathbf{x}|\mathbf{y})$  and  $\hat{\mathbf{F}}_t(\mathbf{Z}_0, \mathbf{y}) \sim \hat{p}_t(\mathbf{x}; \mathbf{y})$ . For simplicity, we abbreviate  $\mathbf{F}_t(\cdot, \mathbf{y})$  and  $\hat{\mathbf{F}}_t(\cdot, \mathbf{y})$  as  $\mathbf{Z}_t^{\mathbf{y}}(\cdot)$  and  $\hat{\mathbf{Z}}_t^{\mathbf{y}}(\cdot)$ , respectively. Now,  $\mathbf{Z}_t^{\mathbf{y}}(\mathbf{Z}_0)$  and  $\hat{\mathbf{Z}}_t^{\mathbf{y}}(\mathbf{Z}_0)$  form a coupling of  $f_t(\mathbf{x}|\mathbf{y})$  and  $\hat{p}_t(\mathbf{x}; \mathbf{y})$ . Denote by  $\nu_0(\mathbf{x})$  the density of  $\mathcal{N}(\mathbf{0}, \mathbf{I}_{d_x})$ . By the definition of Wasserstein-2 distance, we have

$$W_2^2(f_t(\mathbf{x}|\mathbf{y}), \hat{p}_t(\mathbf{x}; \mathbf{y})) \leq \int |\mathbf{Z}_t^{\mathbf{y}}(\mathbf{x}) - \hat{\mathbf{Z}}_t^{\mathbf{y}}(\mathbf{x})|_2^2 \nu_0(\mathbf{x}) d\mathbf{x} =: R_t^{\mathbf{y}}.$$

Due to  $d\mathbf{Z}_t^{\mathbf{y}}(\mathbf{x}) = \mathbf{v}_F(\mathbf{Z}_t^{\mathbf{y}}(\mathbf{x}), \mathbf{y}, t) dt$  and  $d\hat{\mathbf{Z}}_t^{\mathbf{y}}(\mathbf{x}) = \hat{\mathbf{v}}(\hat{\mathbf{Z}}_t^{\mathbf{y}}(\mathbf{x}), \mathbf{y}, t) dt$ , we have

$$\begin{aligned} \frac{dR_t^{\mathbf{y}}}{dt} &= 2 \int \langle \mathbf{v}_F(\mathbf{Z}_t^{\mathbf{y}}(\mathbf{x}), \mathbf{y}, t) - \hat{\mathbf{v}}(\hat{\mathbf{Z}}_t^{\mathbf{y}}(\mathbf{x}), \mathbf{y}, t), \mathbf{Z}_t^{\mathbf{y}}(\mathbf{x}) - \hat{\mathbf{Z}}_t^{\mathbf{y}}(\mathbf{x}) \rangle \nu_0(\mathbf{x}) d\mathbf{x} \\ &= 2 \int \langle \mathbf{v}_F(\mathbf{Z}_t^{\mathbf{y}}(\mathbf{x}), \mathbf{y}, t) - \hat{\mathbf{v}}(\mathbf{Z}_t^{\mathbf{y}}(\mathbf{x}), \mathbf{y}, t), \mathbf{Z}_t^{\mathbf{y}}(\mathbf{x}) - \hat{\mathbf{Z}}_t^{\mathbf{y}}(\mathbf{x}) \rangle \nu_0(\mathbf{x}) d\mathbf{x} \\ &\quad + 2 \int \langle \hat{\mathbf{v}}(\mathbf{Z}_t^{\mathbf{y}}(\mathbf{x}), \mathbf{y}, t) - \hat{\mathbf{v}}(\hat{\mathbf{Z}}_t^{\mathbf{y}}(\mathbf{x}), \mathbf{y}, t), \mathbf{Z}_t^{\mathbf{y}}(\mathbf{x}) - \hat{\mathbf{Z}}_t^{\mathbf{y}}(\mathbf{x}) \rangle \nu_0(\mathbf{x}) d\mathbf{x}. \end{aligned}$$

Notice that

$$\begin{aligned} &2 \langle \mathbf{v}_F(\mathbf{Z}_t^{\mathbf{y}}(\mathbf{x}), \mathbf{y}, t) - \hat{\mathbf{v}}(\mathbf{Z}_t^{\mathbf{y}}(\mathbf{x}), \mathbf{y}, t), \mathbf{Z}_t^{\mathbf{y}}(\mathbf{x}) - \hat{\mathbf{Z}}_t^{\mathbf{y}}(\mathbf{x}) \rangle \\ &\leq |\mathbf{v}_F(\mathbf{Z}_t^{\mathbf{y}}(\mathbf{x}), \mathbf{y}, t) - \hat{\mathbf{v}}(\mathbf{Z}_t^{\mathbf{y}}(\mathbf{x}), \mathbf{y}, t)|_2^2 + |\mathbf{Z}_t^{\mathbf{y}}(\mathbf{x}) - \hat{\mathbf{Z}}_t^{\mathbf{y}}(\mathbf{x})|_2^2. \end{aligned}$$

Since  $\hat{\mathbf{v}}(\mathbf{x}, \mathbf{y}, t) \in \text{FNN}$  defined in Proposition 2 is  $\gamma_1$ -Lipschitz continuous w.r.t.  $\mathbf{x}$ , we have

$$\langle \hat{\mathbf{v}}(\mathbf{Z}_t^{\mathbf{y}}(\mathbf{x}), \mathbf{y}, t) - \hat{\mathbf{v}}(\hat{\mathbf{Z}}_t^{\mathbf{y}}(\mathbf{x}), \mathbf{y}, t), \mathbf{Z}_t^{\mathbf{y}}(\mathbf{x}) - \hat{\mathbf{Z}}_t^{\mathbf{y}}(\mathbf{x}) \rangle \leq d_x^{1/2} \gamma_1 |\mathbf{Z}_t^{\mathbf{y}}(\mathbf{x}) - \hat{\mathbf{Z}}_t^{\mathbf{y}}(\mathbf{x})|_2^2.$$

Therefore,

$$\frac{dR_t^{\mathbf{y}}}{dt} \leq (1 + 2d_x^{1/2} \gamma_1) R_t^{\mathbf{y}} + \int |\mathbf{v}_F(\mathbf{Z}_t^{\mathbf{y}}(\mathbf{x}), \mathbf{y}, t) - \hat{\mathbf{v}}(\mathbf{Z}_t^{\mathbf{y}}(\mathbf{x}), \mathbf{y}, t)|_2^2 \nu_0(\mathbf{x}) d\mathbf{x}.$$

Denote by  $g_t(\cdot, \cdot)$  the joint density of  $(t\mathbf{X} + \sqrt{1-t^2}\mathbf{W}, \mathbf{Y})$ . By Lemma 3 and  $R_0^{\mathbf{Y}} = 0$ , it holds that

$$\begin{aligned} \int W_2^2(f_T(\mathbf{x}|\mathbf{y}), \hat{p}_T(\mathbf{x}; \mathbf{y}))p_y(\mathbf{y}) \, d\mathbf{y} &\leq \int R_T^{\mathbf{Y}} p_y(\mathbf{y}) \, d\mathbf{y} \\ &\leq e^{1+2d_x^{1/2}\gamma_1} \int_0^T \int \int |\mathbf{v}_F(\mathbf{Z}_t^{\mathbf{Y}}(\mathbf{x}), \mathbf{y}, t) - \hat{\mathbf{v}}(\mathbf{Z}_t^{\mathbf{Y}}(\mathbf{x}), \mathbf{y}, t)|_2^2 \nu_0(\mathbf{x}) p_y(\mathbf{y}) \, d\mathbf{x} d\mathbf{y} dt \\ &= e^{1+2d_x^{1/2}\gamma_1} \int_0^T \int \int |\mathbf{v}_F(\mathbf{x}, \mathbf{y}, t) - \hat{\mathbf{v}}(\mathbf{x}, \mathbf{y}, t)|_2^2 f_t(\mathbf{x}|\mathbf{y}) p_y(\mathbf{y}) \, d\mathbf{x} d\mathbf{y} dt \\ &= e^{1+2d_x^{1/2}\gamma_1} \int_0^T \|\mathbf{v}_F(\mathbf{x}, \mathbf{y}, t) - \hat{\mathbf{v}}(\mathbf{x}, \mathbf{y}, t)\|_{L^2(g_t)}^2 \, dt. \end{aligned}$$

As given in Proposition 2,  $\gamma_1 = 10d_x^2(1-T)^{-2}$ . By Proposition 2, with probability at least  $1 - n^{-2}$ , we have

$$\int W_2^2(f_T(\mathbf{x}|\mathbf{y}), \hat{p}_T(\mathbf{x}; \mathbf{y}))p_y(\mathbf{y}) \, d\mathbf{y} = \tilde{\mathcal{O}} \left\{ e^{20d_x^{5/2}(1-T)^{-2}} \frac{(1-T)^{-(4d_x+14)/(d_x+d_y+5)}}{n^{2/(d_x+d_y+5)}} \right\}.$$

We complete the proof of Proposition 3. □

## F Proof of Proposition 4

Recall that the flow map related to  $\hat{\mathbf{Z}}_t^{\mathbf{Y}}$  in (8) is defined as  $\hat{\mathbf{F}}_t(\cdot, \mathbf{y})$  in Section E. Denote by  $\tilde{\mathbf{F}}_t(\cdot, \mathbf{y})$  the flow map related to  $\tilde{\mathbf{Z}}_t^{\mathbf{Y}}$  in (9). Then, given  $\mathbf{Z}_0 \sim \mathcal{N}(\mathbf{0}, \mathbf{I}_{d_x})$ , we have  $\hat{\mathbf{F}}_t(\mathbf{Z}_0, \mathbf{y}) \sim \hat{p}_t(\mathbf{x}; \mathbf{y})$  and  $\tilde{\mathbf{F}}_t(\mathbf{Z}_0, \mathbf{y}) \sim \tilde{p}_t(\mathbf{x}; \mathbf{y})$ . For simplicity, we abbreviate  $\hat{\mathbf{F}}_t(\cdot, \mathbf{y})$  and  $\tilde{\mathbf{F}}_t(\cdot, \mathbf{y})$  as  $\hat{\mathbf{Z}}_t^{\mathbf{Y}}(\cdot)$  and  $\tilde{\mathbf{Z}}_t^{\mathbf{Y}}(\cdot)$ , respectively. Now,  $\hat{\mathbf{Z}}_t^{\mathbf{Y}}(\mathbf{Z}_0)$  and  $\tilde{\mathbf{Z}}_t^{\mathbf{Y}}(\mathbf{Z}_0)$  form a coupling of  $\hat{p}_t(\mathbf{x}; \mathbf{y})$  and  $\tilde{p}_t(\mathbf{x}; \mathbf{y})$ . Denote by  $\nu_0(\mathbf{x})$  the density of  $\mathcal{N}(\mathbf{0}, \mathbf{I}_{d_x})$ . By the definition of Wasserstein-2 distance, we have

$$W_2^2(\hat{p}_t(\mathbf{x}; \mathbf{y}), \tilde{p}_t(\mathbf{x}; \mathbf{y})) \leq \int |\hat{\mathbf{Z}}_t^{\mathbf{Y}}(\mathbf{x}) - \tilde{\mathbf{Z}}_t^{\mathbf{Y}}(\mathbf{x})|_2^2 \nu_0(\mathbf{x}) \, d\mathbf{x} =: L_t^{\mathbf{Y}}.$$

Since  $\tilde{\mathbf{Z}}_t(\mathbf{x})$  is piece-wise linear, we consider the evolution of  $L_t^{\mathbf{Y}}$  on each split interval  $(t_k, t_{k+1})$ . Due to  $d\hat{\mathbf{Z}}_t^{\mathbf{Y}}(\mathbf{x}) = \hat{\mathbf{v}}(\hat{\mathbf{Z}}_t^{\mathbf{Y}}(\mathbf{x}), \mathbf{y}, t) dt$  and  $d\tilde{\mathbf{Z}}_t^{\mathbf{Y}}(\mathbf{x}) = \hat{\mathbf{v}}(\tilde{\mathbf{Z}}_t^{\mathbf{Y}}(\mathbf{x}), \mathbf{y}, t_k) dt$  for any

$t \in (t_k, t_{k+1})$ , it holds that

$$\begin{aligned}
\frac{dL_t^y}{dt} &= \int 2 \langle \hat{\mathbf{v}}(\hat{\mathbf{Z}}_t^y(\mathbf{x}), \mathbf{y}, t) - \hat{\mathbf{v}}(\tilde{\mathbf{Z}}_{t_k}^y(\mathbf{x}), \mathbf{y}, t_k), \hat{\mathbf{Z}}_t^y(\mathbf{x}) - \tilde{\mathbf{Z}}_t^y(\mathbf{x}) \rangle \nu_0(\mathbf{x}) \, d\mathbf{x} \\
&= \int 2 \langle \hat{\mathbf{v}}(\hat{\mathbf{Z}}_t^y(\mathbf{x}), \mathbf{y}, t) - \hat{\mathbf{v}}(\tilde{\mathbf{Z}}_t^y(\mathbf{x}), \mathbf{y}, t), \hat{\mathbf{Z}}_t^y(\mathbf{x}) - \tilde{\mathbf{Z}}_t^y(\mathbf{x}) \rangle \nu_0(\mathbf{x}) \, d\mathbf{x} \\
&\quad + \int 2 \langle \hat{\mathbf{v}}(\tilde{\mathbf{Z}}_t^y(\mathbf{x}), \mathbf{y}, t) - \hat{\mathbf{v}}(\tilde{\mathbf{Z}}_{t_k}^y(\mathbf{x}), \mathbf{y}, t), \hat{\mathbf{Z}}_t^y(\mathbf{x}) - \tilde{\mathbf{Z}}_t^y(\mathbf{x}) \rangle \nu_0(\mathbf{x}) \, d\mathbf{x} \\
&\quad + \int 2 \langle \hat{\mathbf{v}}(\tilde{\mathbf{Z}}_{t_k}^y(\mathbf{x}), \mathbf{y}, t) - \hat{\mathbf{v}}(\tilde{\mathbf{Z}}_{t_k}^y(\mathbf{x}), \mathbf{y}, t_k), \hat{\mathbf{Z}}_t^y(\mathbf{x}) - \tilde{\mathbf{Z}}_t^y(\mathbf{x}) \rangle \nu_0(\mathbf{x}) \, d\mathbf{x}
\end{aligned}$$

for any  $t \in (t_k, t_{k+1})$ . Since  $\hat{\mathbf{v}}(\mathbf{x}, \mathbf{y}, t)$  is  $\gamma_1$ -Lipschitz continuous w.r.t.  $\mathbf{x}$ , we have

$$\begin{aligned}
&\int \langle \hat{\mathbf{v}}(\hat{\mathbf{Z}}_t^y(\mathbf{x}), \mathbf{y}, t) - \hat{\mathbf{v}}(\tilde{\mathbf{Z}}_t^y(\mathbf{x}), \mathbf{y}, t), \hat{\mathbf{Z}}_t^y(\mathbf{x}) - \tilde{\mathbf{Z}}_t^y(\mathbf{x}) \rangle \nu_0(\mathbf{x}) \, d\mathbf{x} \\
&\leq d_x^{1/2} \gamma_1 \int |\hat{\mathbf{Z}}_t^y(\mathbf{x}) - \tilde{\mathbf{Z}}_t^y(\mathbf{x})|_2^2 \nu_0(\mathbf{x}) \, d\mathbf{x} = d_x^{1/2} \gamma_1 L_t^y.
\end{aligned}$$

Note that  $\tilde{\mathbf{Z}}_t^y(\mathbf{x}) = \tilde{\mathbf{Z}}_{t_k}^y(\mathbf{x}) + (t - t_k) \hat{\mathbf{v}}(\tilde{\mathbf{Z}}_{t_k}^y(\mathbf{x}), \mathbf{y}, t_k)$ . So it holds that

$$\begin{aligned}
&2 \int \langle \hat{\mathbf{v}}(\tilde{\mathbf{Z}}_t^y(\mathbf{x}), \mathbf{y}, t) - \hat{\mathbf{v}}(\tilde{\mathbf{Z}}_{t_k}^y(\mathbf{x}), \mathbf{y}, t), \hat{\mathbf{Z}}_t^y(\mathbf{x}) - \tilde{\mathbf{Z}}_t^y(\mathbf{x}) \rangle \nu_0(\mathbf{x}) \, d\mathbf{x} \\
&\leq \int |\hat{\mathbf{v}}(\tilde{\mathbf{Z}}_t^y(\mathbf{x}), \mathbf{y}, t) - \hat{\mathbf{v}}(\tilde{\mathbf{Z}}_{t_k}^y(\mathbf{x}), \mathbf{y}, t)|_2^2 \nu_0(\mathbf{x}) \, d\mathbf{x} + \int |\hat{\mathbf{Z}}_t^y(\mathbf{x}) - \tilde{\mathbf{Z}}_t^y(\mathbf{x})|_2^2 \nu_0(\mathbf{x}) \, d\mathbf{x} \\
&\leq d_x \gamma_1^2 (t - t_k)^2 \sup_{\mathbf{x}, \mathbf{y}, t} |\hat{\mathbf{v}}(\mathbf{x}, \mathbf{y}, t)|_2^2 + L_t^y \leq d_x \gamma_1^2 (t - t_k)^2 K^2 + L_t^y.
\end{aligned}$$

Finally, since  $\hat{\mathbf{v}}(\mathbf{x}, \mathbf{y}, t)$  is  $\gamma_3$ -Lipschitz continuous w.r.t.  $t$ , we have

$$\begin{aligned}
&\int 2 \langle \hat{\mathbf{v}}(\tilde{\mathbf{Z}}_{t_k}^y(\mathbf{x}), \mathbf{y}, t) - \hat{\mathbf{v}}(\tilde{\mathbf{Z}}_{t_k}^y(\mathbf{x}), \mathbf{y}, t_k), \hat{\mathbf{Z}}_t^y(\mathbf{x}) - \tilde{\mathbf{Z}}_t^y(\mathbf{x}) \rangle \nu_0(\mathbf{x}) \, d\mathbf{x} \\
&\leq d_x \gamma_3^2 (t - t_k)^2 + \int |\hat{\mathbf{Z}}_t^y(\mathbf{x}) - \tilde{\mathbf{Z}}_t^y(\mathbf{x})|_2^2 \nu_0(\mathbf{x}) \, d\mathbf{x} = d_x \gamma_3^2 (t - t_k)^2 + L_t^y.
\end{aligned}$$

All above tells us

$$\frac{dL_t^y}{dt} \leq 2(d_x^{1/2} \gamma_1 + 1)L_t^y + d_x(\gamma_1^2 K^2 + \gamma_3^2)(t - t_k)^2, \quad t \in (t_k, t_{k+1}).$$

By Lemma 3, we obtain

$$L_{t_{k+1}}^y \leq L_{t_k}^y e^{2(d_x^{1/2} \gamma_1 + 1)(t_{k+1} - t_k)} + e^{2(d_x^{1/2} \gamma_1 + 1)(t_{k+1} - t_k)} d_x(\gamma_1^2 K^2 + \gamma_3^2)(t_{k+1} - t_k)^3,$$

which implies

$$e^{-2(d_x^{1/2}\gamma_1+1)t_{k+1}}L_{t_{k+1}}^{\mathbf{y}} - e^{-2(d_x^{1/2}\gamma_1+1)t_k}L_{t_k}^{\mathbf{y}} \leq d_x(\gamma_1^2K^2 + \gamma_3^2)(t_{k+1} - t_k)^3.$$

Recall that  $t_{k+1} - t_k = \Delta t = N^{-1}T$ . Since  $t_0 = 0$ ,  $t_N = T < 1$  and  $L_0^{\mathbf{y}} = 0$ , we have

$$L_T^{\mathbf{y}} \leq d_x e^{2(d_x^{1/2}\gamma_1+1)}(\gamma_1^2K^2 + \gamma_3^2) \sum_{k=0}^{N-1} (t_{k+1} - t_k)^3 \leq d_x e^{2(d_x^{1/2}\gamma_1+1)}(\gamma_1^2K^2 + \gamma_3^2)N^{-2}.$$

As shown in Proposition 2, for fixed  $(d_x, d_y)$ , we have  $K = \tilde{\mathcal{O}}\{(1-T)^{-1}\}$ ,  $\gamma_1 = 10d_x^2(1-T)^{-2}$

and  $\gamma_3 = \tilde{\mathcal{O}}\{(1-T)^{-3}\}$ , where  $\tilde{\mathcal{O}}(\cdot)$  omits the polynomial term of  $\log n$ . Hence,

$$\sup_{\mathbf{y} \in [0, B]^{d_y}} W_2^2(\hat{p}_T(\mathbf{x}; \mathbf{y}), \tilde{p}_T(\mathbf{x}; \mathbf{y})) \leq \sup_{\mathbf{y} \in [0, B]^{d_y}} L_T^{\mathbf{y}} = \tilde{\mathcal{O}}\{e^{20d_x^{5/2}(1-T)^{-2}}(1-T)^{-6}N^{-2}\}.$$

We complete the proof of Proposition 4. □

## G Proofs of Lemmas

### G.1 Proof of Lemma 4

The first result is directly obtained from Lemma 7 of [Chen, Jiang, Liao and Zhao \(2022\)](#), with a slight modification of the input region. To prove the second result, it suffices to show there exists a function  $C(\cdot)$  such that

$$\|\ell(\mathbf{x}, \mathbf{y}, \mathbf{v}_1) - \ell(\mathbf{x}, \mathbf{y}, \mathbf{v}_2)\|_{L^\infty([0,1]^{d_x} \times [0,B]^{d_y})} \leq \delta \tag{S.49}$$

for any  $\mathbf{v}_1, \mathbf{v}_2 \in \text{FNN}$  satisfying

$$\|\mathbf{v}_1(\mathbf{x}, \mathbf{y}, t) - \mathbf{v}_2(\mathbf{x}, \mathbf{y}, t)\|_{L^\infty([-R,R]^{d_x} \times [0,B]^{d_y} \times [0,1])} \leq C(\delta), \tag{S.50}$$

where  $R > 0$  will be specified later. We rewrite  $\ell(\mathbf{x}, \mathbf{y}, \mathbf{v})$  as follows:

$$\begin{aligned} \ell(\mathbf{x}, \mathbf{y}, \mathbf{v}) &= \frac{1}{T} \int_0^T \left[ \mathbb{E}_{\mathbf{W}} \left( \left\| \mathbf{x} - \frac{t}{\sqrt{1-t^2}} \mathbf{W} \right\|_2^2 \right) + \mathbb{E}_{\mathbf{W}} \{ |\mathbf{v}(t\mathbf{x} + \sqrt{1-t^2}\mathbf{W}, \mathbf{y}, t)|_2^2 \} \right] dt \\ &\quad - \frac{2}{T} \int_0^T \mathbb{E}_{\mathbf{W}} \left\{ \left( \mathbf{x} - \frac{t}{\sqrt{1-t^2}} \mathbf{W} \right)^\top \mathbf{v}(t\mathbf{x} + \sqrt{1-t^2}\mathbf{W}, \mathbf{y}, t) \right\} dt. \end{aligned}$$

Then

$$\begin{aligned}
|\ell(\mathbf{x}, \mathbf{y}, \mathbf{v}_1) - \ell(\mathbf{x}, \mathbf{y}, \mathbf{v}_2)| &\leq \underbrace{\frac{2}{T} \int_0^T \mathbb{E}_{\mathbf{W}} \left( \left| \mathbf{x} - \frac{t}{\sqrt{1-t^2}} \mathbf{W} \right|_2 \cdot |\mathbf{v}_1 - \mathbf{v}_2|_2 \right) dt}_{(A)} \\
&\quad + \underbrace{\frac{1}{T} \int_0^T \mathbb{E}_{\mathbf{W}} (|\mathbf{v}_1 - \mathbf{v}_2|_2 \cdot |\mathbf{v}_1 + \mathbf{v}_2|_2) dt}_{(B)},
\end{aligned} \tag{S.51}$$

where we omit the input of  $\mathbf{v}_1$  and  $\mathbf{v}_2$  for brevity. In the sequel, we always assume (S.50) holds.

We first focus on the upper bound for term (A). By Cauchy-Schwartz inequality,

$$\begin{aligned}
&\frac{1}{T} \int_0^T \mathbb{E}_{\mathbf{W}} \left( \left| \mathbf{x} - \frac{t}{\sqrt{1-t^2}} \mathbf{W} \right|_2 \cdot |\mathbf{v}_1 - \mathbf{v}_2|_2 \right) dt \\
&\leq \frac{1}{T} \left\{ \int_0^T \mathbb{E}_{\mathbf{W}} \left( \left| \mathbf{x} - \frac{t}{\sqrt{1-t^2}} \mathbf{W} \right|_2^2 \right) dt \right\}^{1/2} \left\{ \int_0^T \mathbb{E}_{\mathbf{W}} (|\mathbf{v}_1 - \mathbf{v}_2|_2^2) dt \right\}^{1/2} \\
&\leq \frac{d_x^{1/2}}{(1-T)^{1/2}} \left\{ \frac{1}{T} \int_0^T \mathbb{E}_{\mathbf{W}} (|\mathbf{v}_1 - \mathbf{v}_2|_2^2) dt \right\}^{1/2}.
\end{aligned} \tag{S.52}$$

Recall  $\mathbf{W}_t = t\mathbf{X} + \sqrt{1-t^2}\mathbf{W}$ . Denote by  $p_{w_t|x}(\mathbf{u}|\mathbf{x})$  the conditional density of  $\mathbf{W}_t$  given  $\mathbf{X} = \mathbf{x}$ . Since  $\mathbf{v}_1, \mathbf{v}_2 \in \text{FNN} = \text{FNN}(L, M, J, K, \kappa, \gamma_1, \gamma_2, \gamma_3)$ , then  $|\mathbf{v}_1(\mathbf{x}, \mathbf{y}, t)|_2 \leq K$  and  $|\mathbf{v}_2(\mathbf{x}, \mathbf{y}, t)|_2 \leq K$ . Furthermore, we have

$$\begin{aligned}
&\mathbb{E}_{\mathbf{W}} \left\{ |\mathbf{v}_1(t\mathbf{x} + \sqrt{1-t^2}\mathbf{W}, \mathbf{y}, t) - \mathbf{v}_2(t\mathbf{x} + \sqrt{1-t^2}\mathbf{W}, \mathbf{y}, t)|_2^2 \right\} \\
&= \int_{|\mathbf{u}|_\infty \leq R} |\mathbf{v}_1(\mathbf{u}, \mathbf{y}, t) - \mathbf{v}_2(\mathbf{u}, \mathbf{y}, t)|_2^2 p_{w_t|x}(\mathbf{u}|\mathbf{x}) d\mathbf{u} \\
&\quad + \int_{|\mathbf{u}|_\infty > R} |\mathbf{v}_1(\mathbf{u}, \mathbf{y}, t) - \mathbf{v}_2(\mathbf{u}, \mathbf{y}, t)|_2^2 p_{w_t|x}(\mathbf{u}|\mathbf{x}) d\mathbf{u} \\
&\leq C^2(\delta) + 2K^2 \mathbb{P}(|\mathbf{W}_t|_\infty > R | \mathbf{X} = \mathbf{x}) \\
&= C^2(\delta) + 2K^2 \mathbb{P}(|t\mathbf{x} + \sqrt{1-t^2}\mathbf{W}|_\infty > R).
\end{aligned}$$

Notice that  $\mathbf{W} \sim \mathcal{N}(\mathbf{0}, \mathbf{I}_{d_x})$ . Write  $\mathbf{W} = (W_1, \dots, W_{d_x})^\text{T}$  and  $\mathbf{x} = (x_1, \dots, x_{d_x})^\text{T}$ . Then

$$\mathbb{P}(|t\mathbf{x} + \sqrt{1-t^2}\mathbf{W}|_\infty > R) \leq \sum_{i=1}^{d_x} \mathbb{P}(|tx_i + \sqrt{1-t^2}W_i| > R)$$

$$\leq d_x \mathbb{P}\left(|W_1| > \frac{R-1}{\sqrt{1-t^2}}\right) \leq 2d_x \exp\left\{-\frac{(R-1)^2}{2(1-t^2)}\right\}$$

for any  $R > 1$ , which implies

$$\begin{aligned} & \mathbb{E}_{\mathbf{W}}\left\{|\mathbf{v}_1(\mathbf{t}\mathbf{x} + \sqrt{1-t^2}\mathbf{W}, \mathbf{y}, t) - \mathbf{v}_2(\mathbf{t}\mathbf{x} + \sqrt{1-t^2}\mathbf{W}, \mathbf{y}, t)|_2^2\right\} \\ & \leq C^2(\delta) + 4K^2 d_x \exp\left\{-\frac{(R-1)^2}{2(1-t^2)}\right\} \leq C^2(\delta) + 4K^2 d_x \exp\left\{-\frac{(R-1)^2}{2}\right\}. \end{aligned} \quad (\text{S.53})$$

Combining (S.52) and (S.53), we get

$$\begin{aligned} & \frac{1}{T} \int_0^T \mathbb{E}_{\mathbf{W}}\left(\left|\mathbf{x} - \frac{t}{\sqrt{1-t^2}}\mathbf{W}\right|_2 \cdot |\mathbf{v}_1 - \mathbf{v}_2|_2\right) dt \\ & \leq \frac{d_x^{1/2}}{(1-T)^{1/2}} \left[ C^2(\delta) + 4K^2 d_x \exp\left\{-\frac{(R-1)^2}{2}\right\} \right]^{1/2} \\ & \leq \frac{d_x^{1/2}}{(1-T)^{1/2}} \left[ C(\delta) + 2K d_x^{1/2} \exp\left\{-\frac{(R-1)^2}{4}\right\} \right]. \end{aligned} \quad (\text{S.54})$$

Now we consider term (B). Again, using Cauchy-Schwartz inequality, we have

$$\begin{aligned} & \frac{1}{T} \int_0^T \mathbb{E}_{\mathbf{W}}(|\mathbf{v}_1 - \mathbf{v}_2|_2 \cdot |\mathbf{v}_1 + \mathbf{v}_2|_2) dt \\ & \leq \frac{1}{T} \left\{ \int_0^T \mathbb{E}_{\mathbf{W}}(|\mathbf{v}_1 - \mathbf{v}_2|_2^2) dt \right\}^{1/2} \left\{ \int_0^T \mathbb{E}_{\mathbf{W}}(|\mathbf{v}_1 + \mathbf{v}_2|_2^2) dt \right\}^{1/2} \\ & \leq 2K \left[ C(\delta) + 2K d_x^{1/2} \exp\left\{-\frac{(R-1)^2}{4}\right\} \right]. \end{aligned} \quad (\text{S.55})$$

Combining (S.51), (S.54) and (S.55), we obtain

$$\begin{aligned} & \sup_{\mathbf{x}, \mathbf{y} \in [0,1]^{d_x} \times [0,B]^{d_y}} |\ell(\mathbf{x}, \mathbf{y}, \mathbf{v}_1) - \ell(\mathbf{x}, \mathbf{y}, \mathbf{v}_2)| \\ & \leq \left\{ 2K + \frac{2d_x^{1/2}}{(1-T)^{1/2}} \right\} \left[ C(\delta) + 2K d_x^{1/2} \exp\left\{-\frac{(R-1)^2}{4}\right\} \right]. \end{aligned} \quad (\text{S.56})$$

Letting

$$R = 2 \log^{1/2} [8K\delta^{-1} d_x^{1/2} \{K + (1-T)^{-1/2} d_x^{1/2}\}] + 1,$$

$$C(\delta) = \frac{\delta}{4\{K + (1-T)^{-1/2} d_x^{1/2}\}},$$

by (S.56), we have (S.49) holds for any  $\|\mathbf{v}_1(\mathbf{x}, \mathbf{y}, t) - \mathbf{v}_2(\mathbf{x}, \mathbf{y}, t)\|_{L^\infty([-R, R]^{d_x} \times [0, B]^{d_y} \times [0, T])} \leq C(\delta)$ . Hence, a  $C(\delta)$ -covering of FNN w.r.t.  $\|\cdot\|_{L^\infty([-R, R]^{d_x} \times [0, B]^{d_y} \times [0, T])}$  induces a  $\delta$ -covering of  $\mathcal{H}$ , which implies

$$\begin{aligned} & \log \mathcal{N}(\delta, \mathcal{H}, \|\cdot\|_{L^\infty([0, 1]^{d_x} \times [0, B]^{d_y})}) \\ & \leq \log \mathcal{N}\{C(\delta), \text{FNN}, \|\cdot\|_{L^\infty([-R, R]^{d_x} \times [0, B]^{d_y} \times [0, T])}\} \\ & \leq C J L \log\left(\{K + (1 - T)^{-1/2} d_x^{1/2}\} L M \kappa \delta^{-1} \log^{1/2}[K d_x^{1/2} \delta^{-1} \{K + (1 - T)^{-1/2} d_x^{1/2}\}]\right), \end{aligned}$$

where  $C > 1$  is a universal constant. We complete the proof of Lemma 4.  $\square$

## G.2 Proof of Lemma 6

By Proposition 1(i), we have

$$\mathbf{v}_F(\mathbf{x}, \mathbf{y}, t) = \mathbb{E}\left(\mathbf{X} - \frac{t}{\sqrt{1-t^2}} \mathbf{W} \mid \mathbf{W}_t = \mathbf{x}, \mathbf{Y} = \mathbf{y}\right),$$

where  $\mathbf{W}_t = t\mathbf{X} + \sqrt{1-t^2}\mathbf{W}$ . By (S.47) and (S.48), we define

$$\tilde{K} := \sup_{(\mathbf{x}, \mathbf{y}, t) \in \mathbb{R}^{d_x} \times [0, B]^{d_y} \times [0, T]} |\tilde{\mathbf{v}}(\mathbf{x}, \mathbf{y}, t)|_2^2 \leq \frac{\bar{C}^2 R^2 d_x}{(1-T)^2}.$$

For any  $R > 1$ , it holds that

$$\begin{aligned} & \|\{\mathbf{v}_F(\mathbf{x}, \mathbf{y}, t) - \tilde{\mathbf{v}}(\mathbf{x}, \mathbf{y}, t)\} \mathbb{I}(|\mathbf{x}|_\infty > R)\|_{L^2(g_t)}^2 \\ & = \int \int_{|\mathbf{x}|_\infty > R} |\mathbf{v}_F(\mathbf{x}, \mathbf{y}, t) - \tilde{\mathbf{v}}(\mathbf{x}, \mathbf{y}, t)|_2^2 g_t(\mathbf{x}, \mathbf{y}) \, d\mathbf{x} \, d\mathbf{y} \\ & \leq 2 \int \int_{|\mathbf{x}|_\infty > R} \{|\mathbf{v}_F(\mathbf{x}, \mathbf{y}, t)|_2^2 + |\tilde{\mathbf{v}}(\mathbf{x}, \mathbf{y}, t)|_2^2\} g_t(\mathbf{x}, \mathbf{y}) \, d\mathbf{x} \, d\mathbf{y} \\ & \leq 2 \int \int_{|\mathbf{x}|_\infty > R} \left| \mathbb{E}\left(\mathbf{X} - \frac{t}{\sqrt{1-t^2}} \mathbf{W} \mid \mathbf{W}_t = \mathbf{x}, \mathbf{Y} = \mathbf{y}\right) \right|_2^2 g_t(\mathbf{x}, \mathbf{y}) \, d\mathbf{x} \, d\mathbf{y} \\ & \quad + \tilde{K} \mathbb{P}(|\mathbf{W}_t|_\infty > R) \\ & \leq 2 \int \int_{|\mathbf{x}|_\infty > R} \mathbb{E}\left(\left|\mathbf{X} - \frac{t}{\sqrt{1-t^2}} \mathbf{W}\right|_2^2 \mid \mathbf{W}_t = \mathbf{x}, \mathbf{Y} = \mathbf{y}\right) g_t(\mathbf{x}, \mathbf{y}) \, d\mathbf{x} \, d\mathbf{y} \\ & \quad + \tilde{K} \mathbb{P}(|\mathbf{W}_t|_\infty > R). \end{aligned} \tag{S.57}$$

By Cauchy-Schwarz inequality and Jensen's inequality, it holds that

$$\begin{aligned}
& \int \int_{|\mathbf{x}|_\infty > R} \mathbb{E} \left( \left| \mathbf{X} - \frac{t}{\sqrt{1-t^2}} \mathbf{W} \right|_2^2 \middle| \mathbf{W}_t = \mathbf{x}, \mathbf{Y} = \mathbf{y} \right) g_t(\mathbf{x}, \mathbf{y}) \, d\mathbf{x} \, d\mathbf{y} \\
&= \int \int \mathbb{E} \left( \left| \mathbf{X} - \frac{t}{\sqrt{1-t^2}} \mathbf{W} \right|_2^2 \middle| \mathbf{W}_t = \mathbf{x}, \mathbf{Y} = \mathbf{y} \right) \mathbb{I}(|\mathbf{x}|_\infty > R) g_t(\mathbf{x}, \mathbf{y}) \, d\mathbf{x} \, d\mathbf{y} \\
&\leq \left[ \mathbb{E} \left\{ \mathbb{E} \left( \left| \mathbf{X} - \frac{t}{\sqrt{1-t^2}} \mathbf{W} \right|_2^2 \middle| \mathbf{W}_t, \mathbf{Y} \right) \right\} \right]^{1/2} \{ \mathbb{P}(|\mathbf{W}_t|_\infty > R) \}^{1/2} \\
&\leq \left\{ \mathbb{E} \left( \left| \mathbf{X} - \frac{t}{\sqrt{1-t^2}} \mathbf{W} \right|_2^4 \right) \right\}^{1/2} \{ \mathbb{P}(|\mathbf{W}_t|_\infty > R) \}^{1/2}.
\end{aligned} \tag{S.58}$$

By Assumption 2, it holds that  $|\mathbf{X}|_\infty \leq 1$ . Write  $\mathbf{W} = (W_1, \dots, W_{d_x})^\top$ . Using the inequality

$(a + b)^2 \leq 2a^2 + 2b^2$ , we have

$$\begin{aligned}
\mathbb{E} \left( \left| \mathbf{X} - \frac{t}{\sqrt{1-t^2}} \mathbf{W} \right|_2^4 \right) &\leq \mathbb{E} \left\{ 4|\mathbf{X}|_2^4 + \frac{4t^4}{(1-t^2)^2} |\mathbf{W}|_2^4 \right\} \\
&\leq 4d_x^2 + \frac{4t^4}{(1-t^2)^2} \mathbb{E} \left( \sum_{k=1}^{d_x} W_k^4 + \sum_{i \neq j} W_i^2 W_j^2 \right) \\
&\leq 4d_x^2 + \frac{4t^4}{(1-t^2)^2} d_x(d_x + 2) \leq \frac{8(d_x + 2)^2}{(1-t^2)^2}
\end{aligned} \tag{S.59}$$

for any  $t \in [0, 1)$ . Write  $\mathbf{X} = (X_1, \dots, X_{d_x})^\top$  and  $\mathbf{W}_t = (W_{t,1}, \dots, W_{t,d_x})^\top$ . Since  $W_i$  is a standard Gaussian, using the union inequality, we have

$$\begin{aligned}
\mathbb{P}(|\mathbf{W}_t|_\infty > R) &= \mathbb{P} \left( \bigcup_{i=1}^{d_x} \{ |W_{t,i}| > R \} \right) \leq \sum_{i=1}^{d_x} \mathbb{P}(|W_{t,i}| > R) \\
&\leq \sum_{i=1}^{d_x} \mathbb{P}(t|X_i| + \sqrt{1-t^2}|W_i| > R) \\
&\leq \sum_{i=1}^{d_x} \mathbb{P} \left( |W_i| > \frac{R-1}{\sqrt{1-t^2}} \right) \leq 2d_x \exp \left\{ -\frac{(R-1)^2}{2(1-t^2)} \right\}
\end{aligned} \tag{S.60}$$

for any  $R > 1$ . Combining (S.57), (S.58), (S.59) and (S.60) for  $t \in [0, T]$  with  $T < 1$ , we have

$$\begin{aligned}
& \|(\mathbf{v}_F(\mathbf{x}, \mathbf{y}, t) - \tilde{\mathbf{v}}(\mathbf{x}, \mathbf{y}, t)) \mathbb{I}\{|\mathbf{x}|_\infty > R\}\|_{L^2(g_t)}^2 \\
&\leq \frac{8(d_x + 2)^{3/2}}{1-t^2} \exp \left\{ -\frac{(R-1)^2}{4(1-t^2)} \right\} + \frac{2\bar{C}^2 R^2 d_x^2}{(1-T)^2} \exp \left\{ -\frac{(R-1)^2}{2(1-t^2)} \right\} \\
&\leq \frac{8\bar{C}^2 (R+1)^2 (d_x + 2)^2}{(1-T)^2} \exp \left\{ -\frac{(R-1)^2}{4(1-t^2)} \right\} \leq C_1 (R+1)^2 \exp \left\{ -\frac{(R-1)^2}{4} \right\},
\end{aligned}$$

where  $C_1 = 8\bar{C}^2(d_x + 2)^2(1 - T^2)^{-2}$ . Letting the right-hand side in the above inequality be smaller than  $\varepsilon^2$ , we need to choose  $R$  satisfying

$$\log C_1 + 2\log(R + 1) - \frac{(R - 1)^2}{4} \leq 2\log \varepsilon.$$

Since  $\log(R + 1) \leq R$ , it suffices to require

$$\log C_1 + 2R - \frac{(R - 1)^2}{4} \leq 2\log \varepsilon,$$

which leads to

$$R \geq 5 + 2\sqrt{\log C_1 + 2\log(\varepsilon^{-1})} + 6.$$

Hence,  $\|\{\mathbf{v}_F(\mathbf{x}, \mathbf{y}, t) - \tilde{\mathbf{v}}(\mathbf{x}, \mathbf{y}, t)\}\mathbb{I}(|\mathbf{x}|_\infty > R)\|_{L^2(g_t)}^2 \leq \varepsilon^2$  if  $R \geq C\sqrt{\log\{d_x\varepsilon^{-1}(1 - T)^{-1}\}}$  for some sufficiently large universal constant  $C > 0$ .  $\square$

## References

- Ambrosio, L. (2004). Transport equation and cauchy problem for bv vector fields, *Inventiones mathematicae* **158**(2): 227–260.
- Ambrosio, L. and Crippa, G. (2014). Continuity equations and ode flows with non-smooth velocity, *Proceedings of the Royal Society of Edinburgh Section A: Mathematics* **144**(6): 1191–1244.
- Bainov, D. and Simeonov, P. (1992). *Integral Inequalities and Applications*, Vol. 57, Springer Science & Business Media.
- Bogachev, V. I., Krylov, N. V., Röckner, M. and Shaposhnikov, S. V. (2022). *Fokker–Planck–Kolmogorov Equations*, Vol. 207, American Mathematical Society.
- Boucheron, S., Lugosi, G. and Bousquet, O. (2003). Concentration inequalities, *Summer school on machine learning*, Springer, pp. 208–240.

Chen, M., Jiang, H., Liao, W. and Zhao, T. (2022). Nonparametric regression on low-dimensional manifolds using deep relu networks: Function approximation and statistical recovery, *Information and Inference: A Journal of the IMA* **11**(4): 1203–1253.

Dai, Y., Gao, Y., Huang, J., Jiao, Y., Kang, L. and Liu, J. (2023). Lipschitz transport maps via the follmer flow, *arXiv:2309.03490*.

DiPerna, R. J. and Lions, P.-L. (1989). Ordinary differential equations, transport theory and sobolev spaces, *Inventiones mathematicae* **98**(3): 511–547.